U.S. DEPARTMENT OF COMMERCE
National Technical Information Service

PB80-112394

Development of Superior Entrainment Separators

Air Pollution Technology, Inc, San Diego, CA

Prepared for

Industrial Environmental Research Lab, Research Triangle Park, NC

Aug 79

United States
Environmental Protection
Agency

Industrial Environmental Research
Laboratory
Research Triangle Park NC 27711

EPA-600/7-79-180
August 1979

PB80-112394

EPA

Development of Superior Entrainment Separators

Interagency Energy/Environment R&D Program Report

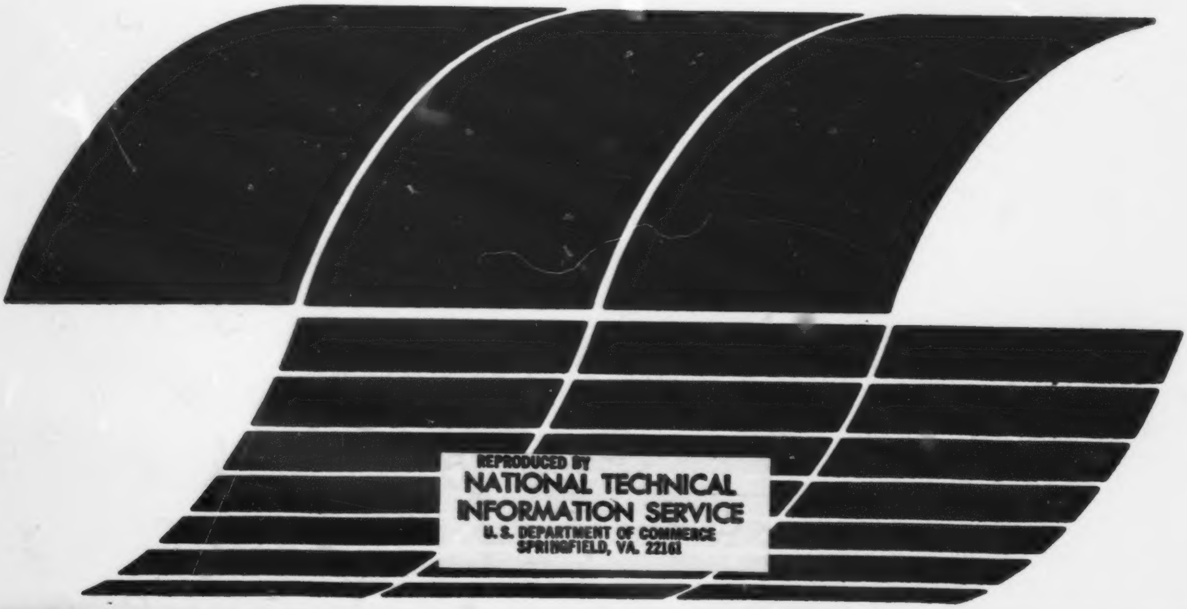

REPRODUCED BY
NATIONAL TECHNICAL
INFORMATION SERVICE
U.S. DEPARTMENT OF COMMERCE
SPRINGFIELD, VA. 22161

RESEARCH REPORTING SERIES

Research reports of the Office of Research and Development, U.S. Environmental Protection Agency, have been grouped into nine series. These nine broad categories were established to facilitate further development and application of environmental technology. Elimination of traditional grouping was consciously planned to foster technology transfer and a maximum interface in related fields. The nine series are:

1. Environmental Health Effects Research
2. Environmental Protection Technology
3. Ecological Research
4. Environmental Monitoring
5. Socioeconomic Environmental Studies
6. Scientific and Technical Assessment Reports (STAR)
7. Interagency Energy-Environment Research and Development
8. "Special" Reports
9. Miscellaneous Reports

This report has been assigned to the INTERAGENCY ENERGY-ENVIRONMENT RESEARCH AND DEVELOPMENT series. Reports in this series result from the effort funded under the 17-agency Federal Energy/Environment Research and Development Program. These studies relate to EPA's mission to protect the public health and welfare from adverse effects of pollutants associated with energy systems. The goal of the Program is to assure the rapid development of domestic energy supplies in an environmentally-compatible manner by providing the necessary environmental data and control technology. Investigations include analyses of the transport of energy-related pollutants and their health and ecological effects; assessments of, and development of, control technologies for energy systems; and integrated assessments of a wide-range of energy-related environmental issues.

EPA REVIEW NOTICE

This report has been reviewed by the participating Federal Agencies, and approved for publication. Approval does not signify that the contents necessarily reflect the views and policies of the Government, nor does mention of trade names or commercial products constitute endorsement or recommendation for use.

This document is available to the public through the National Technical Information Service, Springfield, Virginia 22161.

TECHNICAL REPORT DATA

(Please read Instructions on the reverse before completing)

1. REPORT NO. EPA-600/7-79-180	2.	3. RECIPIENT'S ACCESSION NO. PB80-112394
4. TITLE AND SUBTITLE Development of Superior Entrainment Separators		5. REPORT DATE August 1979
		6. PERFORMING ORGANIZATION CODE
7. AUTHOR(S) Seymour Calvert and Harry F. Barbarika		8. PERFORMING ORGANIZATION REPORT NO.
9. PERFORMING ORGANIZATION NAME AND ADDRESS Air Pollution Technology, Inc. 4901 Morena Boulevard, Suite 402 San Diego, California 92117		10. PROGRAM ELEMENT NO. EHE624
		11. CONTRACT/GRANT NO. 68-02-2184
12. SPONSORING AGENCY NAME AND ADDRESS EPA, Office of Research and Development Industrial Environmental Research Laboratory Research Triangle Park, NC 27711		13. TYPE OF REPORT AND PERIOD COVERED Final; 10/76 - 3/79
		14. SPONSORING AGENCY CODE EPA/600/13

15. SUPPLEMENTARY NOTES IERL-RTP project officer is Leslie E. Sparks, Mail Drop 61, 919/541-2925.

16. ABSTRACT The report describes an experimental and theoretical program carried out to develop an improved design for entrainment separators for scrubbers. The problems of separation efficiency, suspended solids deposition, and plugging of the entrainment separator (ES) were of primary concern. A pilot scale ES, coupled to a scrubber and designed to handle a nominal gas flow rate of 1.4 cu m/s (3000 acfm), was designed, built, and tested. Vertical discontinuous zigzag baffles was the ES design selected after a review of both theory and practical experience with slurry scrubbers. The effect of ES performance on particulate emissions of a typical fossil-fueled boiler was evaluated. The experimental program included measurements of entrainment size distribution and loading, entrainment collection efficiency, solids deposition character and rate, and ES washing efficiency. Results were compared with available models and new criteria for effective washing were developed.

17. KEY WORDS AND DOCUMENT ANALYSIS

a. DESCRIPTORS	b. IDENTIFIERS/OPEN ENDED TERMS	c. COSATI Field/Group
Pollution	Pollution Control	13B
Separators	Stationary Sources	13I,07A
Washing	Entrainment Separators	13H
Scrubbers	Mist Eliminators	
Dust	Particulate	11G
Flue Gases		21B
Fossil Fuels		21D

18. DISTRIBUTION STATEMENT Release to Public	19. SECURITY CLASS *(This Report)* Unclassified	21. NO. OF PAGES 163
	20. SECURITY CLASS *(This page)* Unclassified	22. PRICE PC A08/MF A01

EPA Form 2220-1 (9-73)

EPA-600/7-79-180

August 1979

Development of Superior Entrainment Separators

by

Seymour Calvert and Harry F. Barbarika

Air Pollution Technology, Inc.
4901 Morena Boulevard, Suite 402
San Diego, California 92117

Contract No. 68-02-2184
Program Element No. EHE624

EPA Project Officer: Leslie E. Sparks

Industrial Environmental Research Laboratory
Office of Energy, Minerals, and Industry
Research Triangle Park, NC 27711

Prepared for

U.S. ENVIRONMENTAL PROTECTION AGENCY
Office of Research and Development
Washington, DC 20460

ABSTRACT

An experimental and theoretical program was carried out to develop an improved design for entrainment separators for scrubbers. The problems of separation efficiency, suspended solids deposition and plugging of the entrainment separator were of primary concern.

A pilot scale entrainment separator (E.S.) coupled to a scrubber and designed to handle a nominal gas flow rate of 1.4 m^3/s (3,000 ACFM) was designed, built and tested. Vertical discontinuous, zigzag baffles was the E.S. design selected after a review of both theory and practical experience with slurry scrubbers. The effect of E.S. performance on particulate emissions of a typical fossil-fueled boiler was evaluated.

The experimental program included measurements of entrainment size distribution and loading, entrainment collection efficiency, solids deposition character and rate, and E.S. washing efficiency. Results were compared with available models and new criteria for effective washing were developed.

TABLE OF CONTENTS

ABSTRACT. iii
FIGURES vii
TABLES. xi
ABBREVIATIONS AND SYMBOLS xiii
ACKNOWLEDGMENT xvi

SECTIONS

1. SUMMARY AND CONCLUSIONS. 1
    Summary. 1
    Conclusions. 5
2. INTRODUCTION 11
    Application to Slurry Scrubbers. 12
    Background 13
        Other Programs. 13
        Conclusions from EPA Studies. 14
    Objectives 14
3. ENTRAINMENT SEPARATOR DESIGN FOR PILOT PLANT 17
    Design Approach. 17
        Background Information. 17
        Emission Limit. 19
        Entrainment Separator Types 20
        Performance of Selected Entrainment Separators. 21
        Scrubber/E.S. Performance Balance 21
        Final Selection and Performance Prediction. 25
    Pilot Plant. 32
        Scrubber/Entrainment Separator Shell. 34
        Entrainment Separator Design. 37
        Scrubber Operating Conditions 37
        Drop Disengagement in Vertical Duct 41
        Particle Collection Efficiency of Turning Vanes 41

TABLE OF CONTENTS, continued

Gravity Settling in the Horizontal Duct. 43
Overall Penetration Through Duct 46
4. ENTRAINMENT CHARACTERIZATION. 49
Drop Sizing Techniques. 50
Range of Drop Sizes Expected 50
Review of Drop Sizing Methods. 50
Sizing Methods Chosen. 51
Entrainment Data. 54
E.S. Drainage Data 54
Sphere Drainage Data 56
Concentration from C.I. Measurements 56
Auxiliary Sizing Techniques 58
Entrainment Drop Size Distributions 58
Types of Size Distributions. 59
Cascade Impactor Data. 60
Size from E.S. Penetration 62
Size Distributions from Sphere Collector Data. 72
Expected "σ_g" of Large Drops 76
Sphere Data Analysis 77
Nozzle Manufacturers' Drop Size Data 79
Conclusions 81
5. ENTRAINMENT SEPARATOR PERFORMANCE 91
E.S. Configurations 91
Performance Measurements. 92
Comparison with Theoretical Model 95
Pressure Loss 95
Reentrainment Characteristics 97
E.S. Outlet Solids Emission Levels. 98
6. SOLIDS DEPOSITION 100
Introduction. 100
Slurry. 100
Procedures. 100

TABLE OF CONTENTS, continued

Measurements 101
Results 104
Comparison with Solids Deposition Model 106
Conclusions 110
Operating Experience 110
7. WASHING SYSTEM 114
Introduction 114
Needs and Requirements 114
Requirements/Constraints 115
Experimental Design 117
Results 117
Washing Flux Calculation 117
Minimum Flux Required 119
Comparison with Prediction 121
Design Criteria 121
Typical Design 121
8. FUTURE RESEARCH RECOMMENDATIONS 124
Grade Efficiency 124
Reentrainment Limit 125
Solids Deposition Model 125
Demonstration Program 126

REFERENCES 131

APPENDIX "A" 134

FIGURES

Number		Page
1	Performance cut diameter for several types of entrainment separators.	22
2	Cumulative solids concentration from a mobile bed scrubber for two levels of entrainment concentration.	24
3	Top view diagram of example zigzag baffles.	27
4	Predicted grade efficiency of 3 rows of zigzag baffles	29
5	Predicted grade efficiency of 6 rows of zigzag baffles	29
6	Predicted grade efficiency of zigzag baffles at 4.6 m/s superficial gas velocity.	30
7	Predicted overall penetration for 6 rows of baffles .	31
8	Measured overall collection efficiency of vertical zigzag baffles.	33
9	Reentrainment limits for 6 rows of vertical zigzag baffles (data by Calvert, et al., 1974)	33
10	Schematic diagram of scrubber/entrainment separator system.	35
11	Scrubber/E.S. system.	36
12	Scrubber/entrainment separator system	38
13	Gravity settling velocity of water drops in air (Fuchs, 1964)	42
14	Theoretical centrifugal deposition velocity of water drops in air.	44
15	Theoretical grade efficiency of turning vanes	44
16	Theoretical grade efficiency of horizontal duct . . .	48

FIGURES (continued)

Number		Page
17	Theoretical overall penetration through turning vanes and horizontal duct of log-normally distributed drops.	48
18	Photograph of glass cascade impactor	52
19	Body collector drop sizing system.	57
20	Theoretical overall penetration through zigzag baffles of drops with cubic distribution	64
21	Measured entrainment concentration vs. drop diameter at the E.S. inlet for the mobile bed (mode 1) scrubber	66
22	Measured entrainment concentration vs. drop diameter at the E.S. inlet for the mobile bed (mode 2) scrubber	66
23	Measured entrainment concentration vs. drop diameter at the E.S. inlet for the mobile bed (mode 3) scrubber	67
24	Measured entrainment concentration vs. drop diameter at the E.S. inlet for the mobile bed (mode 4) scrubber	67
25	Measured entrainment concentration vs. drop diameter at the E.S. inlet for the mobile bed (mode 5) scrubber	68
26	Measured entrainment concentration vs. drop diameter at the E.S. inlet for the sieve high scrubber. . . .	68
27	Measured entrainment concentration vs. drop diameter at the E.S. inlet for the sieve low scrubber	69
28	Measured entrainment concentration vs. drop diameter at the E.S. inlet for the spray 5 scrubber	69
29	Measured entrainment concentration vs. drop diameter at the E.S. inlet for the spray 7 scrubber	70
30	Measured entrainment concentration vs. drop diameter at the E.S. inlet for the spray 4 scrubber	70
31	Measured entrainment concentration vs. drop diameter at the E.S. inlet for the spray 6 scrubber	71

FIGURES (continued)

Number Page

32 Theoretical overall efficiency of sphere collectors on log-normally distributed drops. 75

33 Theoretical overall efficiency of sphere collectors on drops with the cubic distribution 75

34 Calculated outlet drop size distribution of turning vane/horizontal run. 78

35 Composite drop size distributions at entrainment separator inlet and at scrubber outlet, for mobile bed (mode 1) scrubber. 85

36 Composite drop size distribution at entrainment separator inlet and at scrubber outlet, for mobile bed (mode 2) scrubber. 85

37 Composite drop size distributions at entrainment separator inlet and at scrubber outlet, for mobile bed (mode 3) scrubber. 86

38 Composite drop size distributions at entrainment separator inlet and at scrubber outlet, for mobile bed (mode 4) scrubber. 86

39 Composite drop size distributions at entrainment separator inlet and at scrubber outlet, for mobile bed (mode 5) scrubber. 87

40 Composite drop size distributions at entrainment separator inlet and at scrubber outlet, for the sieve high scrubber. 87

41 Composite drop size distributions at entrainment separator inlet and at scrubber outlet, for sieve low scrubber 88

42 Composite drop size distributions at entrainment separator inlet and at scrubber outlet, for spray 5 scrubber 88

43 Composite drop size distributions at entrainment separator inlet and at scrubber outlet, for spray 7 scrubber 89

FIGURES (continued)

Number Page

44 Composite drop size distributions at entrainment separator inlet and at scrubber outlet, for spray 4 scrubber. 89

45 Composite drop size distributions at entrainment separator inlet and at scrubber outlet, for spray 6 scrubber. 90

46 Comparison of E.S. size distributions of mobile bed, mode 1 vs. data of Calvert, et al. (1977). . . 90

47 Measured overall penetration correlated to cumulative mass fraction of drops smaller than 20 μmA . . 94

48 Measured deposition thickness rate for spray scrubber operation. 105

49 Measured deposition thickness rate for sieve plate scrubber operation. 105

50 Comparison of measured and predicted deposition rate for spray scrubber run sets 2 and 3. 109

51 Comparison of measured and predicted rates for the sieve plate scrubber operation. 109

52 Slurry flux for maximum deposition rate 116

53 Washing flux vs. percent of baffle surface cleaned after 10 minutes of $u_G = 2.3$ m/s. 118

54 Washing flux vs. percent of baffle surface cleaned after 10 minutes of $u_G = 3.4$ m/s. 118

55 Proposed program schedule 130

TABLES

Number Page

1 Summary of Experimental Conditions. 4

2 Mobile Bed Scrubber Operating Conditions. 39

3 Single Sieve Plate Scrubber Operating Conditions. . . 39

4 Spray Scrubber Operating Conditions 40

5 Superficial Velocity in Entrainment Separator 55

6 Average Size Distributions Based on Cascade Impactor Data at E.S. Inlet. 61

7 Measured Overall Penetration Through E.S. 63

8 Size Distributions Derived from E.S. Penetration Data 65

9 Overall Efficiency of Sphere Collectors 73

10 Size Distributions at E.S. Inlet Derived from Sphere Collector Data. 80

11 Summary of Performance of the Entrainment Separator Based on Cascade Impactor Sampling. 93

12 E.S. Outlet Solids Emissions Based on Drop Penetration 99

13 Calculated Slurry Flux on Rows 1 Through 6. 108

14 Calculated Penetrations of Wash Spray Drops 120

15 Predicted Total Washing Rates for Typical E.S. for Ten-Minute Operation. 123

16 Program Cost Estimate 129

TABLES (continued)

Number | Page

Appendix

A-1 Entrainment Separator Inlet Data Mobile Bed Scrubber Operation. 135

A-2 Entrainment Separator Inlet Data Sieve Plate Scrubber Operation. 138

A-3 Entrainment Separator Inlet Data Spray Scrubber Operation. 140

A-4 Entrainment Separator Outlet Data Mobile Bed Scrubber Operation. 142

A-5 Entrainment Separator Outlet Data Sieve Plate Scrubber Operation. 144

A-6 Entrainment Separator Outlet Data Spray Scrubber Operation. 145

LIST OF ABBREVIATIONS AND SYMBOLS

Latin

a - constant in sphere collection efficiency equation

a - centrifugal acceleration, m/s^2

A_D - deposition area, cm^2 or m^2

b - section width per baffle, m

C' - Cunningham slip correction factor, dimensionless

C_D - drag coefficient, dimensionless

C_n - drop concentration hitting row n, ml/m^3

C_T - total drop concentration, ml/m^3

d_d - drop diameter, μm, (or μmA, cm, m)

d_{dg} - geometric mass mean drop diameter, μm

d_{d50} - drop diameter collected with 50% efficiency, μm

d_{max} - cubic distribution maximum drop diameter, μm

d_{mm} - cubic distribution mass median drop diameter, μm

d_p - particle diameter, μm (or μmA, cm, m)

d_{pa} - particle aerodynamic diameter, $\mu mA = \mu m\ (g/cm^3)^{1/2}$

d_{pg} - geometric mass mean particle diameter, μm

d_{pmm} - mass median particle diameter, μm

f - distribution density function, dimensionless

f_{cub} - cubic density function

f_{LN} - log-normal density function

f_p - pressure loss coefficient, dimensionless

f_v - volume fraction

f_τ - deposition thickness rate correction factor

F_{cub} - cubic distribution function

F_{noz} - spray nozzle distribution function

g - acceleration of gravity, m/s^2 or cm/s^2

h - height, cm or m

k - factor in solids deposition equation

K_p - particle impaction parameter, dimensionless

LIST OF ABBREVIATIONS AND SYMBOLS (continued)

Latin

L - length, cm or m
L_{cr} - critical length, cm or m
n - number of rows of baffles
n_b - number of baffles in a row
N_{Re} - Reynolds number, dimensionless
Pt - penetration, fraction
$\overline{Pt}$ - overall penetration, fraction
Q_G - gas volumetric flow rate, m^3/s
Q_L - liquid volumetric flow rate, m^3/s or ℓ/s
r_c - radius of curvature, cm or m
R_s - solid deposition rate, mg/cm^2-s
T - temperature, °C or °K
u_D - deposition velocity, m/s or cm/s
u_{D1} - deposition velocity on first row, m/s or cm/s
u_G - superficial gas velocity, m/s or cm/s
u_{Gi} - actual gas velocity between baffles of row i, m/s or cm/s
u_t - terminal gravity settling velocity, m/s or cm/s
u_{te} - turbulent eddy velocity, m/s or cm/s
w - baffle or duct width, cm or m
W - solids weight fraction in slurry
x - log-normal distribution parameter

Greek

δ - film thickness, μm
ΔP - pressure loss or drop, Pa or cm W.C.
ε - porosity or void fraction
η - efficiency, fraction
$\overline{\eta}$ - overall efficiency, fraction
θ - baffle angle, degrees or radians
μ_G - gas viscosity, kg/m-s or g/cm-s
μ_L - liquid viscosity, kg/m-s or g/cm-s
ν_G - gas kinematic viscosity, m^2/s or cm^2/s
ρ_d - drop density, kg/m^3 or g/cm^3

LIST OF ABBREVIATIONS AND SYMBOLS (continued)

Greek

ρ_G - gas density, kg/m^3 or g/cm^3
ρ_L - liquid density, kg/m^3 or g/cm^3
ρ_p - particle density, kg/m^3 or g/cm^3
ρ_s - solid cake density, kg/m^3 or g/cm^3
σ_g - geometric standard deviation of diameter
τ - deposition thickness rate, mm/hour
τ' - modified deposition thickness rate, mm/hour
Φ - slurry flux, mg/cm^2-s
Φ_{max} - maximum slurry flux, mg/cm^2-s
Φ_n - slurry flux on row n, mg/cm^2-s
Φ_w - washing flux, mg/cm^2-s

Abbreviations

ACFM - actual cubic feet per minute
BTU - British thermal unit
C.I. - cascade impactor
E.S. - entrainment separator
FGD - flue gas desulfurization
GPM - gallons per minute
ℓ - liter
N - normal conditions : 20°C, 101.325 kPa
NSPS - new source performance standards
psig - pounds force per square inch, gauge
SCF - standard cubic foot : 20°C, 101.325 kPa
W.C. - length of water column
μmA - microns, aerodynamic, μm $(g/cm^3)^{1/2}$

ACKNOWLEDGEMENT

A.P.T., Inc. wishes to express its appreciation for excellent technical coordination and for very helpful assistance in support of our technical effort to Dr. Leslie E. Sparks, EPA Project Officer.

SECTION 1

SUMMARY AND CONCLUSIONS

SUMMARY

Entrainment separation (or mist elimination) has been a major operating problem in scrubber systems, especially those in which dissolved and suspended solids are present in the scrubber liquid, as in lime/limestone scrubbers. The program reported here was initiated by the Particulate Technology Branch of IERL/RTP, EPA in order to develop a superior entrainment separator for FGD lime/limestone scrubbers.

Entrainment separator (E.S.) requirements and performance have been studied in a sequence of research and development programs under several EPA contracts. The results of this work and information from the literature were used as the basis for an experimental program to develop a superior ES for lime/limestone scrubbers. The problems of ES efficiency, suspended solids deposition, and washing were of major concern. The effect of chemical reactions and the resultant precipitation of solids were not included among the parameters studied. It has been shown that proper control of FGD "system chemistry" can essentially eliminate the formation of tightly cemented scale which cannot be removed by washing. Consequently, the present study was restricted to the use of suspended solids.

Pilot Plant

A pilot-scale scrubber and ES system was built to handle a nominal gas flow rate of 1.4 m^3/s (3,000 ACFM). Several scrubbers, typical of those which might be encountered in FGD systems, were used so that the entrainment characteristics would realistically represent what might be encountered. A single stage mobile bed ("ping pong ball"), 1-sieve plate, and spray scrubber were used in this program.

Design criteria for the superior E.S. system were established by considering the effect of the E.S. on particulate emissions from a typical fossil fuel boiler. Estimates of the uncontrolled emissions characteristics and the probable new source performance standards were used to predict the overall efficiency required. Outlet particle concentration depends on both the scrubber and the E.S. acting in series. Consequently, the scrubber and E.S. performances were balanced to define the overall system which would achieve the necessary efficiency with the least power consumption.

The basic theoretical and experimental work on major types of E.S. was carried out on EPA contracts and was presented by Calvert et al. (1974). This research covered the types of E.S. available, drop collection efficiency, gas handling capacity, pressure drop, reentrainment, and solids deposition. Reports of operational experience at the EPA alkali scrubbing facility at the Shawnee Power Station, Paducah, Kentucky detailed many problems with E.S. when used with lime/limestone slurry scrubbers.

Consideration of the overall system, discussed above, led to the conclusion that the E.S. should have an efficiency characterized by a cut diameter (drop collected at 50% efficiency) of about 15 to 20 μm, corresponding to a pressure drop of about 2 cm W.C. A zigzag-type E.S. with vertical or sloping blades and horizontal gas flow was selected for this service. In order to reduce the liquid loading on the E.S. and thereby to increase the allowable gas velocity before reentrainment and to decrease the amount of solids deposition, some "pre-separation" features were employed as follow:

1. Sufficient "free board" was used above the scrubbing zone to permit large drops to settle out or reach the scrubber walls and flow down. A vertical distance of 137 cm was used. Drop diameters with settling velocities corresponding to the upward air velocities used were 700 to 950 μm for the mobile

bed, 300 to 400 μm for the sieve plate, and 600 μm for the spray scrubber.

2. A 90° turn from vertical to horizontal gas flow was fitted with curved turning vanes. Large drops were collected on the turning vanes and flowed back to the scrubbing liquid tank. The turning vanes had a predicted drop cut diameter of 65 μm.
3. A horizontal flow section of sufficient length (235 cm) for substantial drop sedimentation was used between the end of the 90° turn and the upstream face of the E.S. The predicted cut diameter of the horizontal run was 180 μm and the total for freeboard, bend, and horizontal run was 55 μm.

Experimental Program

The experimental program included measurements of entrainment size distribution and concentration, drop collection efficiency, solids deposition character and rate, and E.S. washing efficiency. Flow rates and pressure drops over various segments of the apparatus were also measured. The scrubber had a 76 cm square cross section in which different types of internal structure could be placed to provide the mobile bed, sieve plate, and spray scrubber entrainment emissions.

The E.S. was built in row modules to allow testing with 1 to 6 rows of baffles. Both vertical and forward sloping baffles were tested in 3-row and 6-row configurations. The experimental conditions that were studied are listed in Table 1.

A washing system consisting of sprays of recycled slurry placed upstream of the E.S. was used. The wash period, frequency, drop size, and liquid flow rate were varied to determine the minimum requirements for washing.

Evaluation and Modeling

Experimental results were evaluated to determine how well the theoretical models predicted performance. The drop collection efficiency model agreed generally with the data.

TABLE 1. SUMMARY OF EXPERIMENTAL CONDITIONS

Scrubber	Q_L/Q_G, ℓ/m³	E.S. Velocity, m/s	Scrubber Velocity, m/s	Type of Runs
Mobile Bed - 1	6.5	6.9	3.7	Blank (B), 3 vert.
Mobile Bed - 2	6.0	6.9	3.7	rows (3V), 6V,
Mobile Bed - 3	4.5	6.9	3.7	3 sloping (3S), 6S
Mobile Bed - 4	7.4	6.1	3.3	Drop size and "Pt"
Mobile Bed - 5	8.4	5.3	2.8	
Sieve Plate-low	11.3-13.4	2.3	1.2	B, 3V, 6V, 3S, 6S
Sieve Plate-high	8-9.5	3.4	1.8	Drop size, "Pt", and solids deposition
Spray - 5	1.9	4.6	2.44	Same as sieve plate
Spray - 7	2.6	4.6	2.44	
Spray - 4	1.8	4.6	2.44	
Spray - 6	2.7	4.6	2.44	

The inlet drop size distribution and concentration varied greatly over the cross section of the duct and because of this and the radical difference between the inlet and outlet drop size distributions, the accuracy of the model could not be evaluated with much precision. Reentrainment was not observed for the 6-row E.S. configurations, as would be expected from previous studies. The measured pressure drops agreed with those from previous studies and a mathematical model was developed.

Locations where heavy deposition of solids occurred were predicted with the solids deposition mathematical model, although the deposition rate could not be. Some improvements in the model were made and it is accurate enough to predict potentially troublesome conditions and locations.

The required washing rate was determined experimentally and empirical criteria for satisfactory washing were developed. The continuous flow solids deposition model was not rigorously applicable to the experimental case in which washing was intermittent, but it could be applied to predict a minimum washing flux. General trends can be predicted but not precise flow rates.

CONCLUSIONS

The experience and information gained in the course of this program have led to the formulation of a number of conclusions. Some of these relate to the research objectives, some to the methodology, and some to problems requiring study. For clarity the conclusions are grouped under topical headings below.

Performance Requirements

1. An E.S. drop cut diameter of 15 to 20 μm generally is adequate for lime/limestone scrubbing to meet the EPA NSPS of 13 mg particulates/MJ. (For water drops >5 μm diameter, physical and aerodynamic size are practically equal).

2. Pressure drop, or power requirement, for the combination of scrubber and E.S. can be minimized with an E.S. pressure drop of 2 to 3 cm W.C.

Pre-Separation

1. Pre-separation of entrained drops upstream of the E.S. can significantly reduce the liquid/gas ratio and, thereby, can increase the gas velocity for re-entrainment. Ample freeboard between the scrubber and the next element, turning vanes, and a horizontal run were used in series for pre-separation and gave a drop cut diameter of 55 μm.

2. Turning vanes were the most effective pre-separator and had a predicted drop cut diameter of 65 μm.

Primary Collection Efficiency

1. The vertical, discontinuous zigzag baffle E.S. (Z.Z.E.S.) used with horizontal gas flow in this study had a drop cut diameter of about 20 μm and removed drops larger than 20 μm physical diameter over the range of flow rates investigated.

2. A new mathematical model developed in this study for predicting the primary collection efficiency of zigzag baffles is basically the same as our previous model but easier to comprehend. The effects of drop deposition area and other design parameters are directly apparent in the new model.

3. A Z.Z.E.S. with baffles sloped from vertical and with horizontal gas flow had essentailly the same primary collection efficiency as the vertical baffles.

Reentrainment

1. Both the vertical and sloping baffle, 4-row Z.Z.E.S. had adequate reentrainment characteristics. They did not show drop reentrainment at the limits of pilot plant flow rates (i.e., 8.4 m/s air velocity and 2.4 l/m^3 slurry/air ratio).

2. While four rows of baffles have high primary collection efficiency, they do not have adequate reentrainment characteristics to handle high entrained liquid flow rates. The 4-row Z.Z.E.S. exhibited reentrainment at 6.9 m/s air velocity

and 3 l/m^3 slurry/air ratio.

Solids Deposition

1. Solids deposition is inevitable at some point in the E.S. where the slurry flux to the baffle decreases to a rate which is not "self washing." The predicted minimum rate of washing was approximately 10^{-4} cm^3/cm^2-s and the flux to cause solids deposition on the top 10 cm of a vertical baffle was approximately 2×10^{-5} cm^3/cm^2-s.

2. The mathematical model for solids deposition on vertical surfaces which was developed previously is adequate for estimating the conditions under which deposition will occur.

3. No solids deposition was observed on the backs of baffles, as had been in previous experiments on a single baffle. The gas flow pattern in a multiple baffle Z.Z.E.S. appears to prevent the wake eddy which brought small drops to the back surface of a single baffle.

Washing

1. Solids deposited without cementation (i.e., due to suspended, not dissolved, solids can be removed from baffles by means of intermittent washing with coarse sprays of slurry on the upstream face of the E.S.

2. Effective washing with slurry requires that the slurry flux reaching the last baffle be higher than the minimum self washing rate.

3. Experimental results confirmed the utility of the mathematical model for solids deposition in estimating minimum washing rates.

Drop Sizing Methods

1. A cascade impactor method using a salt tracer provided good drop size distribution data for diameters between 1 and 20 μm.

2. The overall penetration and outlet size distribution data from the E.S. were correlated to log-normal and cubic

inlet size distributions using a mathematical model for E.S. grade penetration. The correlations were very good in a few cases and moderately good in most cases.

3. A new method was developed for sizing drops by means of spherical and cylindrical collection bodies. The volumes of drops collected by the sphere collectors were correlated to log-normal and cubic inlet size distributions using a mathematical model for sphere collection efficiency.

4. The hot wire drop counter did not perform successfully under the conditions of these tests. The fragility of the 5 μm diameter wires and the use at high gas velocities were the probable causes of the poor performance.

Entrainment Size Distribution

The size distributions of the entrainment produced from the three types of scrubbers are represented graphically as the average of the data based on cascade impactor, sphere, and E.S. sampling at the E.S. inlet.

Comparison with Other Data

The only entrainment size distribution data for scrubbers and conditions similar to those used here that could be found were those of Calvert, Yung and Sparks (1977). The present data show a drop concentration about double that of the 1977 measurements for drops smaller than 20 μm diameter.

Future Research Recommendations

The major goals of this research were met, however, a few problems remain to be more fully resolved. These include a more precise determination of the entrainment separator grade efficiency and reentrainment limits and more experimental work to improve the solids deposition model.

The superior E.S. system should undergo a demonstration phase to prove that the design can maintain high performance and not be degraded by a slurry in an actual practical application. Demonstration at a coal-fired utility boiler that uses a lime or limestone flue gas desulfurization scrubber would be desired. The design gas flow rate should be an order of magnitude greater than the present; i.e., at least 14 actual m^3/s (30,000 ACFM).

Report Guide

The following report is devoted mainly to describing the experimental program, its results, our analysis, and conclusions. While only one type of E.S. was used, the program yielded some results which have general applicability. To assist the reader in locating the kind of information he needs, an overview of the major subject categories of the report are given below.

Section 2 presents a brief summary of the background work in the field and the objectives of this program.

Section 3 gives the design basis and rationale for the pilot plant used in this program. The performance characteristics required of the E.S. were established upon consideration of the overall emission limits and the characteristics of FGD scrubbers.

Methods for predicting the primary collection efficiency and re-entrainment conditions for a given zigzag baffle design are given in "Final Selection and Performance Prediction, page 25.

The design rationale and details of the experimental pilot plant are given in "Pilot Plant," page 32. Pre-separation effects on drop size distribution are predicted in this section.

Section 4 deals with the measurement of drop size and concentration. Several methods were used and the results are compared for a number of experimental conditions.

Section 5 presents experimental results on E.S. performance and compares them with theoretical predictions. Penetration, pressure drop, reentrainment, and outlet solids emissions are discussed.

Section 6 covers the experiments and analysis of experimental results on solids deposition. Comparison of experimental results and a mathematical model illustrates the use and limitations of the model.

Section 7 describes the E.S. washing system, experiments, results, and analysis of data.

Section 8 gives the recommendations for future research.

SECTION 2

INTRODUCTION

Entrainment separators, or mist eliminators, are widely used to prevent the carry-over of liquid drops from scrubbers. The liquid drops are the result of the thorough and vigorous liquid-gas contacting in the scrubber which atomizes and entrains some of the scrubbing liquor. Undesirable particulate emissions as well as numerous operational problems may occur if this entrained liquid is not removed from the gas stream.

The liquid entrainment will generally contain both suspended and dissolved solids. The suspended solids may be the particles collected by the scrubber, substances carried in the scrubbing liquid, or products of chemical reaction occurring within the scrubber. Similarly, the dissolved solids may come from the impurities in the gas, reagents carried in the scrubber liquid, or products of reaction.

The residue remaining after the emitted entrainment drops have dried is a particulate emission into the atmosphere. The composition of such residues can be quite different from that of the particles entering the scrubber, especially where reactive solutions or slurries are used for gas scrubbing. Thus, a consequence of excessive entrainment carry-over can be that the particulate concentration in the effluent gas within a certain size range could be higher than that in the gas entering the scrubber.

Many operational problems can arise if the entrainment level is excessive. The drops can be responsible for corrosion, erosion, and ultimately, mechanical failure of fan blades or housing. Pools of liquid and/or residual solids can also deposit in ductwork, on heat-exchange surfaces, and in the stack, causing corrosion or plugging. In the area immediately surrounding the point of emission harmful and unsightly "rain-out" of liquid drops can occur.

Because of the emissions and operational problems that arise from excessive levels of entrainment, the entrainment separator is an important component of the air pollution control system. In many applications it is no less important than the scrubber itself since its inefficiency can allow reemission of particles collected and generated in the scrubber. And, should the entrainment separator fail to remove enough corrosive, erosive, or solids-laden drops, operational problems will occur to seriously affect the availability of the scrubber.

APPLICATION TO SLURRY SCRUBBERS

Many scrubbers which are designed for particle collection use fresh or fairly clean recirculated water as the scrubbing liquid. The solids in the form of collected particulates and impurities would, in this case, usually constitute less than 1% of the liquid mass, depending on the particle loading and the efficiency of the cleaning of the recycled liquid. Thus, the design of the entrainment separator (E.S.) need be mainly concerned with collecting liquid drops. However, if a considerable percentage of suspended solids is present in the scrubbing liquid, one must pay attention to the possibility of solids deposition and accumulation.

Slurries are used primarily when a gaseous component of the effluent stream is to be scrubbed. Chemically reactive slurry solids are used to increase the mass transfer rate and capacity of the liquid. One of the most widely used slurry scrubbers is the lime/limestone system for controlling both particulates and sulfur oxides from coal-fired utility boilers. In these scrubbers the suspended solids concentrations are often in the range of 10 to 20% by mass so that the potential for plugging and other operational problems, as well as high particulate emissions, is great.

BACKGROUND

Because of the increasing usage of lime/limestone scrubbing for flue gas desulfurization (FGD), the U.S. Environmental Protection Agency (E.P.A.) has carried out several research and development programs aimed at developing our capability and engineering knowledge in this subject.

In the "Scrubber Handbook" prepared under E.P.A. contract by Calvert et al. (1972), a subsection was devoted to entrainment separators. It was noted that entrained drops can be removed from the gas stream by a variety of devices similar in principle to particle collecting scrubbers. The devices for which some theoretical or experimental collection information was available were gravity settlers, knitted wire mesh, rods arranged in staggered rows, and cyclones.

Because the available design information was so scarce the E.P.A. contracted with Air Pollution Technology, Inc. (A.P.T.) in 1973 to conduct extensive theoretical and experimental studies of entrainment separators. The study included an evaluation of current technology, experimental studies in a pilot-scale system, and development of theoretical performance models.

Zigzag baffle, knitted mesh, tube bank, packed bed, and cyclone devices were tested. Preliminary studies of the mechanisms for and effects of solids deposition were also made. Two reports were issued for this contract - Calvert et al. (1974), and Calvert et al. (1975). In addition, the results have been reported in the literature by Calvert et al. (1974b), Calvert et al. (1977), Calvert (1978a), and Calvert (1978b).

Other Programs

Since 1972 E.P.A. has been operating a prototype FGD test facility at the Tennessee Valley Authority's Shawnee power plant near Paducah, Kentucky. A number of reports have given details of the operational problems; e.g. Epstein (1975) and Head (1976).

Mist eliminators have also been listed as a major problem area for lime/limestone FGD systems by the Electric Power Research Institute (EPRI) - see Nannen and Yeager (1976). One result of EPRI's efforts to investigate entrainment separator problems has been a study on mist eliminator design by Conkle et al. (1976).

Conclusion of EPA Studies

Several conclusions were drawn by Calvert et al. (1975) concerning primary collection efficiency, capacity, nature of reentrainment, pressure drop, and solids deposition. And, as a result of the studies, it was thought that "Entrainment separator design or specifications by means of rational methods is possible to a useful degree." However, "Several important areas require further study before the state of knowledge will be adequate for the reasonably thorough and accurate design of an entrainment separator. Some of these are:

1. Reentrainment mechanism and loading for separators under various operating conditions.
2. Entrainment loading and drop size distribution from various scrubbers under different operating conditions.
3. Solid depositions and factors affecting the deposition rate.
4. Effective separator washing method and flow rate of washing liquid."

The program that is reported here was undertaken to design and test a superior E.S. for lime/limestone scrubbers and to develop better information for the design of E.S.s. The latter three areas mentioned above were specifically studied in detail. Fulfilling these needs as well as helping to solve the persistent operational problems with slurry scrubber FGD entrainment separators were goals of this program.

OBJECTIVES

The objectives of the program included the following:

Design and Build Pilot Plant

Design and build a pilot scale (1,000 to 3,000 ACFM) entrainment separator, coupled with a scrubber.

Experimental Study

Conduct a pilot scale experimental program using the pilot scale entrainment separator to:

1. Determine locations in the entrainment separator where liquid and entrained solids tend to concentrate.
2. Develop washing techniques to effectively clean the entrainment separator, especially those locations where liquid and solids concentrate. In developing the washing techniques the contractor shall keep in mind that the amount of fresh water available for washing field entrainment separators is limited. Thus, the washing techniques must make use of recirculated scrubber liquid and a minimum of fresh water.
3. Determine the primary droplet collection efficiency, reentrainment properties, and pressure drop of the entrainment separator.
4. Investigate potential operation and maintenance problems such as plugging, corrosion, etc.

Develop Design Criteria

Develop design equations including scale-up criteria which can be used to design larger units.

Determine Emission Effects

Determine the effects of entrained solids (dissolved or suspended) that escape the entrainment separator on particulate emissions from a scrubber system.

Modify Design Models

Previous design methods for entrainment separators should be modified to incorporate the results of this research.

Recommend Test Program

Recommend a test program to demonstrate superior entrainment separators at large pilot scale (up to 30,000 ACFM of gas) for example at EPA's scrubber test facility at Shawnee. Include estimates of the cost and time required for the demonstration.

SECTION 3

ENTRAINMENT SEPARATOR DESIGN FOR PILOT PLANT

DESIGN APPROACH

The approach to the design of the pilot plant entrainment separator (E.S.) was the same as should be followed in designing any E.S., namely:

1. Obtain background information on the gas stream, particulate emissions, and entrainment size and concentration.
2. Determine the required emission limit.
3. Identify suitable types of E.S.
4. Estimate the entrainment separator performance.
5. Determine the compatible combinations of scrubbers and E.S.
6. Final selection and performance prediction.

Background Information

The E.S. design process for a new installation will involve a balance between scrubber and E.S. performance for an optimum design. Thus, particle as well as entrainment information is required. When the E.S. is to be used on an existing scrubber whose performance is fixed, the E.S. efficiency required will also be fixed. Particle information of interest includes:

1. Particle concentration
2. Particle size distribution
3. Particle density
4. Nature, shape, volatility, etc. of the particles
5. Gas temperature, pressure, and composition

To design a suitable E.S. or to select one and predict its collection efficiency, one needs information on the liquid and gas phases, as listed below.

A. Liquid Phase
   1. Entrainment drop size distribution
   2. Entrainment loading
   3. Suspended and dissolved solids
   4. Densities
   5. Vapor pressure
   6. Nature of the entrainment; i.e., is it sticky, corrosive, oily, etc.?

B. Gas Phase
   1. Temperature
   2. Pressure
   3. Composition
   4. Flow rate
   5. Allowable pressure drop

Assumed Properties -

The particle and entrainment properties assumed for this study were based on a typical coal-fired utiltiy boiler application as described by Epstein (1975) for the EPA alkali scrubbing test facility at TVA, Shawnee Station.

Particle concentration: 8.6 g/Nm^3*

Particle size distribution: d_{pg} = 35 μmA** and $\sigma_g = 2.3$

Scrubber type: Mobile bed (because of severe entrainment problems experienced with this type)

---

*'N' refers to "normal" gas conditions, i.e. 20°C and 1 atm.

**'μmA' (micrometers, aerodynamic) are the units of drop or particle aerodynamic impaction diameter (see Galeski, 1977), defined as:

$$d_{pa}\,[\mu mA] = d_p[\mu m] \times (C'\,\rho_p)^{1/2}$$

where d_p = Stokes or physical diameter, μm
C' = Cunningham slip correction factor
ρ_p = particle density, g/cm^3

Entrainment drop size distribution: As described by Calvert, et al. (1977)

Entrainment loading: As described by Calvert, et al. (1977).

Suspended and dissolved solids: Total up to 25% by mass; primarily $CaCO_3$. No attempt was made to match the dissolved and suspended sulfates and sulfites, or the pH of FGD slurries. This study concentrated on performance with suspended solids deposition without chemical precipitation effects. Work at EPA's Shawnee station has shown that scaling resulting from sulfate/sulfite precipitation and other causes can be effectively controlled through the system chemistry - see Williams (1978).

Nature of entrainment: Abrasive

Gas conditions in E.S.: Saturated with H_2O at about 50°C, pressure = 1 atm.

Emission Limit

In order to specify the E.S. performance required one must first determine the overall emission limit for the scrubber/E.S. air pollution control system. The E.S. for this study was designed for a pilot plant which was to simulate a lime/limestone scrubber system used for flue gas desulfurization and particulate removal.

Although it might be ideal to remove all the entrainment, economics dictates some limit, and it is necessary that a tolerable level of removal efficiency be determined. The first consideration should be that of complying with legislated emission standards. In the limestone FGD case the applicable standard would be that for particulate emissions.

The standards for existing fossil-fueled boilers vary from state to state and the EPA was in the process of promulgating a new source performance standard (NSPS) for new facilities. At the time of this study the NSPS for total particulates from fossil-fueled boilers is 13 mg/MJ heat output of fuel (0.03 lbm/10^6 BTU). In terms of concentration of particulates this is about 34 mg/m^3 at 20°C, 1 atm (0.015 grain/SCF).

Entrainment Separator Types

Entrainment separators for scrubbers fall into the following categories:

1. Cyclone
2. Gravity settler
3. Wire mesh
4. Packed bed
5. Discontinuous baffles
6. Tube bank
7. Continuous wave form

The properties and limitations of each category of E.S. have been studied by Calvert, et al. (1975) and descriptions of commercially available designs can be found in McIlvaine (1978). In general the wire mesh, packed bed, and waveforms with "hooks" and other projections are not suitable for applications using slurry as they are easily filled by solids buildup.

The gravity settler is usually not feasible because the efficiency is low and the space required is large. Of the remaining three types, the cyclone and the baffle type are the most widely used on slurry scrubbers. Baffle types are often preferred because of their large clearance dimensions, ease of washing, relatively small size, and moderate cost.

An open, or discontinuous, baffle type E.S. has been used at EPA's Shawnee test facility (Epstein et al.,1976), while continuous sharp-cornered and waveform chevrons have been used extensively in other lime/limestone facilities and pilot plants. Weir, et al. (1976) have successfully used the waveform chevrons at the Mojave Generating Station of Southern California Edison Company. The sharp-cornered chevrons have been used in pilot plant studies at EPA by Hollinden et al. (1976, 1977) and at Ontario Hydro by Sekhar (1977). Conkle et al. (1976) in a broad survey or lime/limestone FGD systems have concluded that "the chevron or baffle-type mist eliminator is used nearly universally in the United States."

Based on its general usage and on our extensive experience with the design (Calvert, et al., 1975) we selected the discontinuous zigzag baffle type of entrainment separator for the pilot plant study.

Performance of Selected Entrainment Separators

The approximate performance of various types of entrainment separators is shown in Figure 1. The performance parameter used in the figure is the aerodynamic cut diameter in units of µmA, which is the drop diameter that will be collected with 50% efficiency. The collection efficiency of drops larger than the cut diameter is usually very high so it can be approximated by assuming that 100% of them are collected.

For our system we arrived at a design pressure drop for the E.S. of about 2 cm W.C. This pressure drop corresponds to a cut diameter ranging from about 15 µmA for the least efficient type of E.S. in Figure 1 to about 2 µmA for the wire mesh. To be conservative, we assumed that 100% of drops larger than 20 µmA are collected for $\Delta P = 2$ cm W.C. in a zigzag baffle E.S. The implications of this E.S. performance on the required scrubber performance are discussed below.

Scrubber/E.S. Performance Balance

The system performance for a mobile bed scrubber and baffle-type E.S. was calculated for representative conditions. The required overall efficiency is assumed to be 99.7% and the assumed entrainment parameters have been listed previously. Most of the particle penetration will be allocated to the scrubber, as discussed below.

In order to predict the E.S. efficiency required we had to assume the entrainment drop size, concentration, and solids content. The drop size and concentration were taken from Calvert, et al. (1977) for $Q_L/Q_G = 7.8$ l/m^3 and $\mu_G \simeq 4$ m/s in a small, 3-stage mobile bed scrubber. A conservatively high slurry concentration of 25 wt% solids was assumed, although this is almost double the usual concentration for lime/limestone scrubbers.

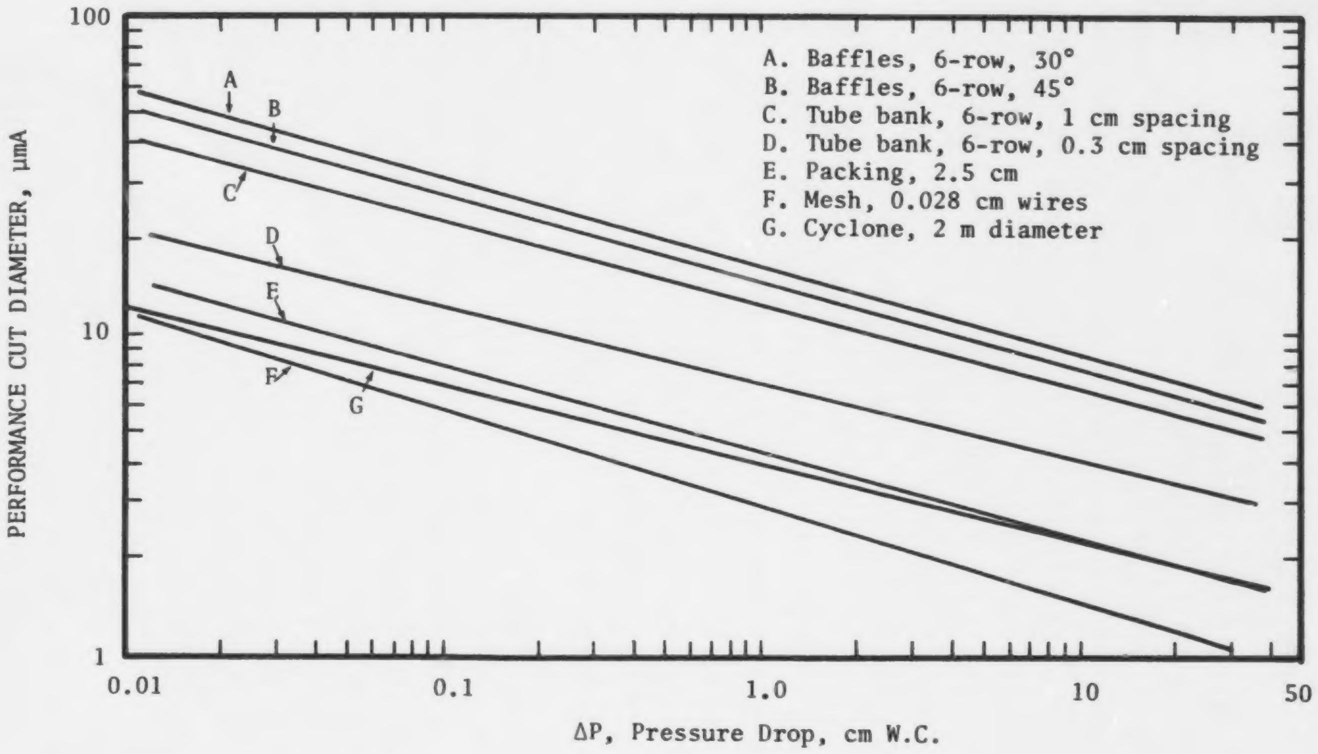

Figure 1. Performance cut diameter for several types of entrainment separators.

Figure 2 is a plot of cumulative mass concentration of solids emission from mobile bed scrubbers as a function of dry particle residue diameters and original drop diameters. The solid curve labeled "1977 data" shows that the cumulative mass concentration of solids in drops 20 μmA diameter and smaller was 4 mg/Nm^3. Consequently, an E.S. with a 20 μmA cut diameter would emit about 4 mg/Nm^3 of solids carried by the drops.

According to Epstein (1975), a mobile bed scrubber with a 21 cm W.C. pressure drop would have a penetration of 0.0035 and would emit 30 mg/Nm^3 (for the representative conditions), so the total emission of ash and entrainment solids would be 34 mg/Nm^3. The solid curves on Figure 2 labeled "Ash" and "Total, 1977 + 21 cm W.C." show the predicted emissions as a function of dry particle diameter.

As will be seen later, the amount of entrainment measured in this study was about twice that in the 1977 research. The dashed curves in Figure 2 shows the cumulative solid mass emitted as entrainment, the ash emission for a 27 cm. W.C. mobile bed scrubber pressure drop, and the total dry particle emission. A relatively small increase, 6 cm W.C., of scrubber pressure drop would permit attainment of the 34 mg/Nm^3 limit with the high assumed value of 25 wt% solids in the entrainment.

At the usual lime/limestone slurry concentration of around 15%, the mass emission due to entrainment would be 4.8 mg/Nm^3 rather than the 8 mg/Nm^3 for 25% slurry. Consequently, even with the benefit of hindsight, the design objective of 15 to 20 μmA drop cut diameter for the E.S. seems reasonable.

The sensitivity of overall pressure drop to E.S. pressure drop can also be estimated from Figures 1 and 2, as given below.

A. Increasing efficiency by having an E.S. absolute cut at 10 μmA instead of 20 μmA would result in an increase in pressure drop of the E. . from 2 cm W.C. to about 20 cm W.C. for the baffle-type E.S. The emissions would be reduced by only about 0.6-1.8 mg/Nm^3 or 2-6% for an 18 cm W.C. increase in ΔP.

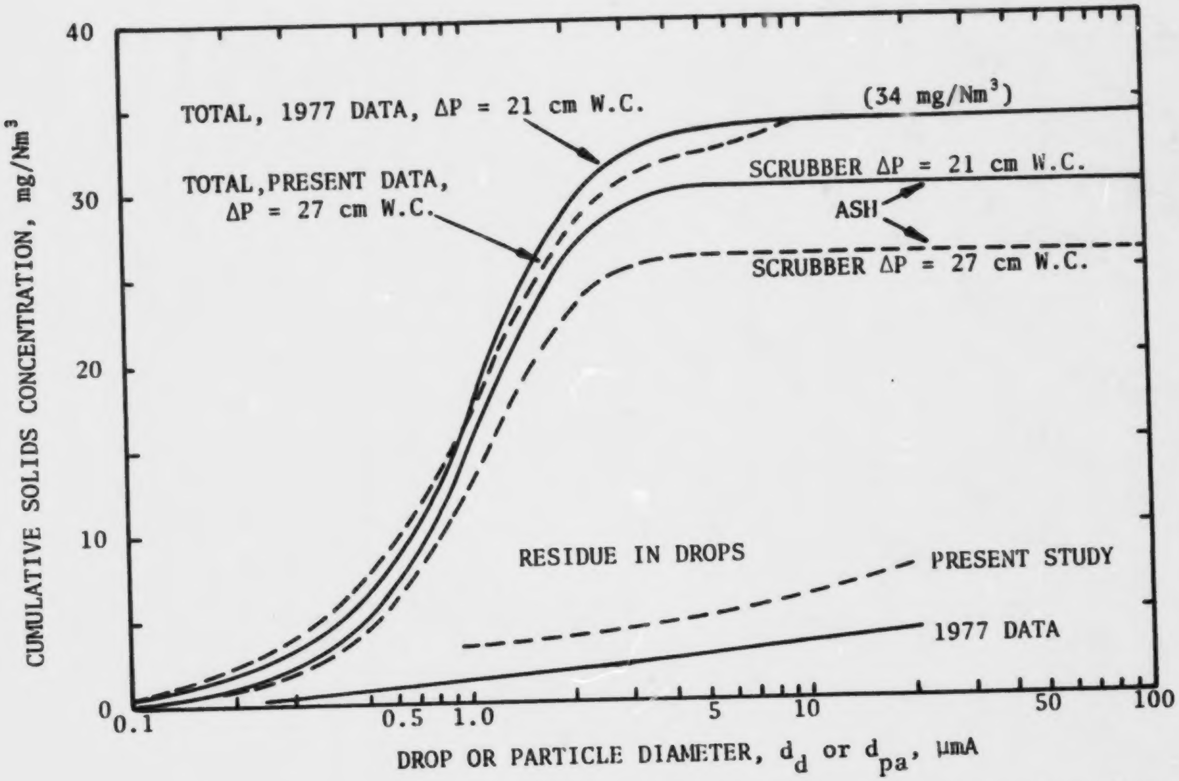

Figure 2. Cumulative solids concentration from a mobile bed scrubber for two levels of entrainment concentration.

B. Increasing efficiency by raising scrubber pressure drop by only 6 cm W.C. from 21 to 27 cm W.C. results in the scrubber being about 99.8% efficient and reduce particulate loading by 4 mg/Nm^3, or 13%.

Thus, increasing E.S. pressure drop has very little effect on overall efficiency, compared to increasing the scrubber pressure drop. This conclusion generally applies, since the scrubber is a much more efficient particle collection device than the entrainment separator.

Final Selection and Performance Prediction

The discontinuous zigzag baffle design was selected for the pilot study. This E.S. type could provide the needed efficiency and had been applied to lime/limestone scrubbers. It was also considered that this design would be less susceptible to solids buildup than others and could easily be washed.

The configuration of the baffles is shown in Figure 3. The approximate performance cut diameter of this configuration was shown as curve "A" in Figure 1. In the following a more detailed performance prediction will be presented.

Primary Collection Efficiency -

The penetration of drops through zigzag baffles, based on perfect turbulent mixing, is:

$$Pt = \exp\left(- \frac{A_D \ u_D}{Q_G}\right) \tag{1}$$

where A_D = deposition surface area, cm^2
u_D = deposition velocity, cm/s
Q_G = gas flow rate, cm^3/s

The deposition surface area is the upstream surface area of the baffles:

$$A_D = w \ h \ n_b \ n \tag{2}$$

where w = baffle width, cm
h = baffle height, cm
n_b = number of baffles in a row
n = number of rows

The drop deposition velocity is the terminal centrifugal velocity, where the centrifugal force acting on the drop is due to the average radius of curvature through which the gas turns in passing through the baffles (see Calvert et al., 1974).

$$u_D = \left(\frac{4}{3}\,\frac{\rho_d\, d_d\, a}{C_D\, \rho_G}\right)^{1/2} \qquad (3)$$

where ρ_d = drop density, g/cm³
ρ_G = gas density, g/cm³
d_d = drop diameter, cm
C_D = drop drag coefficient
a = centrifugal acceleration, cm/s²

$$a \simeq \frac{2\, u_G^2 \sin \Theta}{w \cos^3 \Theta} \qquad (4)$$

where u_G = superficial gas velocity, cm/s
Θ = angle through which gas must turn, degrees or radians

When the drop Reynolds number is less than 0.1 Stokes flow may be assumed, so that:

$$C_D = \frac{24}{N_{Re}} \qquad N_{Re} < 0.1 \qquad (5)$$

where

$$N_{Re} = \frac{\rho_G\, u_D\, d_d}{\mu_G} \qquad (6)$$

and μ_G = gas viscosity, g/cm-s

A more general drag coefficient for spheres, due to Dickinson and Marshall (1968) is,

$$C_D = 0.22 + \frac{24}{N_{Re}}\left(1 + 0.15\, N_{Re}^{0.6}\right) \qquad (7)$$

Combining equations (1), (2), (3) and (4)

$$Pt = \exp\left\{-\frac{w}{b}\left[\frac{u_{D1}}{u_G} + (n-1)\,\frac{u_D}{u_G}\right]\right\} \tag{8}$$

where

$$\frac{u_{D1}}{u_G} = \left[\frac{8}{3}\,\frac{\sin(\Theta/2)\,\rho_d\,d_d}{w\cos^3(\Theta/2)\,C_D\,\rho_G}\right]^{1/2} \tag{9a}$$

$$\frac{u_D}{u_G} = \left[\frac{8}{3}\,\frac{\sin\Theta\,\rho_d\,d_d}{w\cos^3\Theta\,C_D\rho_G}\right]^{1/2} \tag{9b}$$

It is assumed that Θ is the angle the baffle makes with the flow and that except for the first row the gas turns through an angle of 2 Θ. And,

$$u_G = \frac{Q_G}{n_b b} \tag{10}$$

For the dimensions shown in Figure 3:

$w = 7.6$ cm

$b = 8.5$ cm

$n_b = 6$

$\Theta = 30$ degrees

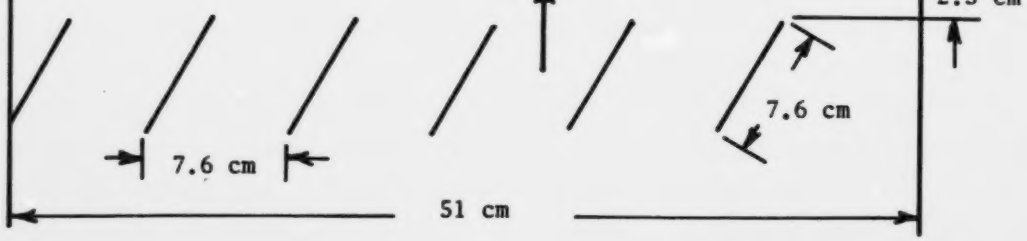

Figure 3. Top view diagram of example zigzag baffles.

We assume typical values for the air and drop properties:

$\rho_G = 1.2 \times 10^{-3}$ g/cm^3

$\rho_d = 1.05$ g/cm^3

$\mu_G = 1.8 \times 10^{-4}$ g/cm-s

The penetrations calculated from these equations for varying drop diameter and superficial gas velocity are shown graphically in Figures 4,5, & 6. The plots show fractional efficiency, which is one minus penetration. The first two show the effect of varying gas velocity and the third shows the efficiency as a function of drop diameter for each row of baffles at a set gas velocity. Coordinates for these plots are logarithm of drop diameter and the Weibull cumulative distribution function. Weibull coordinates have been used because efficiency plots as a straight line function of drop diameter in the low Reynolds number (Stokes flow) regime.

Overall penetration can be predicted by integrating equation (8) over the size distribution of drops. Size distributions, which will be discussed in Section 4, may take a number of forms. Typical size distributions are the log-normal and the cubic. Figure 7 presents the overall penetration based on numerical integration of equation (8) for two log-normal distributions (σ_g = 1.5 and 2.0) and the cubic distribution.

Reentrainment Prediction -

Drop collection in an E.S. is governed by the combination of the primary collection of drops and the reentrainment of collected liquid. The liquid and gas flow capacities of an entrainment separator are limited by the occurrence of reentrainment at high velocities. Experimental data on collection efficiency for various separators have been summarized by Calvert (1978), as follows.

Figure 8 shows collection efficiency vs. horizontal air velocity for vertical zigzag baffles. For horizontal gas flows, Figure 9 shows the superficial (empty cross-section) gas velocity in the separator as a function of the inlet liquid/gas ratio, with reentrainment rate as a prameter. The indicated zones are approximate, and above the shaded area some slight reentrainment was noted.

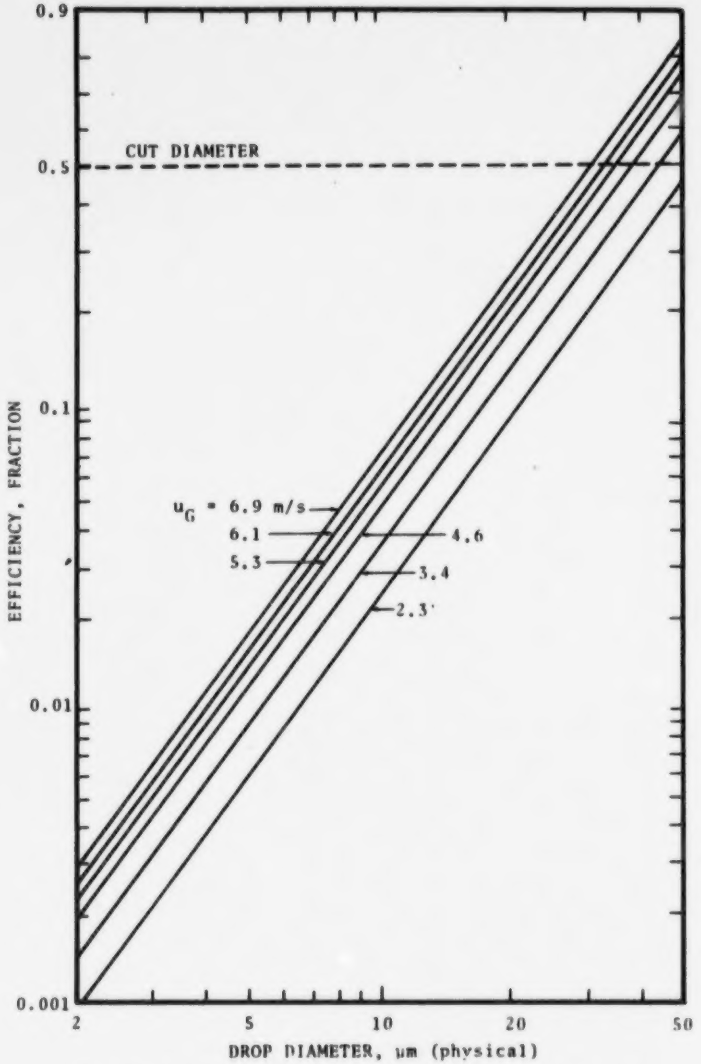

Figure 4. Predicted grade efficiency of 3 rows of zigzag baffles.

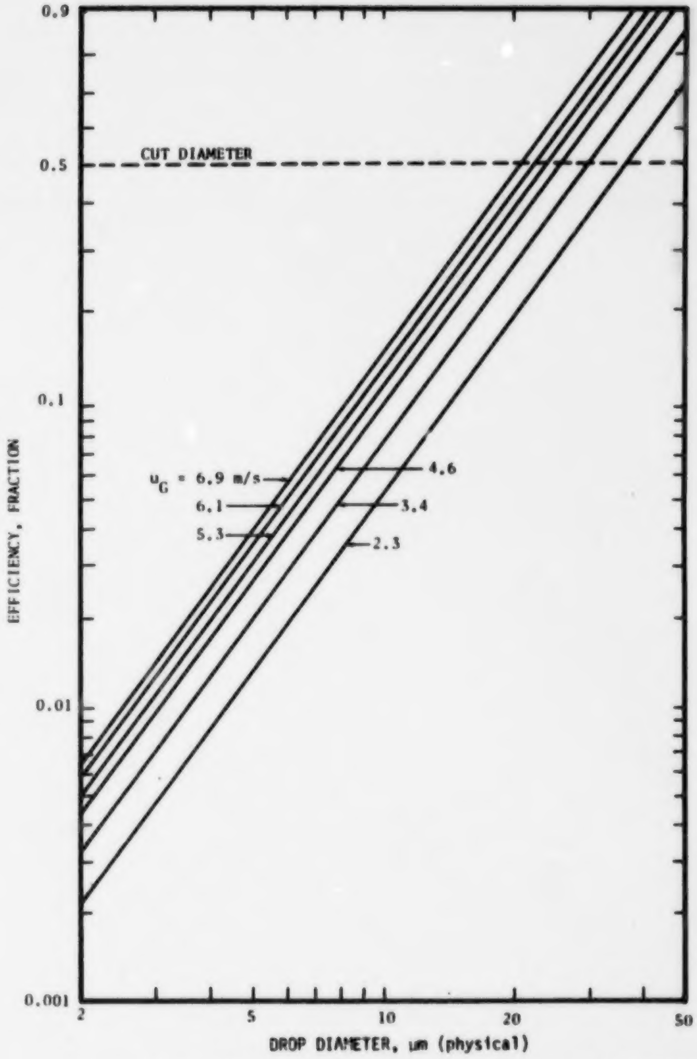

Figure 5. Predicted grade efficiency of 6 rows of baffles.

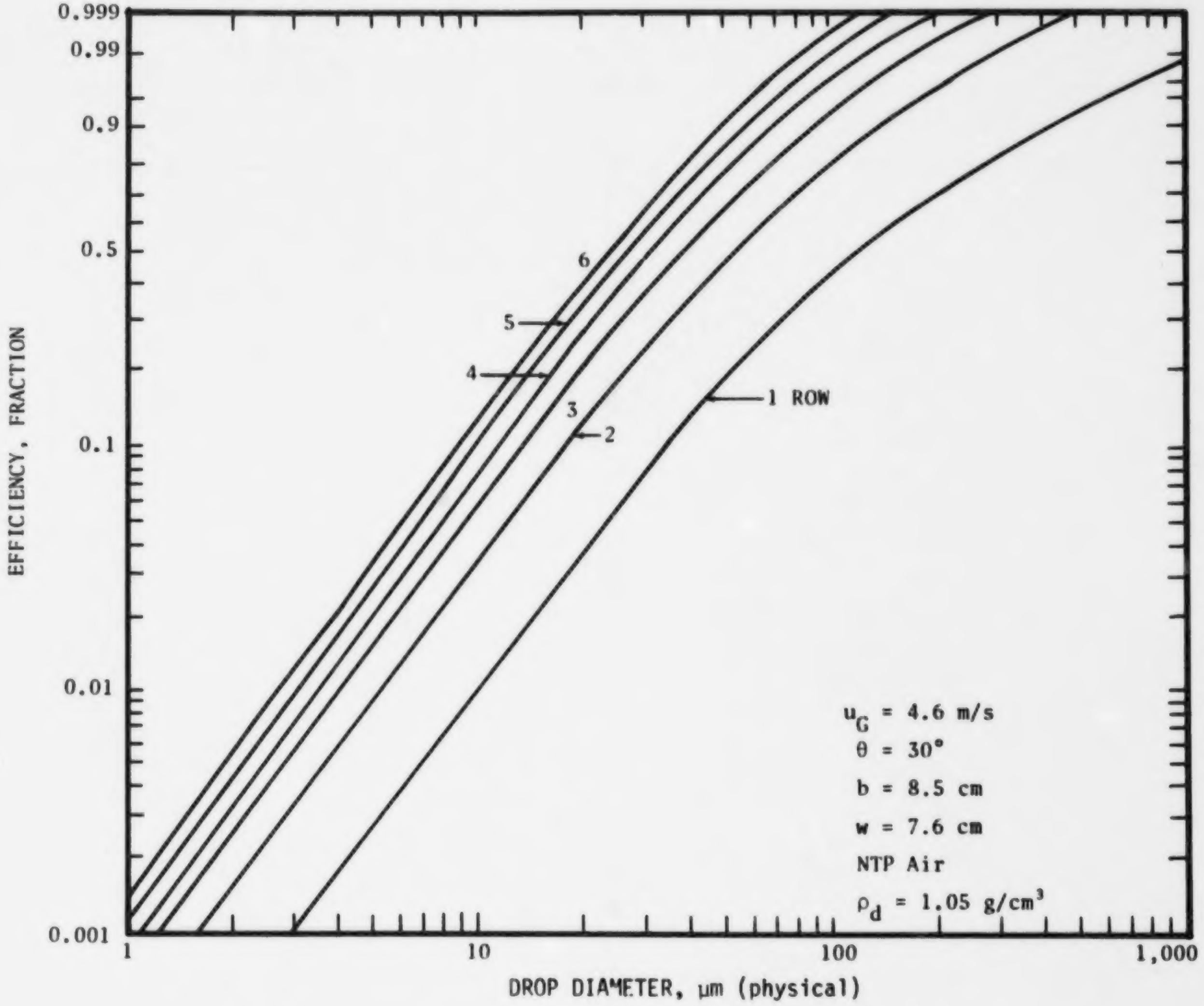

Figure 6. Predicted grade efficiency of zigzag baffles at 4.6 m/s superficial gas velocity.

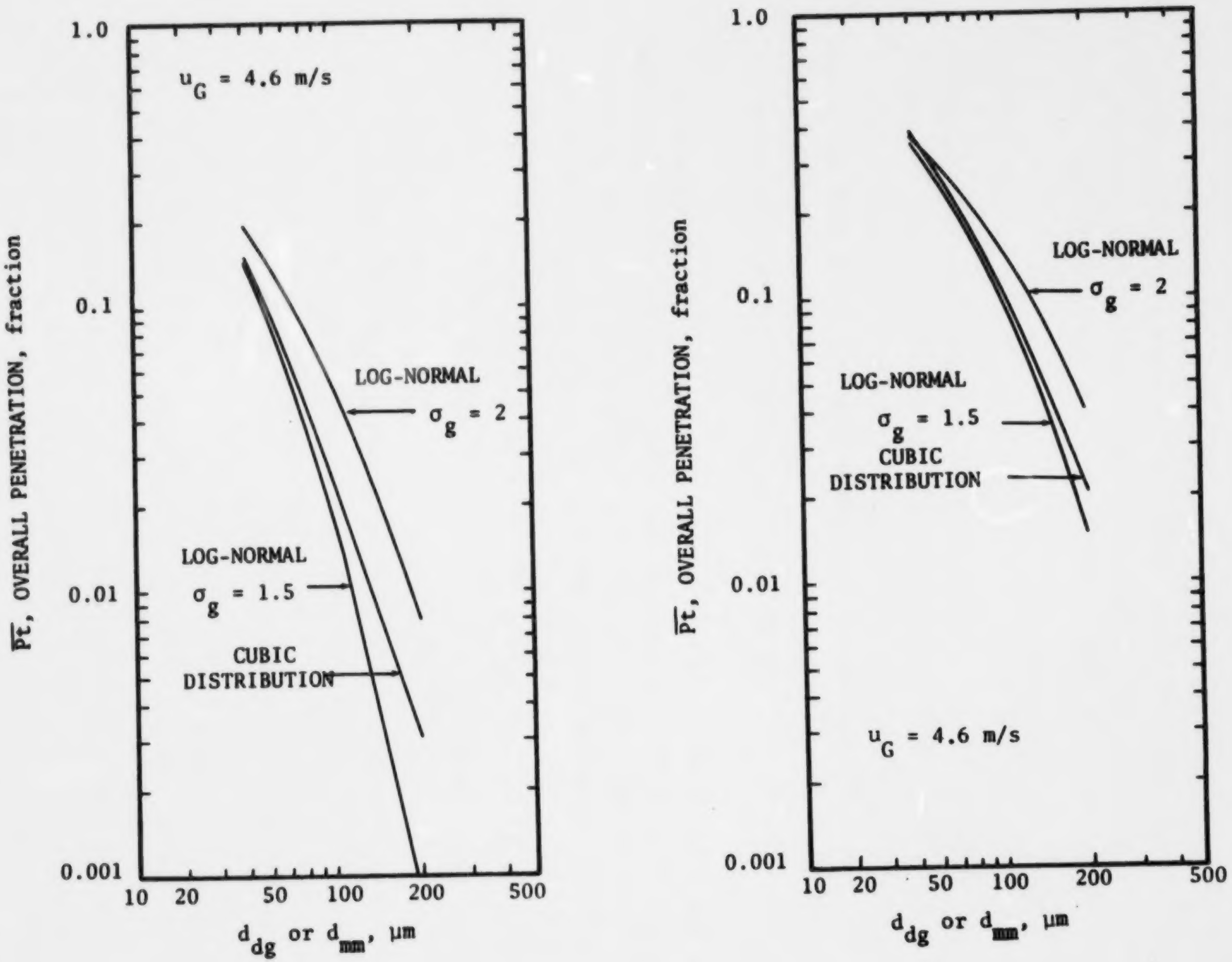

Figure 7. Predicted overall penetration for 6 rows of baffles.

From Figure 8 it appears that about 6 m/s is the limiting superficial gas velocity. This limit is somewhat dependent on entrainment loading and may be raised to about 8 m/s at low loadings, based on data shown in Figure 9. A conservative velocity, allowing for a relatively high entrainment loading, would be 4.6 m/s (15 ft/s), which was selected as the design velocity.

Pre-Separator -

It follows from the relationship between the reentrainment gas velocity and the liquid/gas ratio that higher gas capacity could be obtained if the liquid/gas ratio were reduced. This is the reason for using various means for removing some entrainment upstream from the final E.S. Relatively simple provisions for "pre-separation" can effect significant improvement in the E.S. capacity.

One should note, however, that the use of a pre-separator will not reduce the collection efficiency capability of the final E.S. For example, if a 15 μmA cut diameter is required in order to meet the emission limit, the use of a pre-separator with perhaps, a 50 to 100 μmA cut diameter will not alleviate that requirement.

Pressure Drop Prediction -

Calvert, et al. (1975) present an equation for predicting pressure drop based on the drag of inclined plates. For a velocity of 4.6 m/s the predicted pressure drop was about 1.1 cm W.C. for 6 rows of baffles. Their experimental measurement was slightly higher, about 1.5 cm W.C.

PILOT PLANT

The pilot plant was designed to be representative of an industrial scrubber/entrainment separator system in that it was large enough and of such configuration that its performance could be "scaled-up" reliably. The design gas flow rate was a minimum of 1.42 m^3/s (3,000 CFM) and could be 50% higher, depending on the system pressure drop. Windows and special access and

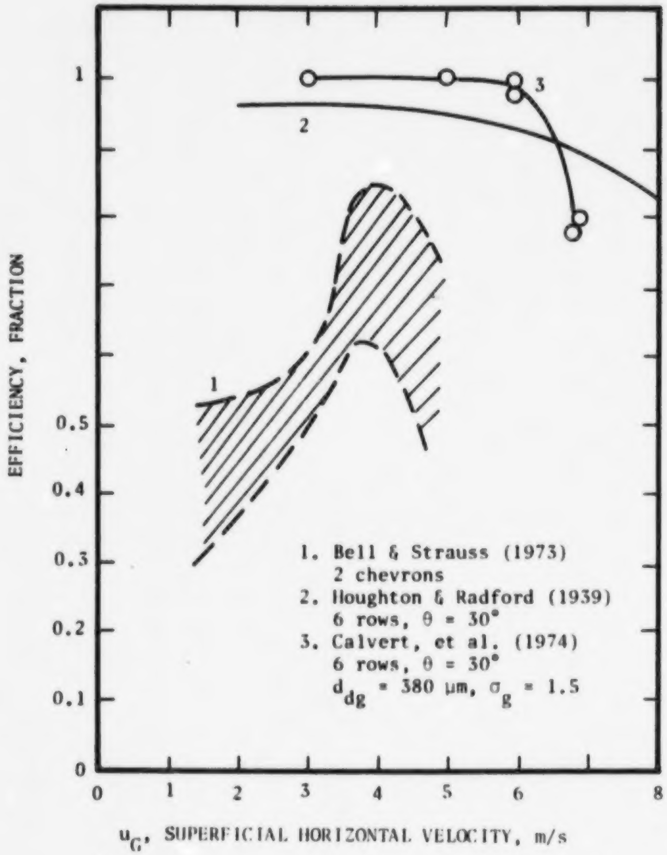

Figure 8. Measured overall collection efficiency of vertical zigzag baffles.

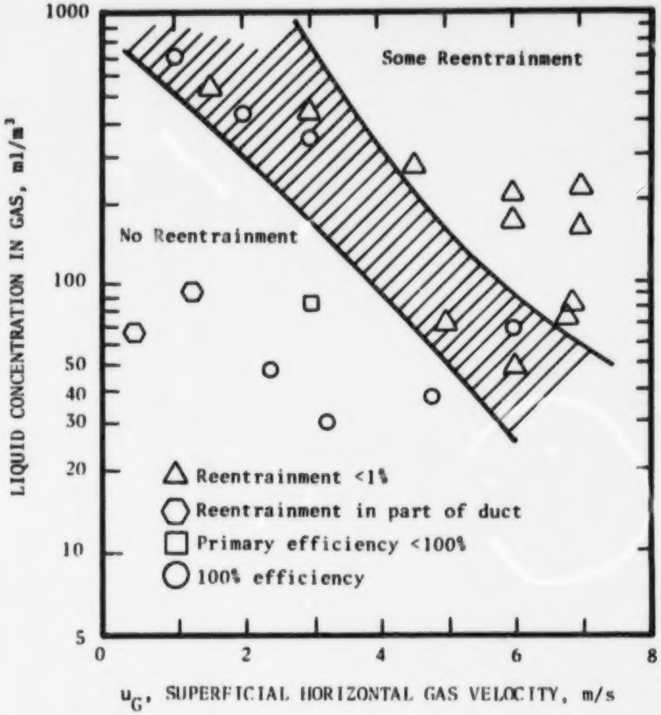

Figure 9. Reentrainment limits for 6 rows of vertical zigzag baffles. (Data by Calvert, et al., 1974).

sampling conveniences were included in the system. The system is shown schematically in Figure 10 and pictorially in Figure 11.

Location of the entrainment separator in a horizontal duct was an important design feature. Previous work reported by Calvert, et al. (1977) had demonstrated that a configuration with the gas flowing horizontal and the drainage surfaces in vertical planes was least subject to reentrainment. The E.S. designed for horizontal gas flow was therefore able to handle the highest entrainment loading and gas velocity for its size.

Pre-Separation -

The scrubber/entrainment separator system was designed with enough vertical height between the scrubber and the entrainment separator so that substantial disengagement of large drops could occur. The loading on the entrainment separator is consequently greatly decreased without using any energy.

Another pre-separator stage was easily incorporated in the form of the turning vanes in the elbow transition between the vertical scrubber and the horizontal entrainment separator duct. The turning vanes collected a considerable amount of the large size entrainment which would otherwise settle on the horizontal duct or overload the E.S.

Finally, the horizontal run between the turning vanes and the E.S. enabled additional entrainment to settle out of the gas stream before the E.S. As discussed previously, the purpose of designing the system was to minimize the loading on the E.S. and thereby increase the allowable gas velocity.

Scrubber/Entrainment Separator Shell

The scrubber and entrainment separator shells were made of molded fiberglass, 4.8 mm (0.19 in) thick. The vertical scrubber section stood in an open polypropylene tank, from which the scrubbing liquor was recirculated. The entrainment separator section was in a horizontal run, accessible from a platform which was 2.44 m (8 ft.) above the floor. The air was moved by a forced draft centrifugal blower. The system had

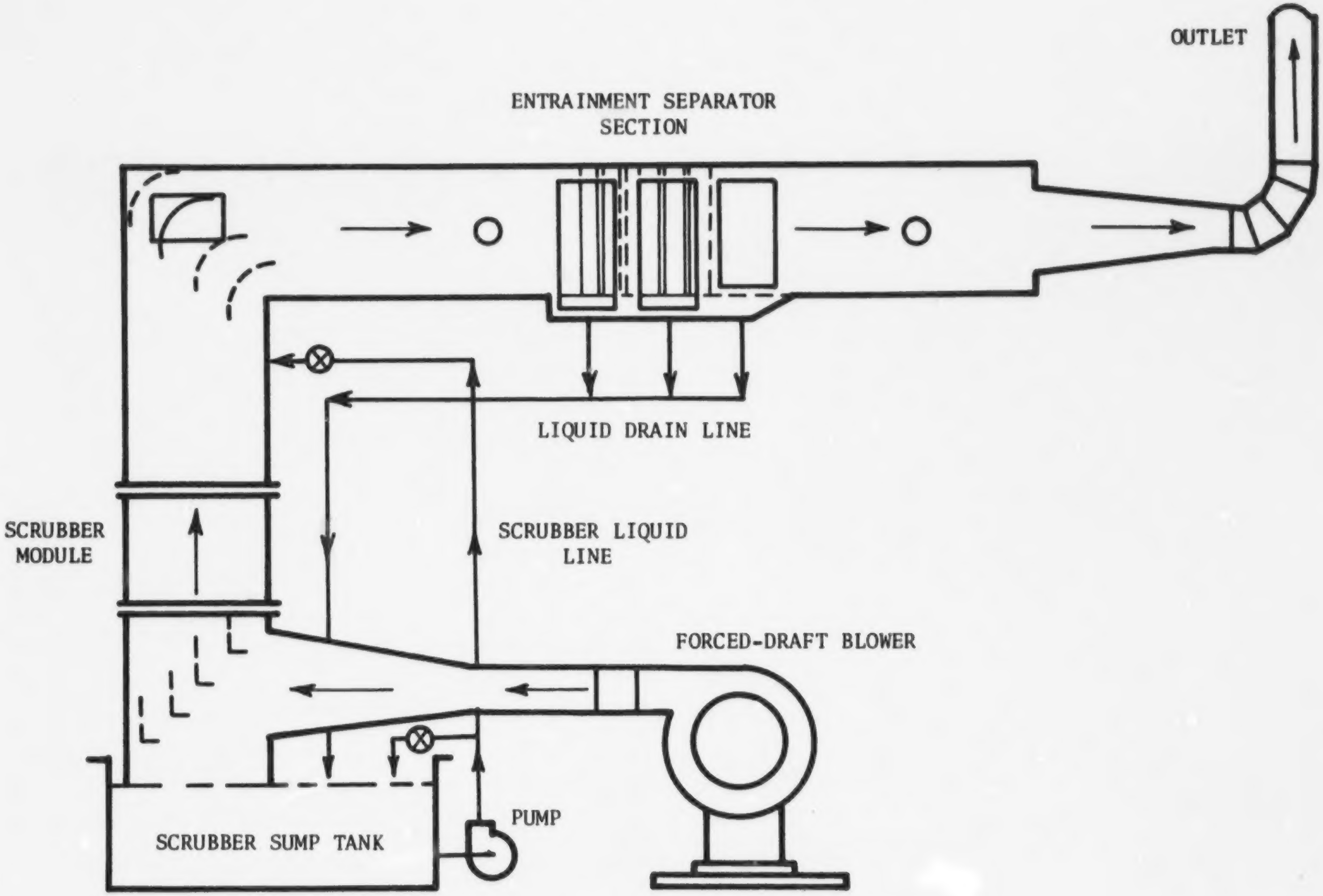
OUTLET
ENTRAINMENT SEPARATOR SECTION
LIQUID DRAIN LINE
SCRUBBER MODULE
SCRUBBER LIQUID LINE
FORCED-DRAFT BLOWER
PUMP
SCRUBBER SUMP TANK

Figure 10. Schematic diagram of scrubber/entrainment separator system.

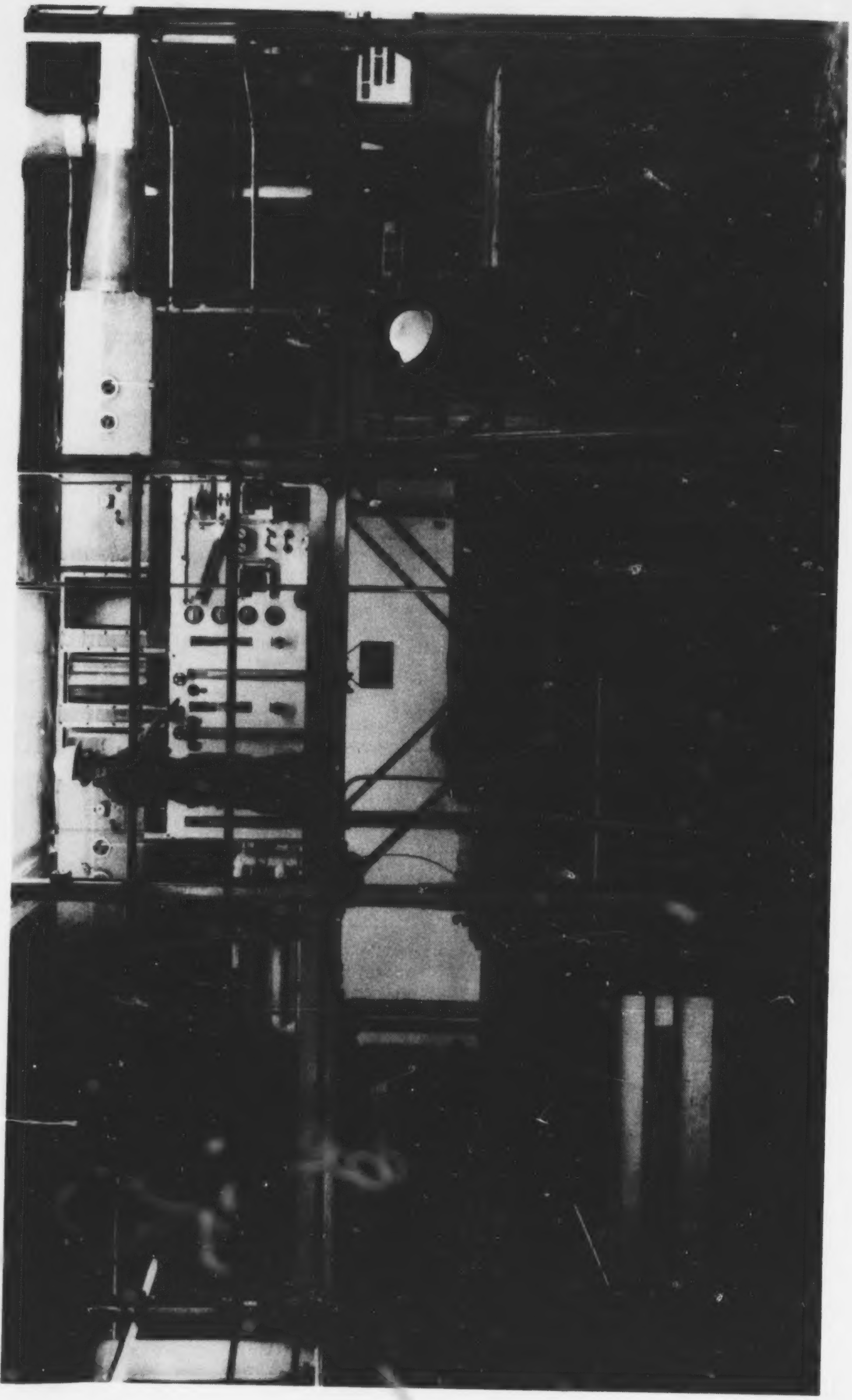

Figure 11. Scrubber/E.S. system.

numerous windows and sampling ports located at strategic points. Basic dimensions are shown in Figure 12.

The scrubber section was square, with a cross-sectional area of 0.581 m^2 (3.33 ft^2). It was 1 m high and flanged at both ends to allow easy removal. The scrubber section was 1.4 m below the horizontal section to allow room for disengagement of large drops generated in the scrubber.

The E.S. section was rectangular, 61 cm high by 51 cm wide (24 in x 20 in). There is a 0.13 m deep recess below the entrainment separator section to collect liquid drainage and to run internal piping. The floor was thin gauge stainless steel sheet with cross-wise slots to accommodate drainage from the E.S. baffles.

Entrainment Separator Design

The entrainment separator was a discontinuous zigzag baffle type, containing up to six rows in two configurations. One configuration was a vertical orientation and the other was a forward sloping orientation of 30° from the vertical. The baffles were made of type 304 stainless steel and constructed in row modules so that any number of rows from one to six could be used. A plan view of the baffles was shown in Figure 3. The lower front edge of the first row was located 2.35 m horizontally downstream from the transition section. Vertical height was 61 cm for all baffles.

Scrubber Operating Conditions

Three types of scrubbers were used to generate entrainment: mobile bed, sieve plate, and spray. A single stage mobile bed scrubber was operated in five modes as described in Table 2. The bed packing consisted of 3.8 cm (1.5 in) diameter hollow polypropylene spheres. A single sieve plate was operated at two conditions, as shown in Table 3 . Two types of spray nozzles were used in the spray scrubbers, as described in Table 4 to achieve different drop size distributions.

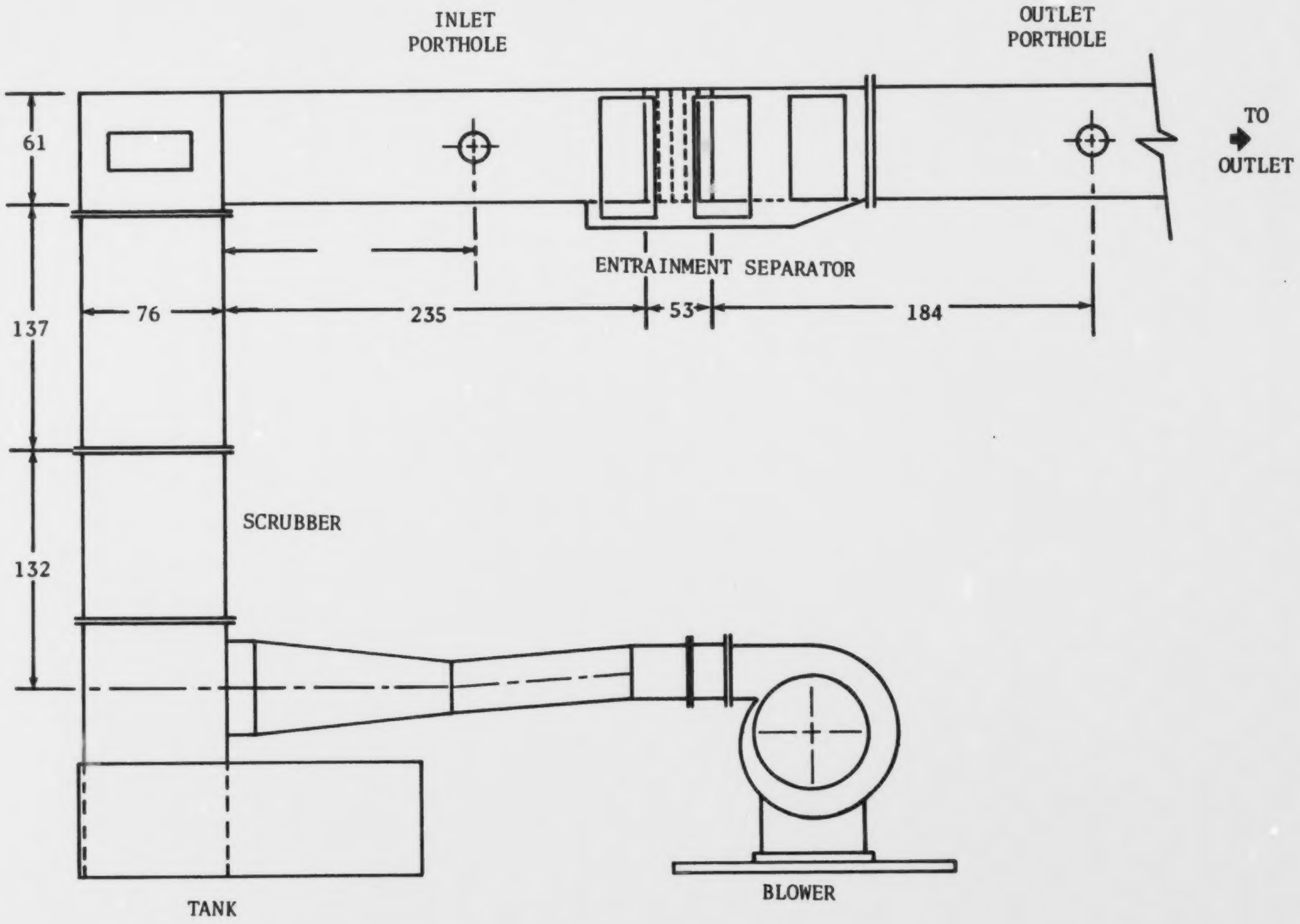
INLET PORTHOLE
OUTLET PORTHOLE
TO
OUTLET
61
137
132
76
235
53
184
ENTRAINMENT SEPARATOR
SCRUBBER
TANK
BLOWER

Figure 12. Scrubber/entrainment separator system (dimensions in cm).

TABLE 2. MOBILE BED SCRUBBER OPERATING CONDITIONS

Mode	Q_G		u_G	Q_L/Q_G	ΔP
	m^3/s	CFM	m/s	ℓ/m^3	cm W.C.
1	2.12	4,500	3.66	6.54	3.9
2	2.12	4,500	3.66	5.94	3.6
3	2.12	4,500	3.66	4.46	3.1
4	1.89	4,000	3.25	7.35	3.7
5	1.65	3,500	2.84	8.40	3.4

Bed static height - 20-23 cm; bed packing - polypropylene spheres 3.8 cm dia., each weighing ~4.7 g; bed support - 0.088 cm dia. galvanized wire screen openings ~1.3 cm x 2.5 cm; located 1.37 m below horizontal section.

TABLE 3. SINGLE SIEVE PLATE SCRUBBER OPERATING CONDITIONS

Stainless Steel - 0.16 cm thick (0.0625 inches)
Hole Diameter - 0.476 cm (3/16 inch)
Column Cross Section - 0.581 m^2 (6.25 ft^2)
Downcomer Cross Section - 0.021 m^2 (0.22 ft^2)
Plate Area Exposed to Flow - 0.386 m^2 (4.15 ft^2)
Open Area - 0.033 m^2 (0.36 ft^2)
Weir Height - 5.1 cm (2 inches)

Located 1.47 m below horizontal section

1. Low ΔP Operation

   Gas flow rate = 0.71 m^3/s (1,500 CFM)
   Water flow rate = 8-9.5 ℓ/s (125-150 GPM)
   Pressure drop ≈ 11 cm W.C.

2. High ΔP Operation

   Gas flow rate = 1.04 m^3/s (2,200 CFM)
   Water flow rate = 8-9.5 ℓ/s (125-150 GPM)
   Pressure drop ≈ 23 cm W.C.

TABLE 4. SPRAY SCRUBBER OPERATING CONDITIONS

Cocurrent operation, nozzles located 2.13 m below horizontal section

Scrubber cross-sectional area = 0.581 m^2 (6.25 ft)

Gas flow rate = 1.42 m^3/s (3,000 CFM)

Scrubber superficial gas velocity = 2.44 m/s

Nozzle type:	Spraying Systems Whirljet	Bete Spiral
Model no.:	1/2-B-50	3/4-ST-24-FCN
Pressure:	207 kPa (30 psig)	55 kPa (8 psig)
Flow rate:	5 nozzles - 2.68 ℓ/s	4 nozzles - 2.52 ℓ/s
	7 nozzles - 3.75 ℓ/s	6 nozzles - 3.79 ℓ/s
Drop sauter mean dia:	1,000 μm	500 μm

Drop Disengagement in Vertical Duct

In a vertical gas flow a drop with a terminal settling velocity greater than the gas velocity will not be emitted from the scrubber, provided enough disengagement space above the scrubber is provided. The terminal settling velocity of a drop or particle is the velocity at which the gravity and fluid drag forces balance. The disengagement space is needed to allow for the higher velocities given to some drops at the top surface of the sieve plate, mobile bed, or spray.

For an air-water drop system at 20°C and 1 atm, the terminal settling velocity of various diameter drops is given in Figure 13. One should note that in systems which are not saturated with water vapor (100% relative humidity) the drops will decrease in size due to evaporation.
Superficial gas velocities for the three scrubber types and the drop diameters corresponding to these terminal settling velocities are given below.

Scrubber	Gas Velocity, m/s	Settling Drop Diameter,μm
Mobile Bed	2.8 to 3.7	700 to 950
Sieve Plate	1.2 to 1.8	300 to 400
Spray	2.44	600

Particle Collection Efficiency of Turning Vanes

The turning vanes cause drop separation due to centrifugal deposition. The four vanes are quarter-sections of 15 cm radius duct arranged diagonally across the turn. The centrifugal deposition velocity is computed by balancing the centrifugal force acting on the drop and the drag.

$$u_D = \left(\frac{4}{3} \frac{\rho_d \; d_d \; u_G{}^2}{C_D \; \rho_G \; r_c} \right)^{\frac{1}{2}} \qquad (11)$$

The deposition area of the four vanes is

$$A_D = 2 \times \pi \times 0.15 \times 0.76 = 0.73 \text{ m}^2$$

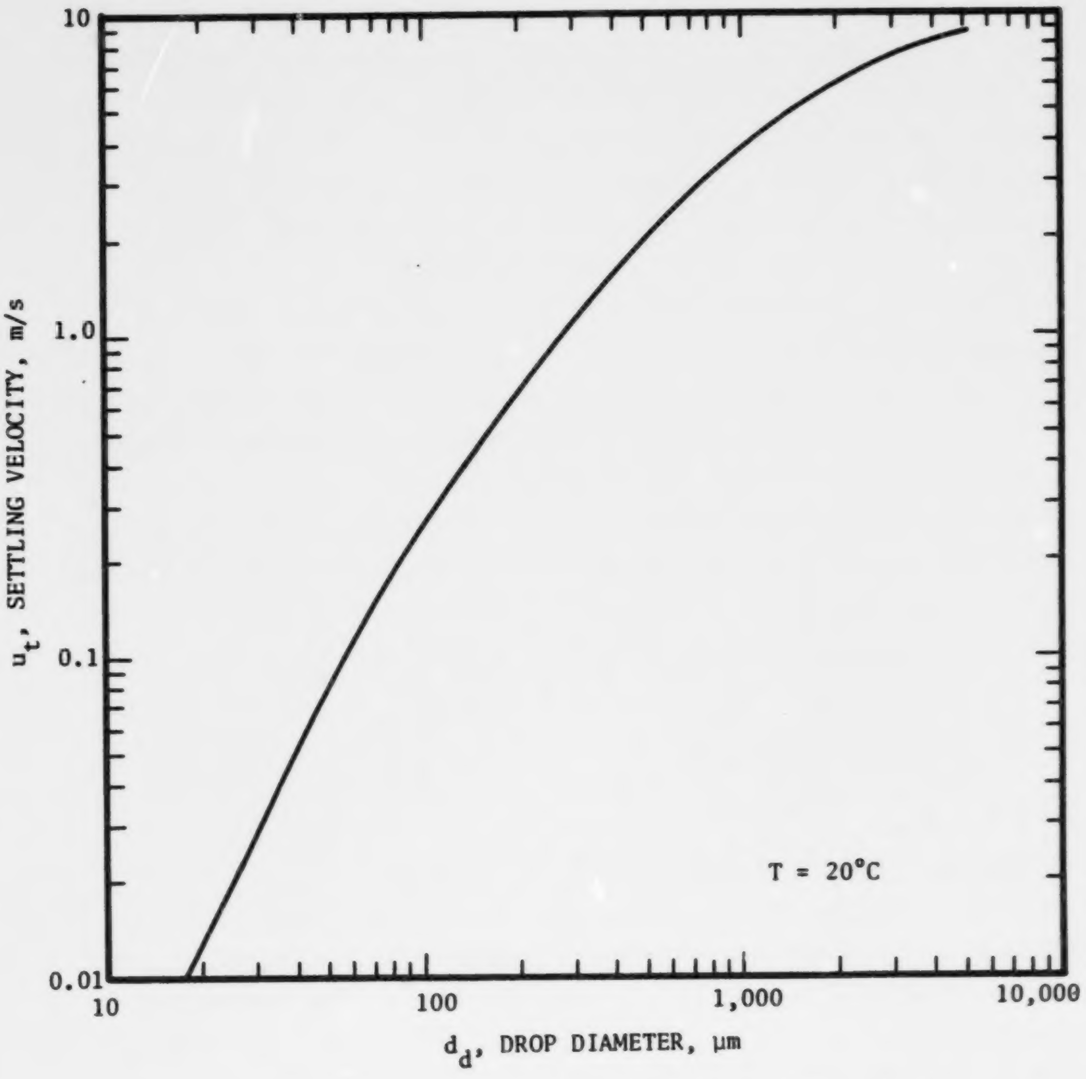

Figure 13. Gravity settling velocity of water drops in air, (Fuchs, 1964).

Penetration through the turning vanes can be analyzed like that through a horizontal duct by substituting centrifugal deposition velocity for gravity settling velocity. Figure 14 is a plot of the centrifugal deposition velocity vs. drop diameter for $u_G = 4.6$ m/s and $r_c = 0.15$ m. The penetration equations for the three drop Reynolds number regimes (described later) are:

$$Pt = 1 - \frac{u_D}{1.93} \qquad d_d > 100\ \mu m \qquad (12)$$

$$Pt = \exp\left[-\frac{u_D}{1.93}\right] \qquad d_d < 100\ \mu m \qquad (13)$$

$$u_D = 4.47 \times 10^{-4}\ d_d^2 \qquad d_d < 50\ \mu m \qquad (14)$$

Equation (12) predicts that no drops larger than 88 μm will penetrate the turning vanes, which makes it unnecessary for this analysis. The efficiency of the turning vanes is plotted in Figure 15 for $u_G = 4.6$ m/s. This figures shows that very few drops larger than 200 μm should penetrate the turning vanes.

Gravity Settling in the Horizontal Duct

The deposition due to gravity settling of water drops in a horizontal rectangular duct was analyzed. The assumed conditions and dimensions were:

$\nu_G = 0.15\ cm^2/s$ (kinematic viscosity)
$h = 0.61$ m (duct height)
$w = 0.508$ m (duct width)
$L = 2.35$ m (duct length)

The Reynolds number of the duct is then

$$N_{Re} = 3.69 \times 10^4\ u_G(m/s)$$

for $u_G = 4.6$ m/s

$$N_{Re} = 170{,}000$$

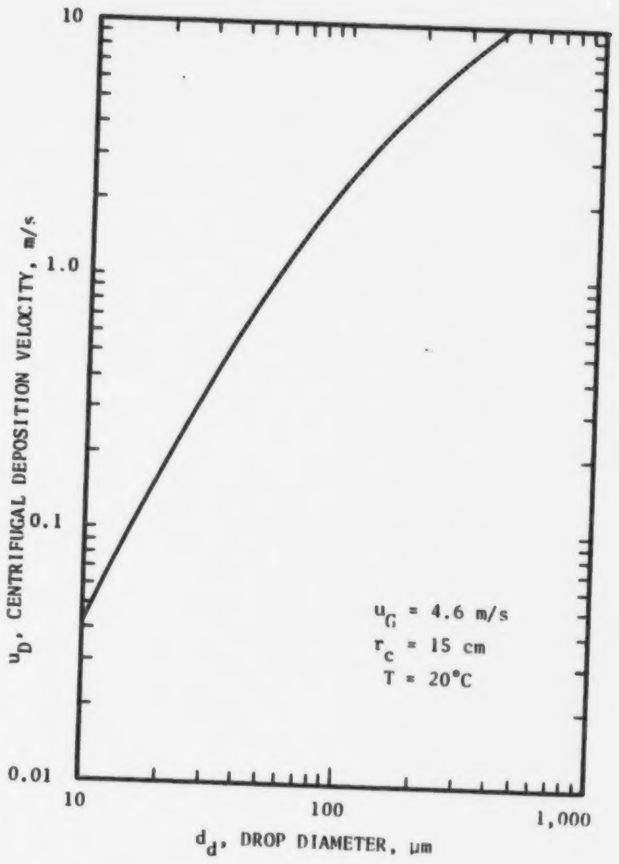

Figure 14. Theoretical centrifugal deposition velocity of water drops in air.

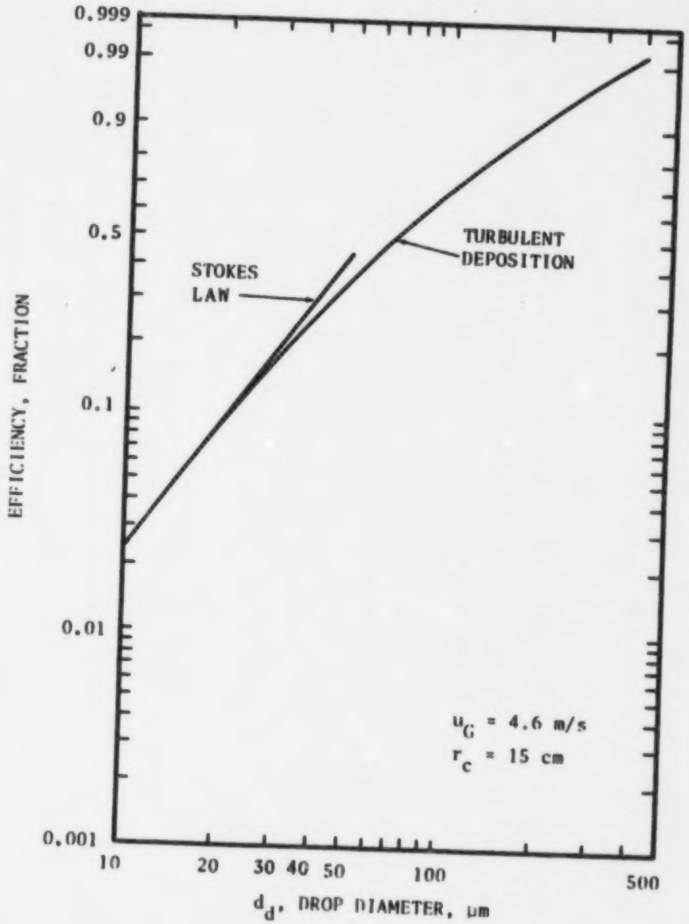

Figure 15. Theoretical grade efficiency of turning vanes.

The turbulent eddy velocity (also known as the friction velocity) is approximately,

$$u_{te} = u_G\sqrt{\frac{f}{8}} \qquad (15)$$

where u_G = mean gas velocity , 4.6 m/s
f = friction factor

At Re = 170,000, f = .016 for smooth pipes. Thus,

$$u_{te} \approx 0.21 \text{ m/s}$$

It is assumed that drops with terminal settling velocities, u_t, greater than u_{te} will not be affected by the turbulent eddies. Thus, for the present case drops larger than 100 μm diameter (see Figure 13) are not affected by the turbulence. Drops this size deposit as if in laminar flow.

Laminar Analysis for Drops Larger than 100 μm-

The penetration is

$$Pt = 1 - \frac{u_t A_D}{Q_G} = 1 - \frac{u_t\ L}{h\ u_G} \qquad (16)$$

which in our case reduces to

$$Pt = 1 - \frac{u_t\ L}{2.81} \qquad (17)$$

for 0% penetration, the minimum or critical length needed is

$$L_{cr} = \frac{2.81}{u_t} \qquad (18)$$

For 100 μm diameter drops, L_{cr} = 11 m.

For the laminar deposition region, at L = 2.35 m

$$Pt = 1 - \frac{u_t}{1.2} \qquad (19)$$

where u_t is found from Figure 13. A plot of predicted efficiency (1-Pt) for laminar settling of large drops is given in Figure 16.

Turbulent Analysis for Drops Smaller than 100 μm -

In turbulent flow the drops are uniformly mixed over the cross section of the duct, except near the walls. Since the vertical eddy velocity approaches zero at the bottom wall of the duct drops which enter this region will be deposited. The concentration of drops entering the wall region is proportional to the concentration in the free stream so the deposition is exponential:

$$Pt = \exp\left(\frac{-u_t\ A_D}{Q_G}\right) = \exp\left(\frac{-u_t\ w\ L}{w\ h\ u_G}\right) \tag{20}$$

$$Pt = \exp\left(\frac{-u_t\ L}{h\ u_G}\right) \tag{21}$$

For drops smaller than 50 μm the terminal settling velocity can be found assuming Stokes law (viscous) resistance.

$$d_d < 50\ \mu m:\quad u_t = \frac{(\rho_d - \rho_G)\ g d_d^2}{18\ \mu_G} \tag{22}$$

where $g = 980\ cm/s^2$

$\mu_G = 1.84 \times 10^{-4}$ g/cm-s

so $u_t = 3.10 \times 10^{-5}\ d_d^2$, m/s ($d_d$ in μm)

For $d_d < 50$ μm, u_t must be found from Figure 11. The penetration at L = 2.35 m, h = 0.61 m, and $u_G = 4.6$ m/s is

$$Pt = \exp\left(\frac{-u_t}{1.2}\right) \tag{23}$$

which is plotted on Figure 16, as efficiency, which is 1 - Pt.

Overall Penetration Through Duct

The overall penetration through the turning vanes and horizontal duct is the penetration integrated over the size distribution function:

$$\overline{Pt} = \int_{-\infty}^{\infty} Pt\ f(x)dx \qquad (24)$$

where for a log-normal inlet distribution,

$$x = \frac{\ell n(d_d/d_{dg})}{\ell n\ \sigma_g} \qquad (25)$$

$$f(x) = \frac{1}{\sqrt{2\pi}}\ \exp\ (-x^2/2) \qquad (26)$$

Pt = Pt (turn vanes) x Pt (horizontal duct)

Figure 17 is a plot of overall penetration for various values of geometric mass mean drop diameter for a standard deviation, σ_g = 2.0, using the grade penetrations from Figures 15 and 16. At higher gas velocities the turning vanes will be more efficient and the horizontal duct will be less efficient, so that Figure 17 is approximately correct over a moderate range of velocities about 4.6 m/s. It also shows that if the scrubber produces a log-normal distribution of drops (σ_g = 2) less than 1% by mass will reach the E.S. if their geometric mass mean diameter is over 550 μm.

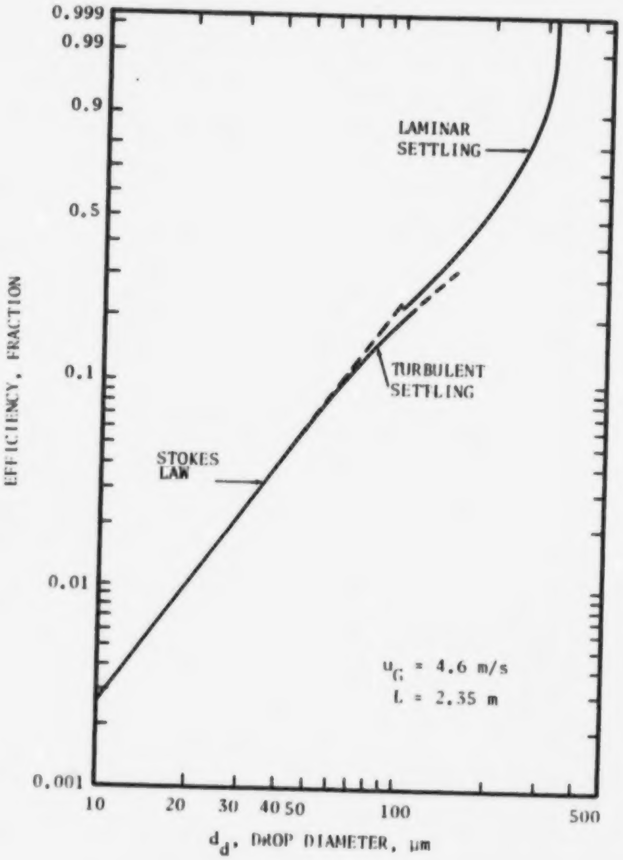

Figure 16. Theoretical grade efficiency of horizontal duct.

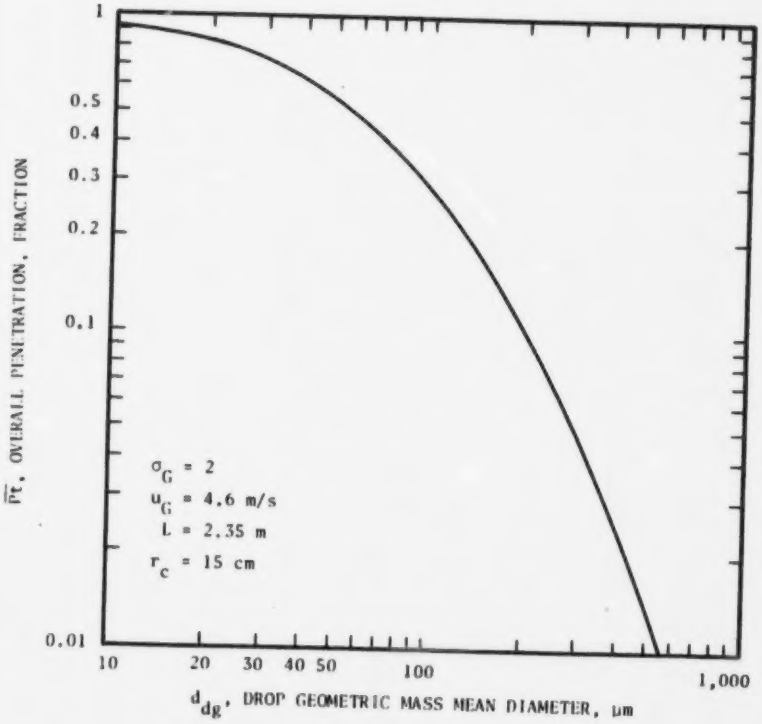

Figure 17. Theoretical overall penetration through turning vanes and horizontal duct of log-normally distributed drops.

SECTION 4

ENTRAINMENT CHARACTERIZATION

The measurement of the drop size distribution and concentration of the entrainment entering the entrainment separator (E.S.) was an important part of this study. Drop size and concentration had to be measured at the E.S. inlet and outlet in order to determine the total and grade efficiency of the E.S.

While the efficiency of the pre-separation stages could be estimated, the entrainment leaving the scrubber modules was not defined. Some data were available for the mobile bed (Calvert, et al., 1974) but substantially none for the other modules. Most of the drops ejected from the scrubbers are very large and subject to sedimentation, which is greatly dependent on gas flow patterns. Consequently, the nature of the entrainment is highly dependent on the configuration and operation of each individual scrubber and would be difficult to generalize.

The approach taken in this study was that the important thing to know about entrainment is its cumulative mass distribution in the size range which penetrates the pre-separator. Application of good engineering design will result in a system which keeps a massive concentration of large drops from reaching the E.S. The difficult problem is to design for a small cut diameter with reasonable pressure drop and freedom from plugging.

In this chapter the available methods and the methods selected for measuring entrained drop sizes are described. Then the data are presented and analyzed. The drop size distributions measured by several methods are discussed.

DROP SIZING TECHNIQUES

Range of Drop Sizes Expected

Most sizing techniques depend on the size of the drops to be measured. The most important range of drop sizes is the range where the E.S. efficiency is changing most rapidly; i.e., about the diameter collected with 50% efficiency. Based on Figures 4 and 5, presented in Section 3, the drop diameters expected to be collected with 50% efficiency range between 20 μm and 50 μm. Thus, the sizing techniques must be able to measure drops with diameters between about 5 μm and 100 μm in order to allow determination of efficiency as a function of drop diameter.

Review of Drop Sizing Methods

Methods for drop size analysis have been developed to meet the requirements of many applications in science, industry, and environmental monitoring. Spray and mist drop size characterization is required for various applications, such as spray nozzles, cooling tower drift eliminators, gas-atomized scrubbers, fuel injection, fog formation and dissipation, and scrubber and chemical process mist eliminators or entrainment separators(E.S.).

Several authors have recently reviewed the state-of-the-art of drop size analysis. Davies (1976), Carter (1970), and Roffman and Van Vleck (1974) present excellent discussions. Chan and Golay (1977) also survey measurement techniques in their report. Davies classified the methods into six categories:

1. Photographic Imaging
2. Collection and Deposition
3. Momentum Transfer
4. Hot-wire Anemometry
5. Electrical Mobility
6. Optical

Total or overall concentration of drops in the gas stream is usually determined by isokinetic sampling with a chemical or radioactive tracer in the liquid; e.g., the method used by Johnson and Statnick (1974).

Sizing Methods Chosen

Hot-wire anemometry and a collection and deposition method were initially selected for use, based on equipment availability and previous experience. A KLD Associates model DC-1 Droplet Counter was available and appeared suitable. As described by Medecki, et al. (1975) it consisted of a 5 μm diameter platinum hot-wire probe sensor and associated electronics to analyze the electrical pulses generated when drops attach to the hot wire. The unit has the following specifications:

Drop size range: 1 μm to 600 μm
Flow velocity: 3 m/s, maximum
Concentration: 500 drops/cm^3, maximum
Temperature: 0°C to 100°C

As discussed later, the KLD device was found not to be practical for this application and yielded no useful data.

The first collection and deposition method used in this research involved a specially designed cascade impactor. In the course of the program we developed a drop sizing method which utilized single body collectors (spheres, cylinders). These methods are discussed below.

Cascade Impactor

The A.P.T. designed cascade impactor (C.I.) consisted of a series of stages of a horizontal flow through single round jet impinging on a flat plate. The nozzle and plate were made of stainless steel and the housing glass, similar in shape to a test tube. Figure 18 is a photograph of the A.P.T. drop sizing C.I. The ratio of jet diameter to jet-to-plate distance was such that the impaction parameter corresponding to 50% collection efficiency, K_{p50} , was approximately 0.2. For the stages with particle cut diameters about 2 μm and smaller, this value was verified by calibration with monodisperse

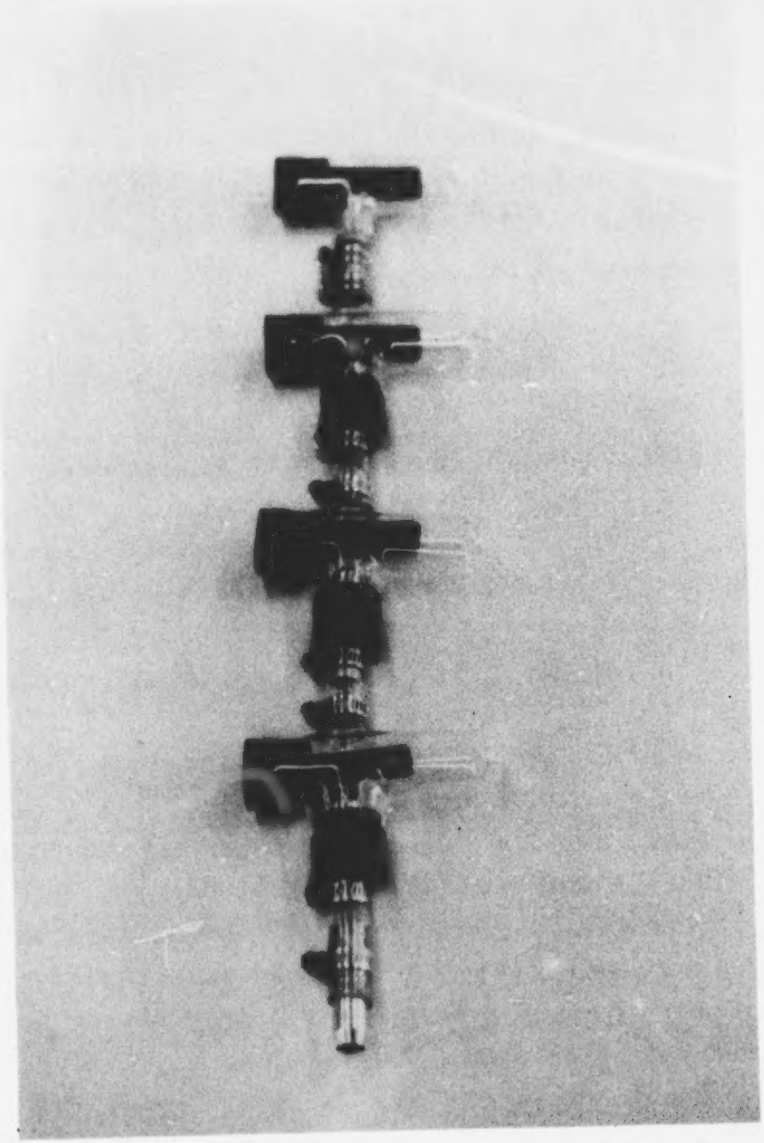

Figure 18. Photograph of glass cascade impactor.

polystyrene latex spheres.

The C.I. was located in the gas stream and isokinetic sampling was used. A glass fiber filter was used after the final impaction stage. While measurable amounts of water were often collected in the first stage, the use of a reasonable sampling time did not cause accumulation of enough water in the other stages.

As in previous studies, we used a salt tracer in the liquid. Sodium chloride was dissolved in the scrubbing water, and the NaCl collected on each C.I. stage and on the final filter was detected using a chloride specific ion electrode method. The measured amount of NaCl was then related to the volume of water drops on each stage since the NaCl concentration in the scrubber was also measured. In addition to its tracer function, the salt reduced the water vapor pressure of the drops to inhibit evaporation and size change before deposition in the C.I.

Single Body Collectors

An impactor for sizing drops larger than 20 μm diameter would be very difficult to design and use. For one thing, it would be so large that it would interfere with the performance of the entrainment separator. As an alternative a system using collection by inertial impaction on single bodies was developed. Spheres and cylinders of different diameters were placed in the entrainment stream. Drops which impacted on the bodies would flow down the wet surface and into a collection flask by way of a thin supporting rod.

Collection efficiency correlations from the literature were used to relate the integrated efficiency of collection to the drop size distribution. The total drop concentration in the stream was measured by the cascade impactor.

While we used both spheres and cylinders, most of the data were taken with spheres. The spheres seemed to provide slightly more reproducible results than the cyliners.

ENTRAINMENT DATA

The measured entrainment loadings from the three types of scrubbers used are compiled in Tables A-1 to A-3 in Appendix "A". The scrubber operating conditions were given in Tables 2-4 and the superficial gas velocities in the entrainment separator (E.S.) are presented in Table 5.

No measurements taken with the KLD Drop Counter are shown because operational difficulties rendered the data useless. The 5 μm probe wires were apparently too fragile for this application. Also, the velocity range was exceeded in all but two scrubber configurations. The data will be discussed in detail in the following paragraphs.

E.S. Drainage Data

The first column of data, after the run number in Tables A1-A3, presents the measured water drop concentrations (ml/DNm^3) based on collection by the E.S. These measurements are based on the water flow rate in the two downstream E.S. drain lines during steady-state operation. (See Figure 10). The upstream drain line, separated from the other drains by a dam, carried away water which settled in the horizontal duct and was forced to flow (creep) along the floor by the drag of the air flow. All the drain lines were sealed so that no gas could flow through them.

The concentrations based on E.S. drawings given in Tables A-1 through A-3 must be considered approximate because they were based on the assumption that the E.S. was 100% efficient. Creep of liquid into the E.S. along the duct walls could not be prevented. The data shown in parentheses qualitatively show the effect of the creeping liquid since no E.S. baffles were in the duct during these runs. Some settling of drops in this 53 cm long space during these empty-duct runs may occur. Thus, concentrations based on the E.S. drainage are higher than they should be.

TABLE 5. SUPERFICIAL VELOCITY IN ENTRAINMENT SEPARATOR

Scrubber Configuration	E.S. Superficial Velocity u_G, m/s
Mobile Bed	
Mode 1	6.9
Mode 2	6.9
Mode 3	6.9
Mode 4	6.1
Mode 5	5.3
Sieve Plate	
Low ΔP	2.3
High ΔP	3.4
Spray	4.6

Sphere Drainage Data

Data are presented in Tables A1 - A3 for drop collection by spheres of two diameters, 7.6 cm and 3.8 cm. The spheres were solid hardwood whose porous surface caused the liquid to spread in sheets rather than rivulets. The spheres were held in the gas stream on a thin wood rod which was held centered inside a length of stainless steel tubing which was connected to a flask. The A.P.T. body collector drop sizing system is shown schematically in Figure 19.

The drops impacting on the spheres formed a sheet which flowed by gravity down the wood supporting rod (which was exposed to the gas stream for less than 0.5 cm) into the tube and then into a flask. The collection system was sealed to prevent gas flow into the drain tube. The rate of liquid flow into the collection flasks was measured after the spheres had become thoroughly wetted.

Drop concentrations were calculated by dividing the liquid flow rate from the sphere by the gas velocity and the sphere cross-sectional area. These concentrations were generally higher than those based on C.I. sampling through a sampling nozzle. The reason is not known, as discussed below.

The relatively large horizontal surface of the spheres offers a possibility for collecting large drops which settle from the gas or drip from the ceiling of the duct. However, computation of the probable drop sedimentation rate based on the drop size measurements indicated that only a small increase in concentration could be accounted for. Sedimentation might increase the measured concentration by 0.1 ml/DNm^3 out of a total on the order of 2.0 ml/DNm^3.

It is possible that the C.I. might "under-sample" large drops by some mechanism such as interception by the nozzle inlet, followed by shattering and/or deflection from the inlet.

Concentration from C.I. Measurements

The concentrations shown for the C.I. method are based on

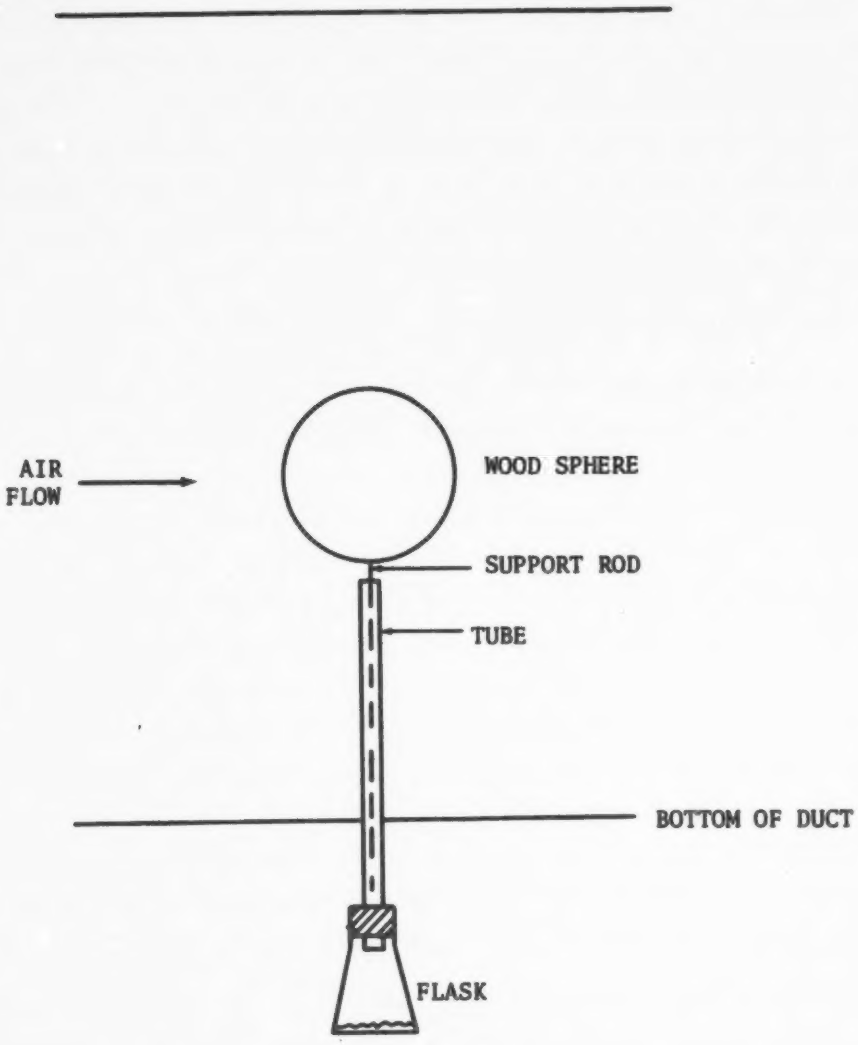
AIR
FLOW
WOOD SPHERE
SUPPORT ROD
TUBE
BOTTOM OF DUCT
FLASK

Figure 19. Body collector drop sizing system.

on analysis of the amount of tracer NaCl collected in the nozzle, cascade impactor (C.I.) and final filter. The sampling nozzle was located 6.5 cm above the center of the duct, about 45 cm upstream of the E.S. (see Figure 12). All the stages of the C.I. were inside the duct.

Because the sampling is done upstream of the E.S. the size distribution and total loading that the E.S. encounters may be slightly different than that measured by the C.I. The location of the sampling nozzle was chosen so that it would sample drops which would enter the center of the E.S. Measured concentrations of drops 20 μm diameter and smaller will not be affected significantly by the sampling location.

AUXILIARY SIZING TECHNIQUES

In addition to making direct measurements one can estimate the maximum drop sizes to reach the entrainment separator. In the vertical section of the scrubber one can estimate that all drops with a settling velocity greater than the upward gas velocity will not reach the E.S. Settling in the rectangular horizontal duct upstream of the E.S. is also predictable.

Centrifugal deposition on the turning vanes in the transition elbow between the vertical tower and the horizontal duct can be predicted with good accuracy because the geometry is simple. When the spray scrubber is operating, the drop size distribution in the scrubber can be estimated by extrapolation of published data. The maximum drop size reaching the E.S. inlet would be approximately the diameter corresponding to the overall mass fraction of the spray at the E.S. inlet.

ENTRAINMENT DROP SIZE DISTRIBUTIONS

As discussed previously, it is important to know the drop size distribution in the crucial range where collection efficiency changes the most with drop size. Several techniques were used to measure drop size over different size intervals within this range. It is necessary to reconcile all of these discontinuous measurements to give a continuous distribution of drop sizes.

The sizes larger than 20 μm were computed from data on drop collection on spheres and collection in the entrainment separator. Comparisons were also made with the nozzle manufacturer's drop size data, theoretical fallout due to gravity in sections between the spray scrubber and the entrainment separator, and theoretical collection by the turning vanes.

Types of Size Distributions

In order to describe the size distribution of drops with a few parameters it is necessary to relate the data to mathematical distribution functions. For liquid atomization processes the log-normal and cubic functions seemed suited to describe the size distribution.

Log-Normal Distribution

The cumulative mass distribution for a log-normal distribution of drop diameters is

$$F_{LN}(\ln d_d) = \int_{-\infty}^{\ln d_d} f_{LN}(\ln d_d)\, d\,(\ln d_d) \qquad (27)$$

where d_d = drop diameter, μm
F_{LN} = log-normal cumulative distribution, fraction

and

$$f_{LN}(\ln d_d) = \frac{1}{\sqrt{2\pi}\,\ln \sigma_g} \exp\left[\frac{-\left(\ln d_d - \ln d_{dg}\right)^2}{2 \ln^2 \sigma_g}\right] \qquad (28)$$

= log-normal density function

where d_{dg} = geometric mass mean diameter, μm
σ_g = geometric standard deviation

These last two parameters fully describe the log-normal distribution.

Cubic Distribution

Plots of the drop size distributions published by spray nozzle manufacturers often fit a cubic distribution:

$$F_{cub} = \left(\frac{d_d}{d_{max}}\right)^3 \qquad (29)$$

where F_{cub} = cubic cumulative distribution, fraction
d_{max} = maximum drop diameter, μm

The cubic density function is,

$$f_{cub} = \frac{3}{d^3_{max}} \quad d_d^{\,2} \qquad (30)$$

The mass median diameter or diameter at which $F_{cub} = 0.5$ is,

$$d_{mm} = 0.794 \quad d_{max} \qquad (31)$$

Thus, only one parameter, either "d_{mm}" or d_{max}" fully describes the cubic size distribution. The "spread" of the distribution has been fixed by the cubic exponent.

Cascade Impactor Data

Data for the concentration of drops on each stage have already been presented. The use of these measurements and the stage cut diameters yields a limited size distribution. Since the maximum stage cut diameter was 20 μmA, only the lower end of the size distribution can be determined. The averaged data are summarized in Table 6. The total size distribution requires correlation with data from the sphere collectors and other means.

TABLE 6. AVERAGE SIZE DISTRIBUTIONS BASED ON CASCADE IMPACTOR DATA AT E.S. INLET

Scrubber Type	Total Loading ml/DNm^3	Cumulative Mass Fraction of drops smaller than indicated diameter (μmA)		
Mobile Bed		8	5	1.5
Mode 1	2.44	0.008	0.007	0.005
Mode 2	1.54	0.026	0.023	0.008
Mode 3	1.26	0.016	0.014	0.008
Mode 4	1.19	0.013	0.014	0.010
Mode 5	0.85	0.080	--	0.041
Sieve Plate		20	8	1.5
Low ΔP	0.086	0.36	0.29	0.21
High ΔP	0.14	0.17	0.14	0.10
Spray		17	8	1.5
5-B50	9.15	0.005	0.003	0.002
7-B50	7.32	0.007	0.006	0.002
4-ST24	3.22	0.011	0.009	0.006
6-ST24	3.76	0.009	0.007	0.005

Size from E.S. Penetration

The efficiency characteristics of the entrainment separator itself can be used to compute the inlet drop size distribution. The overall penetrations through 3 and 6 rows were determined by the cascade impactor/sampling train upstream and downstream of the E.S. Table 7 presents the data.

For zigzag baffles, penetration as a function of drop diameter for drops less than 100 μm can be expressed as:

$$Pt = \exp\left[-\ln 2 \left(\frac{d_d}{d_{d50}}\right)^2\right] \qquad (32)$$

where d_{d50} is the drop diameter collected with 50% efficiency.

The overall penetration is the penetration integrated over the drop size distribution. The two types of size distributions were used to match with the penetration data. The log-normal distribution requires numerical integration, which Calvert, et al. (1972) performed and presented in their Figure 5.3.1-4. The cubic distribution has a mathematical solution:

$$\overline{Pt} = \frac{1.5}{d_{mm}^3}\left\{\frac{d_{d50}^3}{1.3}\,\mathrm{erf}\left(1.05\,\frac{d_{mm}}{d_{50}}\right) - \frac{d_{mm}\,d_{d50}^2}{1.1}\exp\left[-1.1\left(\frac{d_{mm}}{d_{d50}}\right)^2\right]\right\} \qquad (33)$$

where "erf" is the error function. This equation is plotted on Figure 20.

Results

The derived size distribution based on penetration through the E.S. are presented in Table 8. These derived size distributions and the data from the cascade impactor sampling are plotted on Figures 21 through 31. These figures also show the results of the sphere collector data which will be discussed next. In general these figures show a more uniform drop diameter for the larger sizes

TABLE 7. MEASURED OVERALL PENETRATION THROUGH E.S.

Scrubber Configuration	Pt, Overall Penetration (fraction)	
	3 Rows	6 Rows
Mobile Bed, Mode 1	0.0082	0.0082
2		0.0084
3		0.013
4	0.015	0.025
5		0.055
Sieve Plate, Low ΔP	0.31	0.26
High ΔP	0.14	0.20
Spray - 5 B-50	0.029	0.0049
7 B-50	0.014	0.089
4 ST-24	0.014	0.013
6 ST-24	0.030	0.011

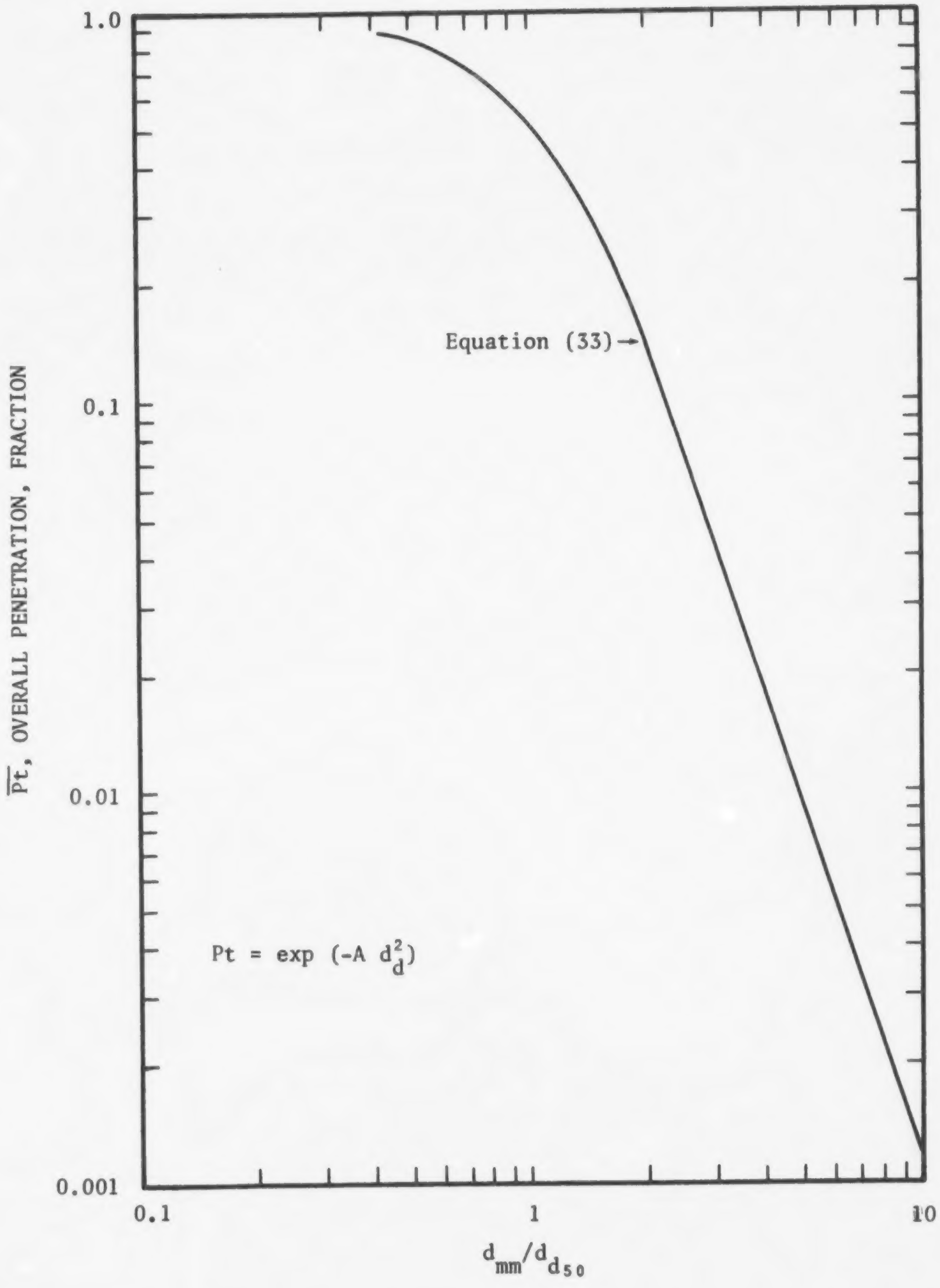

Figure 20. Theoretical overall penetration through zigzag baffles of drops with cubic distribution.

TABLE 8. SIZE DISTRIBUTIONS DERIVED FROM E.S. PENETRATION DATA

Scrubber Configuration	d_{d50}, μm* 3 Row	d_{d50}, μm* 6 Rows	Log-Normal Dist. d_{dg}, μm	σ_g**	Cubic Dist. d_{mm}
Mobile Bed 1	31	21	110	1.5	135
2	31	21	90	1.5	110
3	31	21	80	1.5	95
4	33	21	95	1.5	110
5	35	24	65	1.5	65
Sieve Plant - High ΔP	44	30	50	1.5	55
Low ΔP	54	37	85	1.5	85
Spray 5	38	26	120	1.5***	145
7	38	26	125	1.5	150
4	38	26	120	1.5	140
6	38	26	175	2.0***	125

* See Figures 4 and 5

** Assumed

*** Actual best fit values

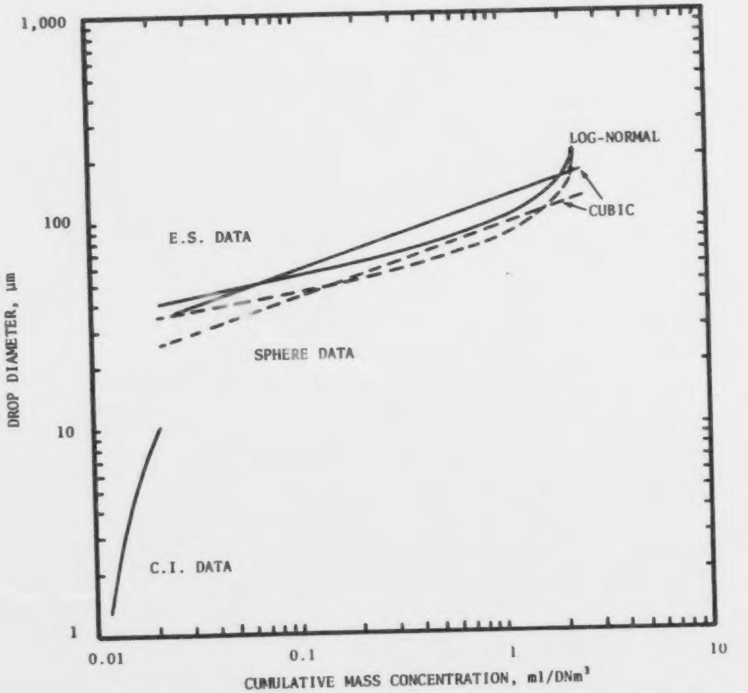

Figure 21. Measured entrainment concentration vs. drop diameter at the E.S. inlet for the mobile bed (mode 1) scrubber.

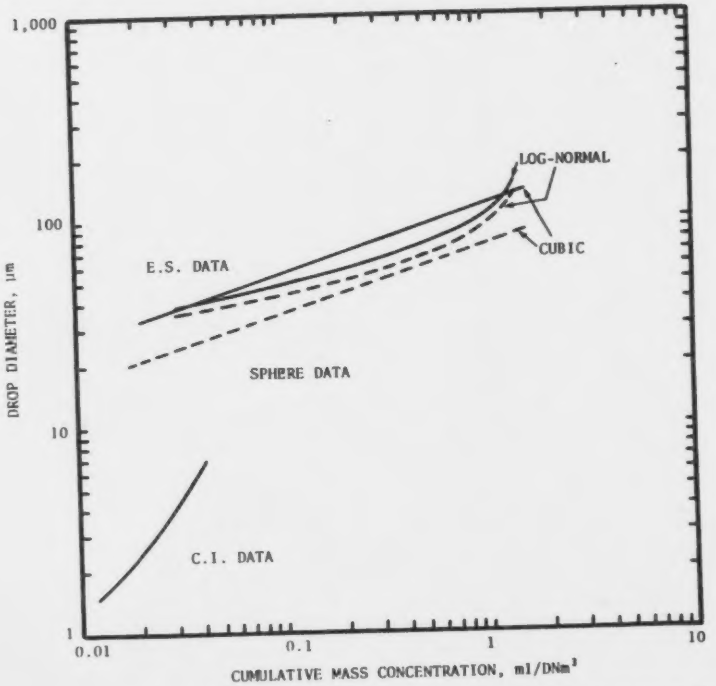

Figure 22. Measured entrainment concentration vs. drop diameter at the E.S. inlet for the mobile bed (mode 2) scrubber.

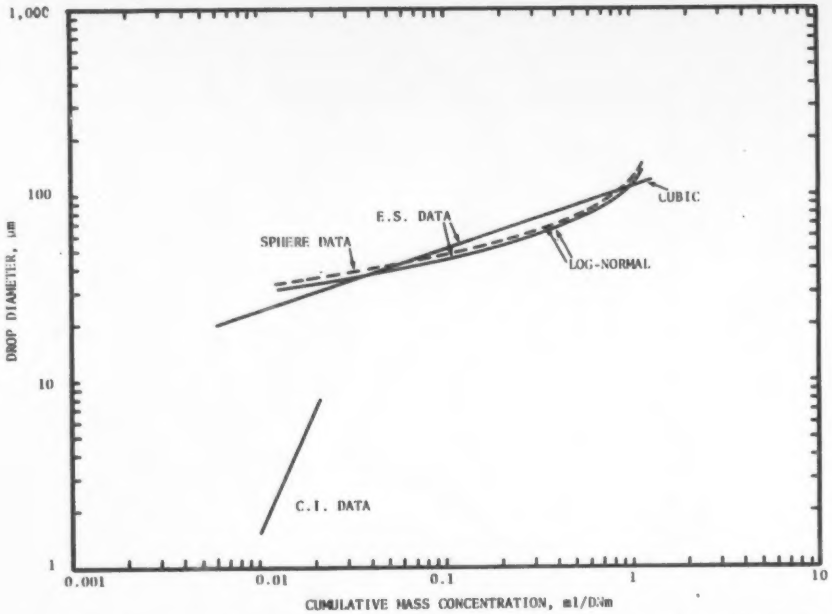

Figure 23. Measured entrainment concentration vs. drop diameter at the E.S. inlet for the mobile bed (mode 3) scrubber.

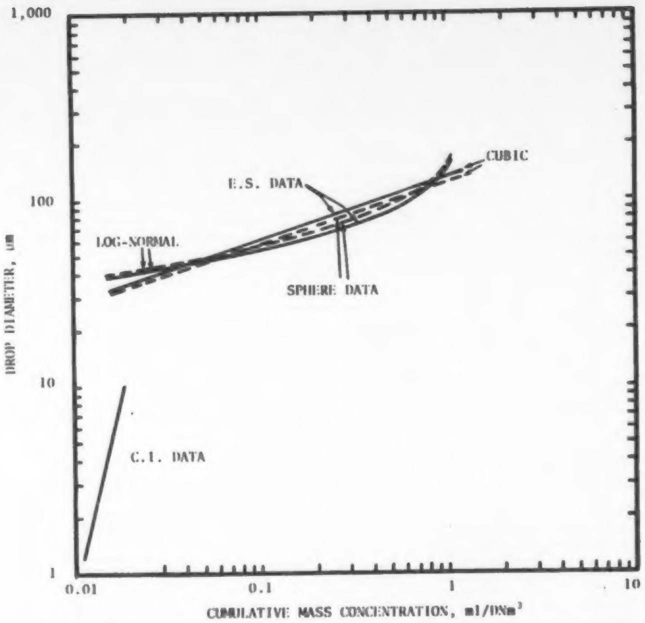

Figure 24. Measured entrainment concentration vs. drop diameter at the E.S. inlet for the mobile bed (mode 4) scrubber.

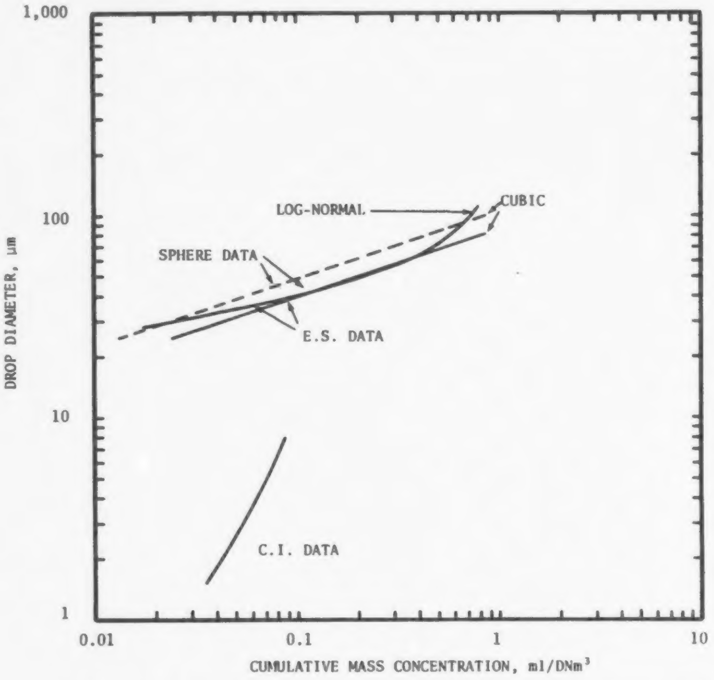

Figure 25. Measured entrainment concentration vs. drop diameter at the E.S. inlet for the mobile bed (mode 5) scrubber.

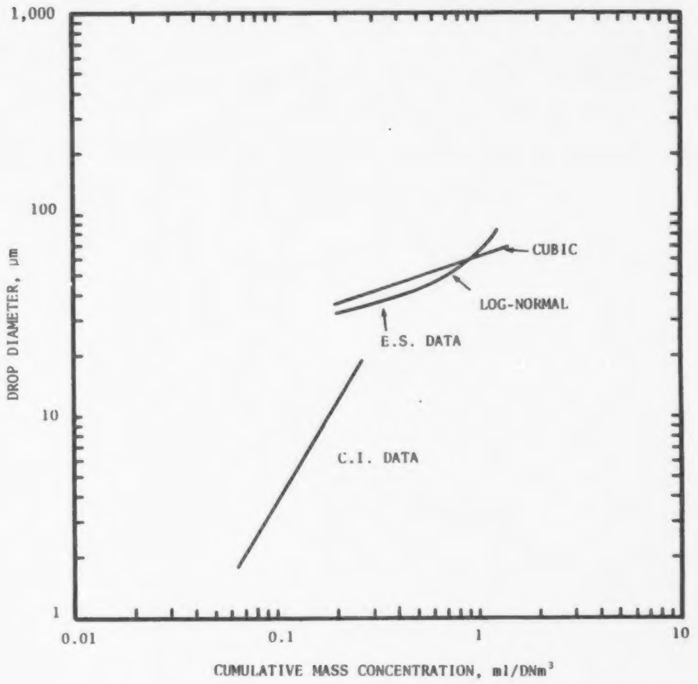

Figure 26. Measured entrainment concentration vs. drop diameter at the E.S. inlet for the sieve high scrubber.

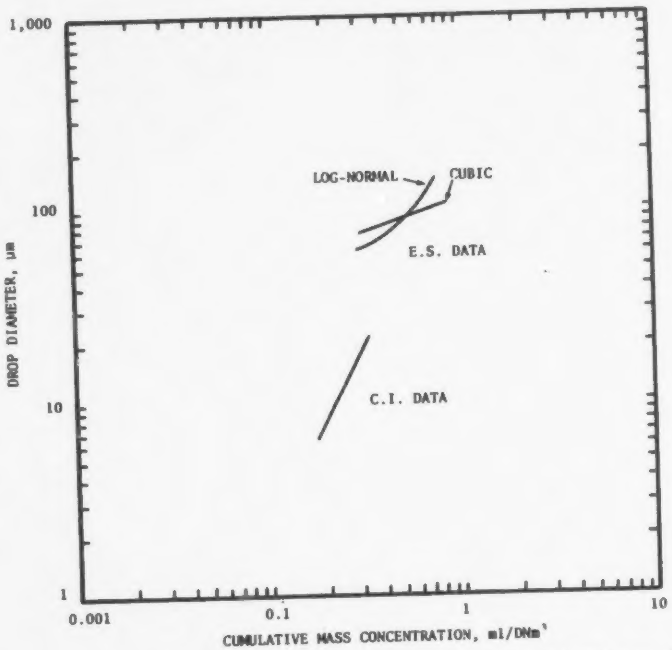

Figure 27. Measured entrainment concentration vs. drop diameter at the E.S. inlet for the sieve low scrubber.

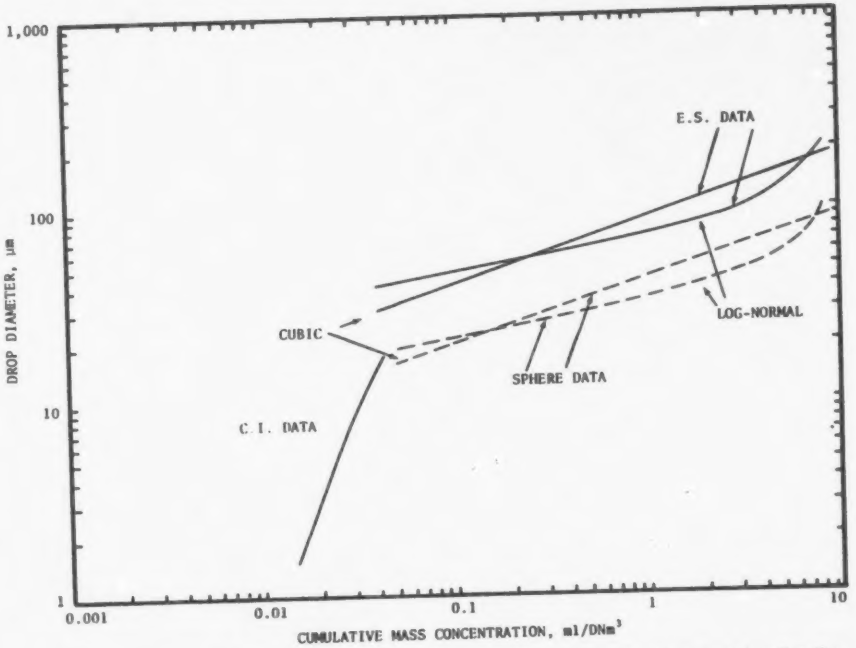

Figure 28. Measured entrainment concentration vs. drop diameter at the E.S. inlet for the spray 5 scrubber.

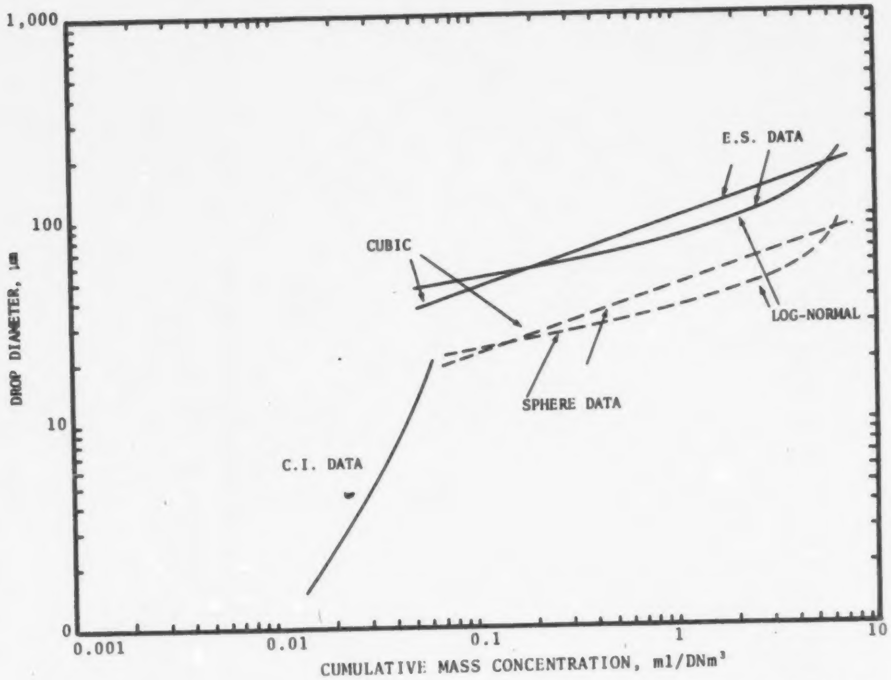

Figure 29. Measured entrainment concentration vs. drop diameter at the E.S. inlet for the spray 7 scrubber.

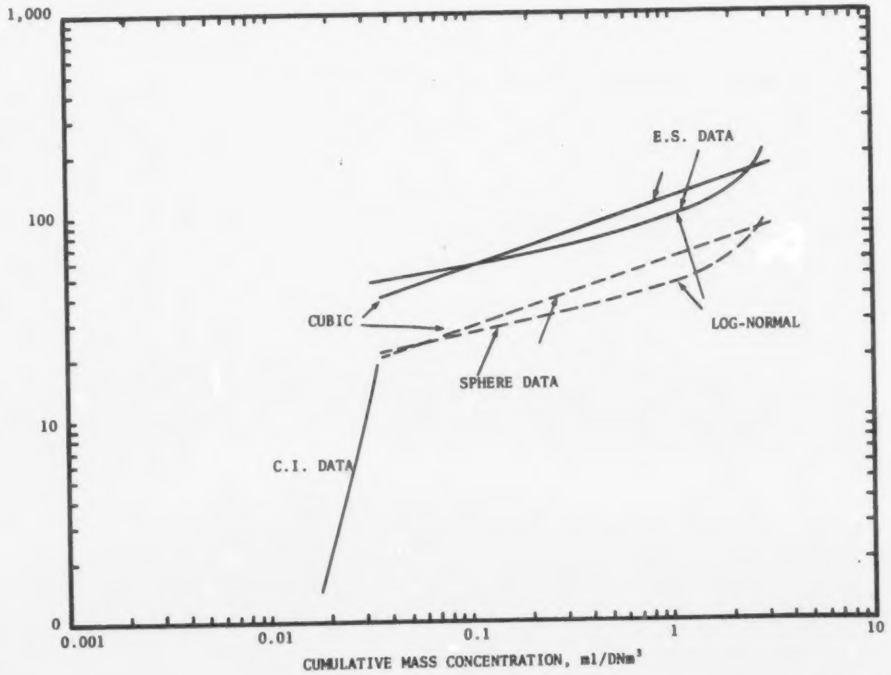

Figure 30. Measured entrainment concentration vs. drop diameter at the E.S. inlet for the spray 4 scrubber.

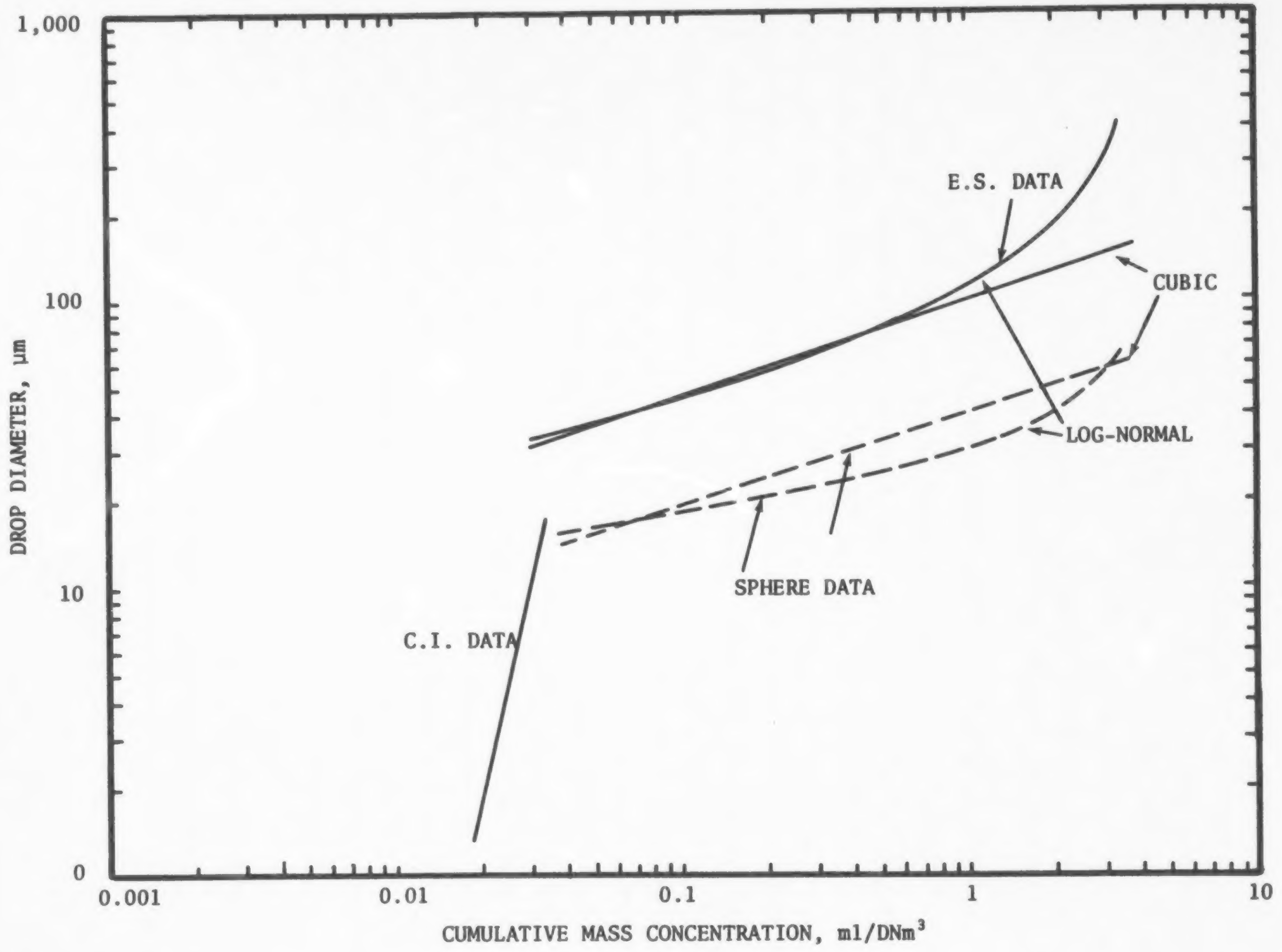

Figure 31. Measured entrainment concentration vs. drop diameter at the E.S. inlet for the spray 6 scrubber.

indicative of the sharp depletion of the large drops due to gravity settling and deposition in the turning vanes. On the other hand, the C.I. data for the smaller sizes show a steep slope, indicating the minor contribution to the total drop concentrations of drops of less than 10 μm diameter. The C.I. distributions for all types of scrubbers and conditions do not vary a great deal, which shows a relative independence of the size distribution of drops smaller than 20 μm diameter to the atomization mechanism within the scrubber.

Size Distributions from Sphere Collector Data

Inertial collection efficiency of drops in a gas stream on solid spheres depends on a number of factors, indluding the drop diameter. If all the factors except drop diameter are known, then the experimentally measured collection efficiency, when compared with empirical correlations, should yield information about the drop diameter. Complications arise when a distribution of drop sizes exists, requiring either a large number of experimental conditions (collector diameter, gas velocity, etc.) or an assumed type of size distribution.

In the experiments the amount of liquid collected by the sphere was divided by the volume of gas swept by the sphere (based on the cross-sectional area) to determine the collected drop concentration. The collection efficiency was then determined by dividing the collected concentration by the total concentration measured at the same location by another means. This other means was usually the cascade impactor. The measured sphere collection efficiencies are presented in Table 9. These are overall efficiencies since a distribution of sizes impacted on the sphere collectors.

The efficiency of collection by spheres has been empirically correlated by Calvert (1970):

$$\eta = \left(\frac{K_p}{K_p + 0.7} \right)^2 \qquad (34)$$

TABLE 9. OVERALL EFFICIENCY OF SPHERE COLLECTORS

Scrubber Configuration	$\bar{\eta}$, Overall Collection Efficiency, fraction	
	3.8 cm Sphere	7.6 cm Sphere
Mobile Bed, Mode 1	1.16	.96
Mode 2	1.83	1.40
Mode 3	2.05	1.67
Mode 4	1.53	1.30
Mode 5	1.20	.93
Sieve Plate, Low ΔP	*	--
High ΔP	*	--
Spray, 5 B-50	0.94	0.68
7 B-50	0.94	0.69
4 ST-24	1.09	0.80
6 ST-24	0.90	0.56

* The entrainment loading for the sieve plate runs was too light to collect a measurable amount of liquid with the spheres.

where $K_p = \frac{d_d^2 \rho_d C' u_G}{9 \mu_G d_c}$, drop impaction parameter

Because the drops collected are not of uniform diameter, the efficiency of the sphere collector is the collection efficiency at each drop diameter integrated over the drop size distribution:

$$\bar{\eta} = \int_0^{\infty} \eta (d_d) f(d_d) dd_d \qquad (35)$$

where $f(d_d)$ = drop size distribution density function
$\bar{\eta}$ = overall efficiency, fraction

The log-normal distribution required numerical integration of equation (35) . The results are shown in Figure 32 for 3 different values of the geometric standard deviation (σ_g).

For the cubic distribution, equation (36) could be integrated analytically, with the result:

$$\bar{\eta} = \frac{1}{(ad_{mm}^2 + 0.7)} \left[ad_{mm}^2 - 3.5 - \frac{3.675}{ad_{mm}^2} + \frac{4.392}{(ad_{mm}^2)^{1.5}} \tan^{-1} \left[\left(\frac{ad_{mm}^2}{0.7} \right)^{\frac{1}{2}} \right] \right] \qquad (36)$$

where the arctangent function is in radians and

$$a = \frac{2.7}{d_{d_{50}}^2} \qquad (37)$$

and $d_{d_{50}}$ was defined on Figure 32. The equation is plotted on Figure 33.

Correlation of the collection data in Table 9 with these log-normal and cubic distributions would normally involve the following procedure:

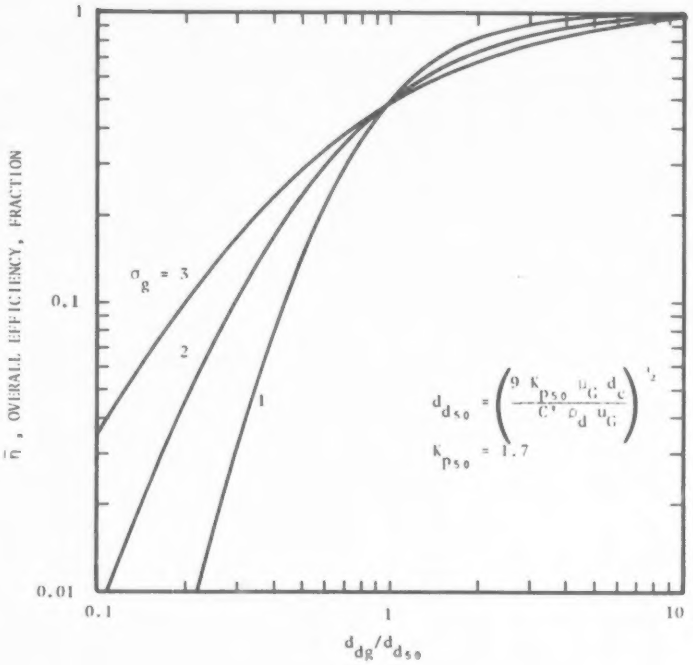

Figure 32. Theoretical overall efficiency of sphere collectors on log-normally distributed drops.

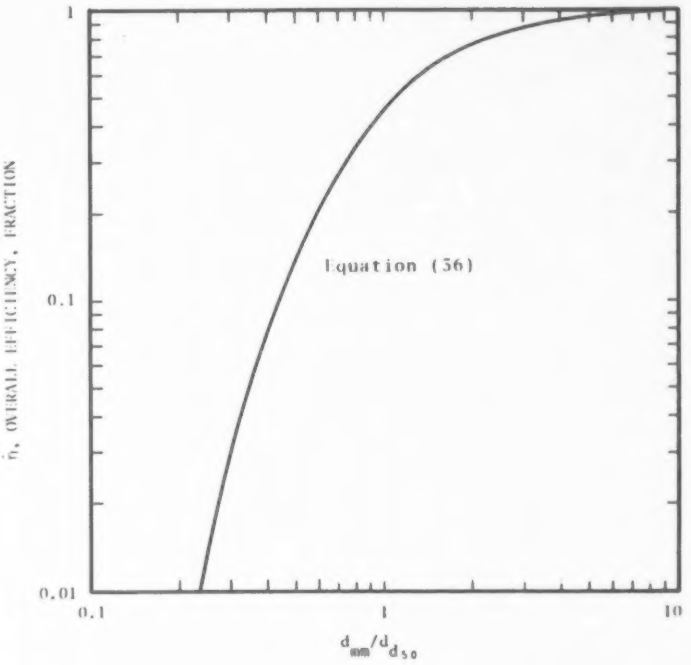

Figure 33. Theoretical overall efficiency of sphere collectors on drops with the cubic distribution.

1. Select a "σ_g" or the cubic distribution.
2. Find the "d_{dg}" or "d_{mm}" for which the two data points ($\bar{\eta}$ vs. d_{dg}/d_{d50}) for each d_{d50} lie on the theoretical line.

Since only two data points were available a unique "σ_g, d_{dg}" combination could usually not be determined for the log-normal distribution. However, the standard deviation was expected to be small (~1.5) so that the data could be used to determine "d_{dg}". A rationale for this expectation is given below.

Expected "σ_g" of Large Drops

Interpretation of size distribution data from the various collection methods would be greatly aided by any additional knowledge of the true distribution. One bit of knowledge available is the standard deviation of large drop diameters.

Few drops larger than 200 μm are expected to penetrate the turning vanes and horizontal run. Predictions of the collection efficiencies of these collectors, made in Section 3, lead to this expectation. Because of the lack of large drops the drop size region immediately below about 200 μm will have a fairly uniform distribution. If we assume a log-normal form of the distribution the expected geometric standard deviation (σ_g) for the distribution of diameters between 50 μm and 200 μm would be around 1.5. In the following discussion this hypothesis is supported.

The cumulative mass concentration is the product of the total mass concentration and the cumulative mass distribution function, $C_T F(d_d)$. The penetration of a drop of diameter, d_d, through a collection device, such as a horizontal run or turning vanes, is the ratio of the derivatives of the outlet and inlet cumulative mass concentrations:

$$Pt\ (d_d) = \frac{\tilde{d}\ [C_{To}\ F_o\ (d_d)]}{\tilde{d}\ [C_{Ti}\ F_i\ (d_d)]} \qquad (38)$$

where 'o' refers to outlet
'i' refers to inlet

Since the derivatives of the cumulative mass loading function (F) are the density functions (f) and the ratio of the total concentrations is the overall penetration, the outlet density function is:

$$f_o = \frac{Pt}{\overline{Pt}} f_i \tag{39}$$

Finally, the outlet cumulative mass distribution is the integral:

$$F_o = \int_o^{d_d} f_o \, \tilde{d}d_d \tag{40}$$

In Section 3 the penetration (Pt) through the turning vanes and the horizontal run were predicted for an E.S. velocity of 4.6 m/s. Also, the overall penetration ($\overline{Pt}$) through the two collectors was predicted, assuming that the drops upstream of the turning vanes had a log-normal distribution with a geometric standard deviation of diameters of 2.0. We need only assume a geometric mass mean inlet drop diameter (d_{dg}) to use these predictions to calculate the distribution at the end of the horizontal run.

Figure 34 shows the calculated size distribution using the two above equations for an assumed d_{dg} of 500 μm at the scrubber which is a reasonably expected drop diameter from the spray scrubber. The distribution in the region of diameters greater than 50 μm is approximately log-normal with d_{dg}=125 and σ_g=1.6. Below μm the size distribution changes, with the standard deviation in diameters increasing. Similar results occur for other types of scrubbers. Thus, in subsequent discussions we will assume where necessary, that the large drops entering the E.S. have a σ_g=1.5 which is very close to that calculated above.

Sphere Data Analysis

Correlations of the sphere collection data in Table 9. with the theoretical graphs could not be made directly because the measured efficiencies were usually above 100%. As discussed previously, gravity settling of drops on the spheres contributed somewhat to the higher measured efficiencies.

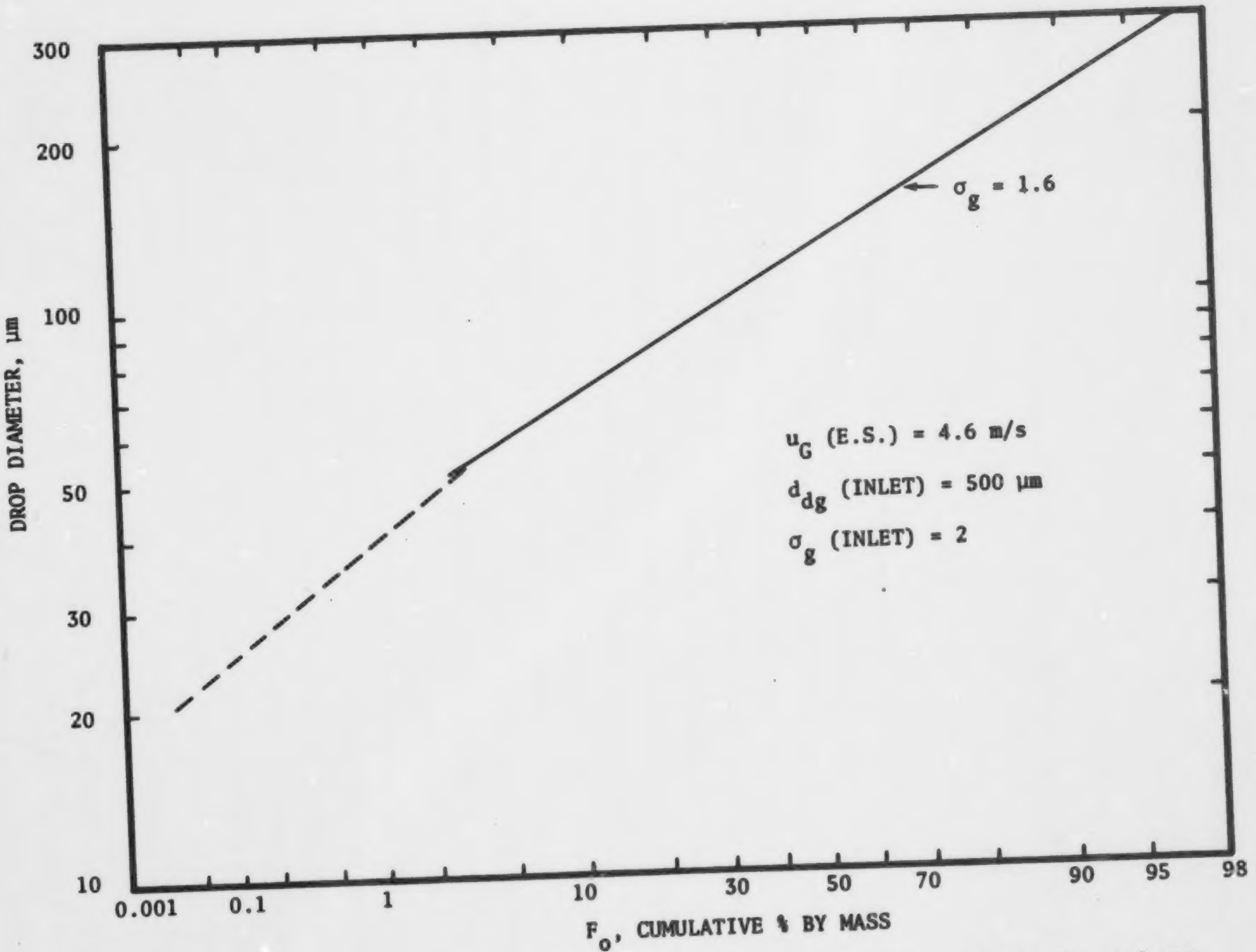

Figure 34. Calculated outlet drop size distribution of turning vane/horizontal run.

However, this contribution was estimated to be only about 5%.

Another contributor to the higher measured collection efficiencies relative to the cascade impactor sampling nozzle could be the higher probability of the larger spheres collecting a few large reentrained drops that drip from the duct ceiling or are sheared from the side walls. Also, the variation in size distribution in the air stream from top to bottom of the spheres was greater than that across the sampling nozzle. Thus, the spheres may have encountered a slightly larger size distribution than the sampling nozzle.

The sphere data are useful if the ratio of the two measured efficiencies are used so that most discrepancies between actual and ideal collection mechanisms can be neglected.

Correlation to the assumed size distributions was done as follows:

1. Assume the smaller, more efficient, sphere has an efficiency predicted by the theory.

2. Assume either a "σ_g" or "σ_g" or the cubic distribution, find the "d_{dg}" or "d_{mm}" for which the ratio of the measured efficiencies matches the theoretical efficiency ratio for the two "d_{d50}'s" of the two spheres.

The results of this correlation procedure are given in Table 10. A standard deviation for the log-normal distribution of 1.5 was assumed, for reasons discussed previously. The size distributions are plotted on Figures 21 through 31 for the three collection devices. For the mobile bed the E.S. and sphere collection data agree closely. The sphere data indicate a smaller size distribution than do the E.S. data for the spray scrubber runs.

Nozzle Manufacturers' Drop Size Data

Another way to check our measured drop size distribution from the spray scrubber is to use the nozzle manufacturer's data to describe nozzle output and to estimate the change in drop size distribution as the entrainment travels to the E.S.

TABLE 10. SIZE DISTRIBUTIONS AT E.S. INLET DERIVED FROM SPHERE COLLECTOR DATA

Scrubber Configuration		d_{d50}, μm 3.8 cm Sphere	d_{d50}, μm 7.6 cm Sphere	Log-Normal Dist.		Cubic Dist.
				dd_g, μm	σ_g*	d_{mm}, μm
Mobile Bed	1	39	56	90	1.5	100
	2	39	56	80	1.5	70
	3	39	56	85	1.5	95
	4	42	59	100	1.5	110
	5	45	63	65	1.5	80
Spray	5	48	68	55	1.5	65
	7	48	68	55	1.5	70
	4	48	68	55	1.5	70
	6	48	68	40	1.5	50

* Assumed

Spraying Systems Company provides some drop size distribution data for their nozzles. The Whirljet size 50, which we used, has a cumulative mass fraction that is a function of the cube of the drop diameter at the lower end (less than 700 μm diameter) at 150 psi (1034 kPa). Assuming that the size distribution is similar at the 30 psi (207 kPa) pressure we used, the equation for the cumulative loading fraction at thw lower end would be:

$$F_{noz} = \left(\frac{d_d}{1,474}\right)^3 \quad (d_d \text{ in } \mu m) \qquad (41)$$

This equation is an extrapolation for diameters smaller than 440 μm.

Based on the spray concentration at the nozzle and the measured entrainment concentration entering the E.S. a maximum expected drop diameter, and a mass median diameter of drop entering the E.S. can be calculated. For the "Spray-5" scrubber configuration the liquid flow rate through the spray nozzles was 2.68 ℓ/s and the gas flow rate was 1.42 m^3/s. Thus, the total initial spray drop concentration was 1.89 ℓ/m^3. The measured concentration at the E.S. inlet was 9.15 ml/m^3, so that $F_{noz} = 9.15 \times 10^{-3}/1.89 = 0.00484$. Using the above equation the drop diameter corresponding to this "F_{noz}" is 249 μm. This diameter is the maximum drop diameter at the E.S. inlet; the corresponding mass median diameter (d_{mm}) at the E.S. inlet is then 198 μm. For the "Spray-7" scrubber configuration a similar analysis yields a d_{mm} = 164 μm.

These values of "d_{mm}" are larger than those derived from sphere collector data and E.S. penetration data, but they are within the expected error bounds.

CONCLUSIONS

The information obtained from the experimental and analytical work on entrainment characterization provides the basis for some conclusions about the methods used, as well as the entrainment. Because of the difficulty of making entrained drop size measurements, it is important to point out what has been demonstrated and what improvement remains to be done. Entrainment characteristics were well enough established to give a useful basis for E.S. design or specification.

Sizing Methods

1. The cascade impactor method using the salt tracer provided good drop size distribution data for diameters between 1 and 20 µm.

2. The overall penetration and outlet size distribution data from the E.S. were correlated to log-normal and cubic inlet size distributions using a mathematical model for E.S. grade penetration. The correlations were very good in a few cases and moderately good in most cases.

3. The volumes of drops collected by the sphere collectors were correlated to log-normal and cubic inlet size distributions using a mathematical model for sphere collection efficiency. After compensating for the greater than theoretical efficiency of the spheres, the data correlated to the size distributions adequately. Further investigations of sphere collection efficiency under more controlled conditions would be needed to completely define the mechanisms involved.

4. The hot wire drop counter did not perform successfully under the conditions of these tests. The fragility of the 5 µm diameter wires and the use at high gas velocities were the probable causes of the poor performance.

Entrainment Size Distribution

The size distributions of the entrainment produced from the three types of scrubbers are summarized in Figure 35 through 45. Drop size was measured at the E.S. inlet not at the scrubber "outlet", so it was necessary to compute the probable distribution at the scrubber outlet. The solid lines represent the average of the data based on cascade impactor, sphere, and E.S sampling at the E.S. inlet. The dashed lines represent the size distribution directly above the scrubbers, before the turning vanes and the horizontal run.

Scrubber outlet size distribution was calculated from the E.S. inlet curve and the theoretical penetrations through the turning vanes and the horizontal run. Because the E.S. inlet data end at a drop diameter of about 150 μm, the scrubber size distribution is shown to end there also. The actual scrubber outlet drop size distribution could include a high concentration of large drops not indicated in these figures. Good scrubber E.S. design practice would prevent these large drops from entering the E.S.
in these figures.

Effectiveness of the Pre-Separators

The turning vanes and horizontal section were very effective at reducing the loading on the E.S. when the entrainment contained a large percentage of large (> 150 μm) drops. This effectiveness can be seen in Figures 35 through 45 where the differences in the two size distributions are due to the pre-separators. As is seen in the case of the sieve plate scrubbers, the pre-separators were not so effective for drops smaller than about 150 μm.

Comparison with Other Data

The only entrainment size distribution data for scrubbers and conditions similar to those used here that could be found were those of Calvert, et al. (1977), cited earlier in Section 3. They measured the entrainment size distribution above a mobile bed scrubber that had a superficial gas velocity of 3.7 m/s and a liquid to gas ratio of 7.8 ℓ/m^3, which was very similar to our Mode 1 conditions.

They sampled in a vertical duct using a University of Washington cascade impactor with filter paper substrates and a precutter to remove large drops. The substrates were analyzed for NaCl used as a tracer. A comparison of the 1977 data with the present data is given in Figure 46.

The present data show a drop concentration about double that of the 1977 data. The reasons for the difference are not clear, although the mobile beds were of different size and configuration and there were dissimilarities in sampling devices and methods. We have noted that gas flow distribution is extremely important to the mode of operation of a mobile bed scrubber, especially if a single stage is used.

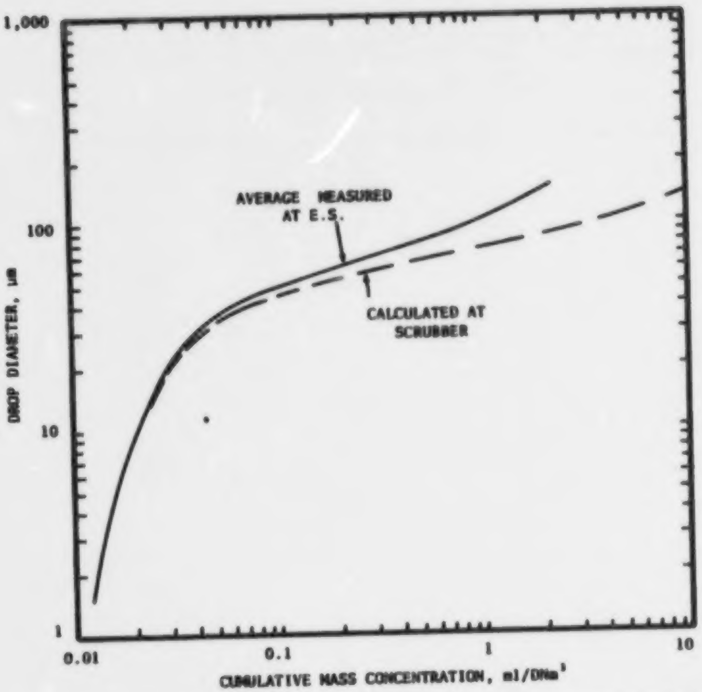

Figure 35. Composite drop size distributions at entrainment separator inlet and at scrubber outlet, for mobile bed (mode 1) scrubber.

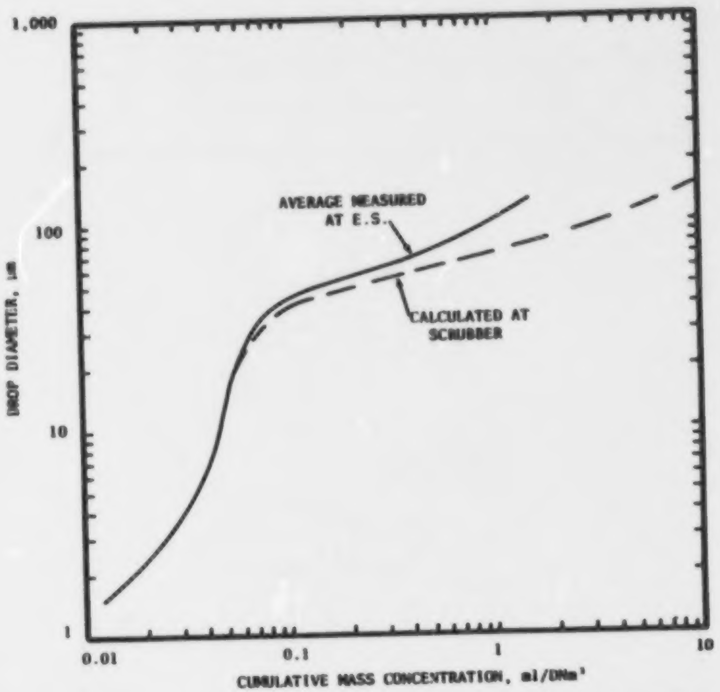

Figure 36. Composite drop size distribution at entrainment separator inlet and at scrubber outlet, for mobile bed (mode 2) scrubber.

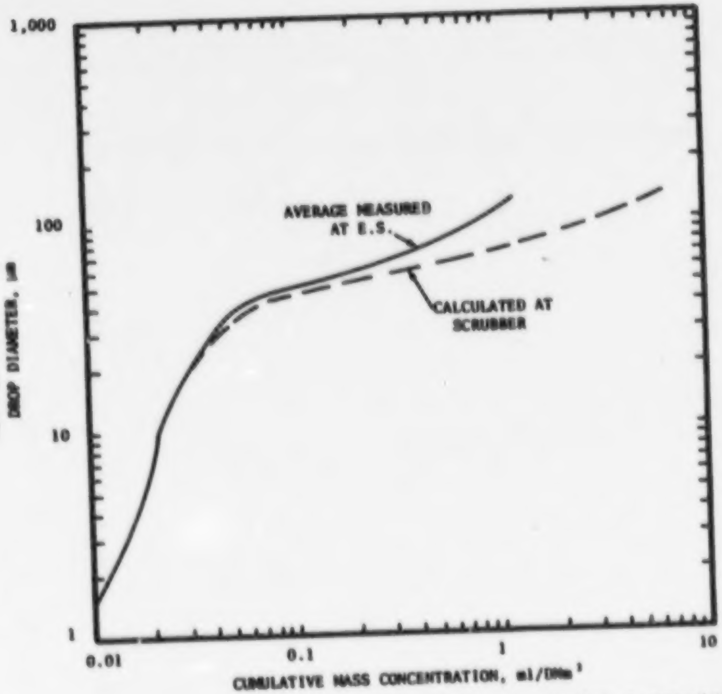

Figure 37. Composite drop size distributions at entrainment separator inlet and at scrubber outlet, for mobile bed (mode 3) scrubber.

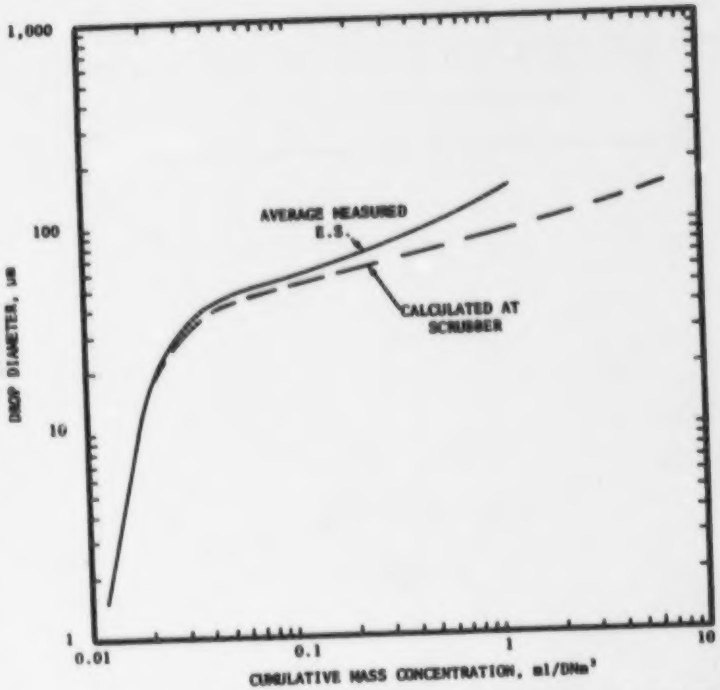

Figure 38. Composite drop size distributions at entrainment separator inlet and at scrubber outlet, for mobile bed (mode 4) scrubber.

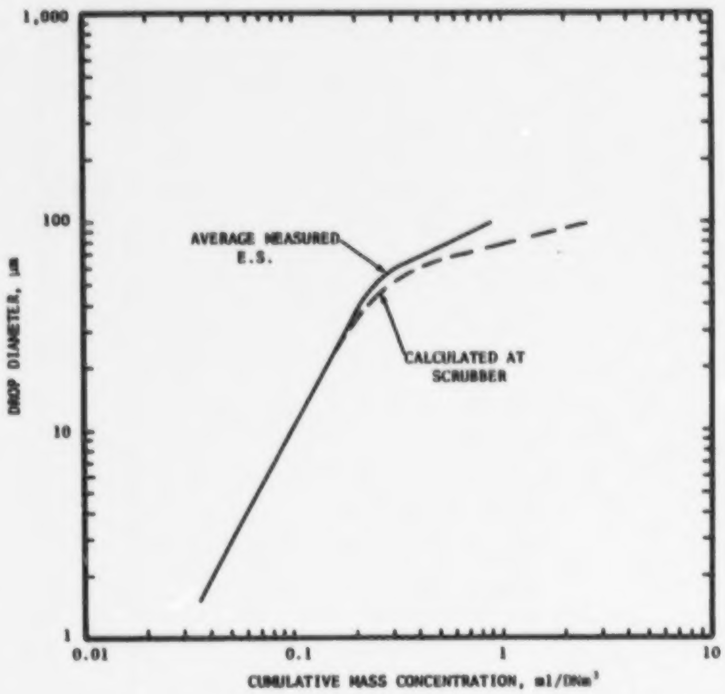

Figure 39. Composite drop size distributions at entrainment separator inlet and at scrubber outlet, for mobile bed (mode 5) scrubber.

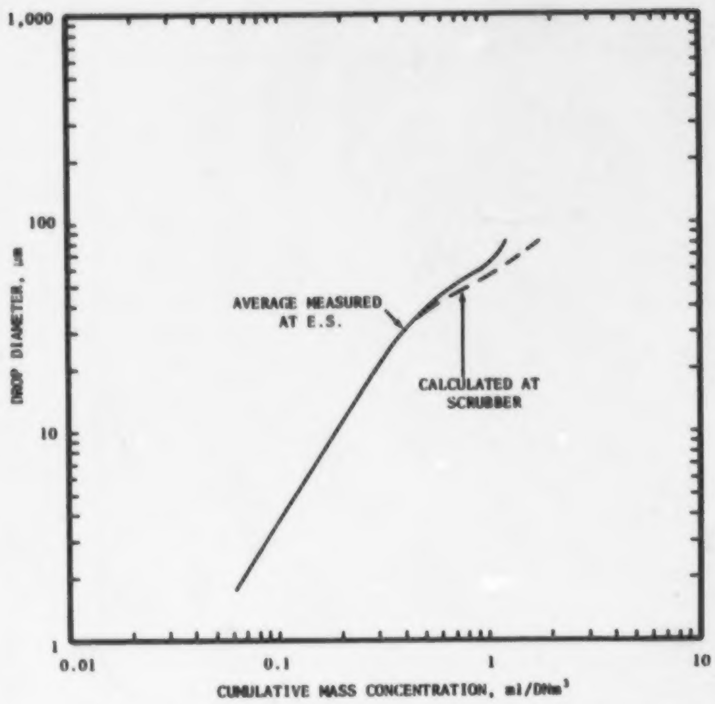

Figure 40. Composite drop size distributions at entrainment separator inlet and at scrubber outlet, for the sieve high scrubber.

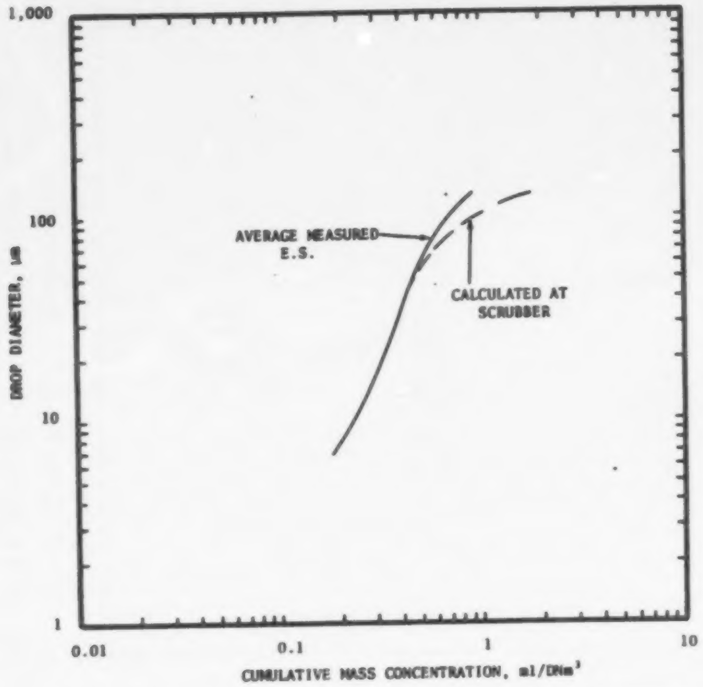

Figure 41. Composite drop size distributions at entrainment separator inlet and at scrubber outlet, for sieve low scrubber.

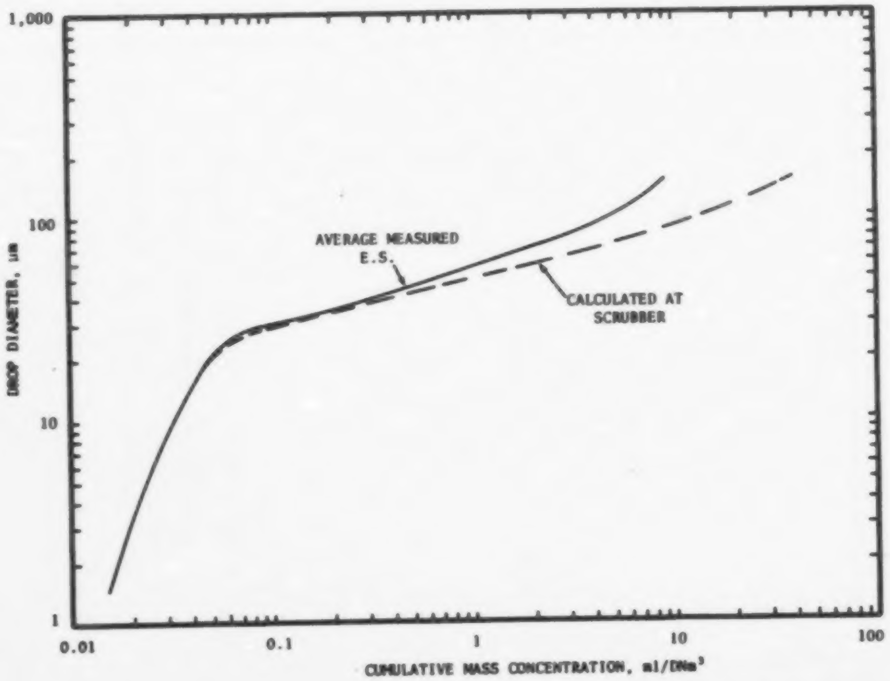

Figure 42. Composite drop size distributions at entrainment separator inlet and at scrubber outlet, for spray 5 scrubber.

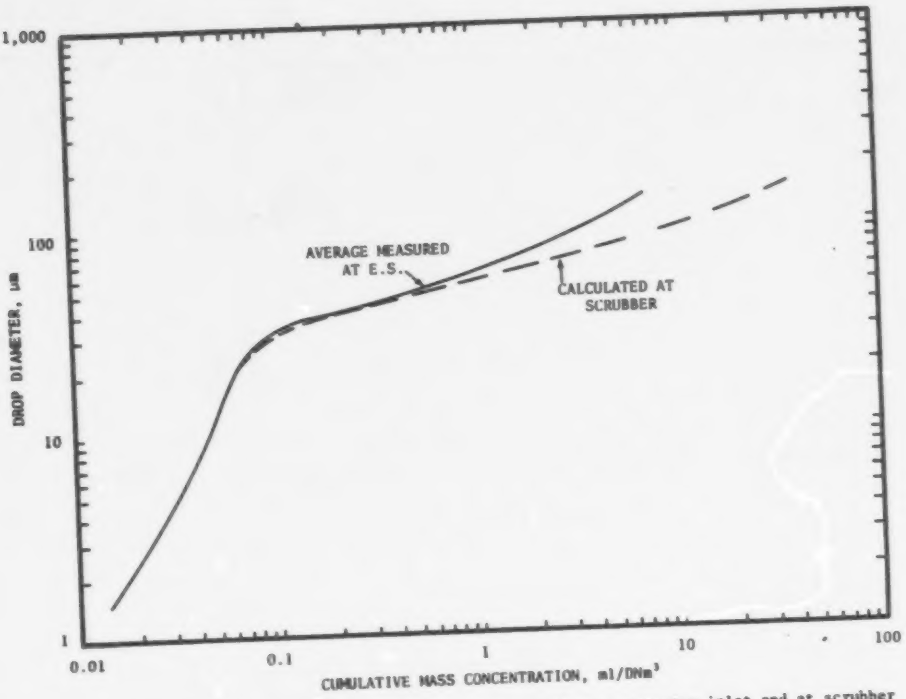

Figure 43. Composite drop size distributions at entrainment separator inlet and at scrubber outlet, for spray 7 scrubber.

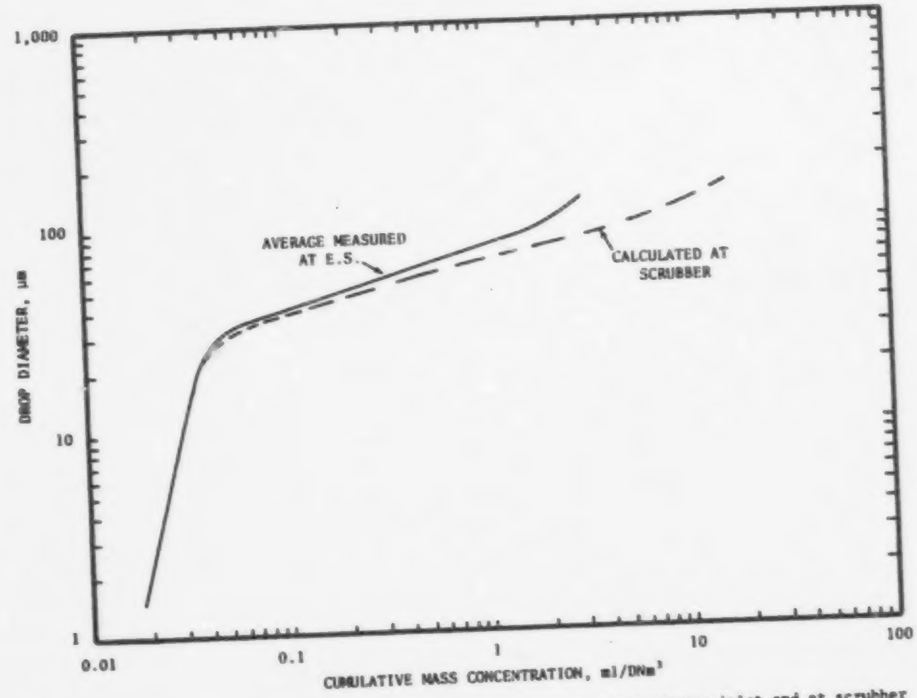

Figure 44. Composite drop size distributions at entrainment separator inlet and at scrubber outlet, for spray 4 scrubber.

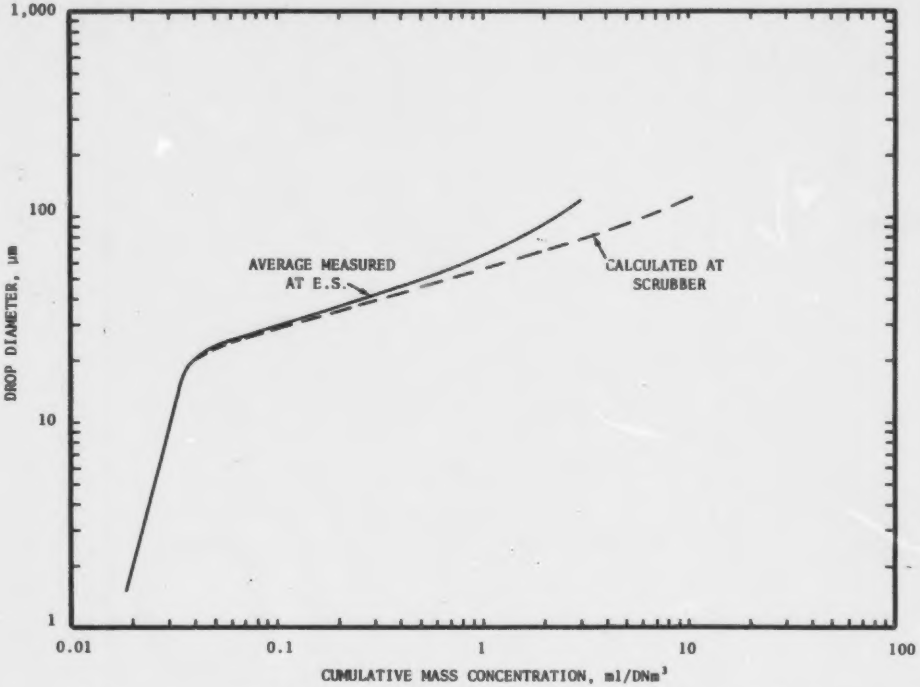

Figure 45. Composite drop size distributions at entrainment separator inlet and at scrubber outlet, for spray 6 scrubber.

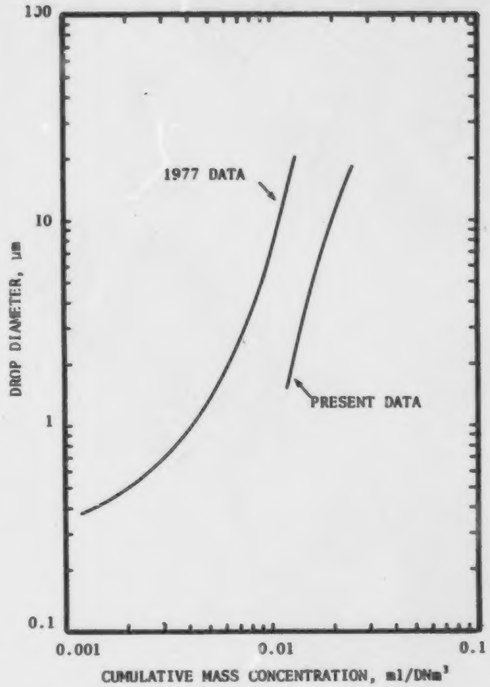

Figure 46. Comparison of E.S. size distributions of mobile bed, mode 1 vs. data of Calvert, et al. (1977).

SECTION 5

ENTRAINMENT SEPARATOR PERFORMANCE

The performance of the entrainment separator (E.S.) on entrainment from the three scrubbers was measured, and compared with the model of Calvert, et al. (1974). The efficiency determinations were based on the drop loading and size distribution at the E.S. inlet, as discussed in Section 4, and outlet drop loading and size distribution as measured with cascade impactors.

E.S. CONFIGURATIONS

The zigzag baffle E.S. depicted in Figure 3 was built in row modules. This construction allowed testing of any number of rows from 1 to 6 at any one time. In this program only 2 configurations were run: 3 rows and 6 rows of baffles.

One other design parameter was varied: the slope of the baffles. In addition to the vertical baffle configuration, a series of tests were run with forward (i.e., upstream) sloping baffles. The design was similar to the vertical design except that all the baffles were sloped forward at the top, 30° from the vertical.

This design should allow the liquid film, which has a horizontal velocity component due to the drag of the gas, to have a better chance flowing the full length of the baffle before reaching the aft edge. Should much liquid flow to the aft edge the film thickness there would increase greatly and the liquid would be susceptible to reentrainment. Thus, it was expected that the sloped configuration would be more efficient than the vertical. The sloped baffles were tested in 3 and 6 rows configurations.

PERFORMANCE MEASUREMENTS

The outlet drop loadings and size distributions were measured with the special cascade impactor (C.I.) using the chloride ion tracer method described in Section 4. The measurements are presented in Tables A4-A6 of Appendix "A". Overall penetrations were calculated based on inlet and outlet C.I. measurements and are presented in Table 11. Overall penetrations for vertical and sloped baffles are not shown separately because there was no significant variation.

Grade Penetrations

Determination of the grade penetration was very difficult because of uncertainties in several measurements. The inlet and outlet size distributions were so different that the outlet size distributions usually had only a few percent of the drops larger than 20 μmA. In the case of the sieve plate scrubber, grade penetrations determination accuracy was limited because the drop concentration was so low.

Figure 47 presents a plot of the overall penetration data versus the cumulative mass fraction of inlet drops smaller than 15-20 μmA diameter. It can be seen that the penetration is substantially equal to the fraction of inlet drops smaller than 20 μm diameter. This is clear evidence that the E.S. cut diameter is about 20 μm, as is should be.

The high penetration of the drops through the 3 row E.S. during spray scrubber operation is an indication that reentrainment was occurring. The drop concentration from the spray scrubber was relatively high and this probably caused more reentrainment. The low penetration for the mobile bed operation suggests that the cut diameter was smaller than about 20 μmA, which is in keeping with the high gas velocity in the E.S. during the mobile bed runs.

TABLE 11. SUMMARY OF PERFORMANCE OF THE ENTRAINMENT SEPARATOR BASED ON CASCADE IMPACTOR SAMPLING

Scrubber Configuration	E.S. Velocity m/s	Overall Penetration %	
		3-Row	6-Row
Mobile Bed - 1	6.9	0.82	0.82
Mobile Bed - 2	6.9		0.84
Mobile Bed - 3	6.9		1.3
Mobile Bed - 4	6.1	1.5	2.5
Mobile Bed - 5	5.3		5.5
Sieve Plate - low	2.3	31.0	26.0
Sieve Plate - high	3.4	14.0	20.0
Spray - 5	4.6	2.9	0.49
Spray - 7	4.6	1.4	0.89
Spray - 4	4.6	1.4	1.3
Spray - 6	4.6	3.0	1.1

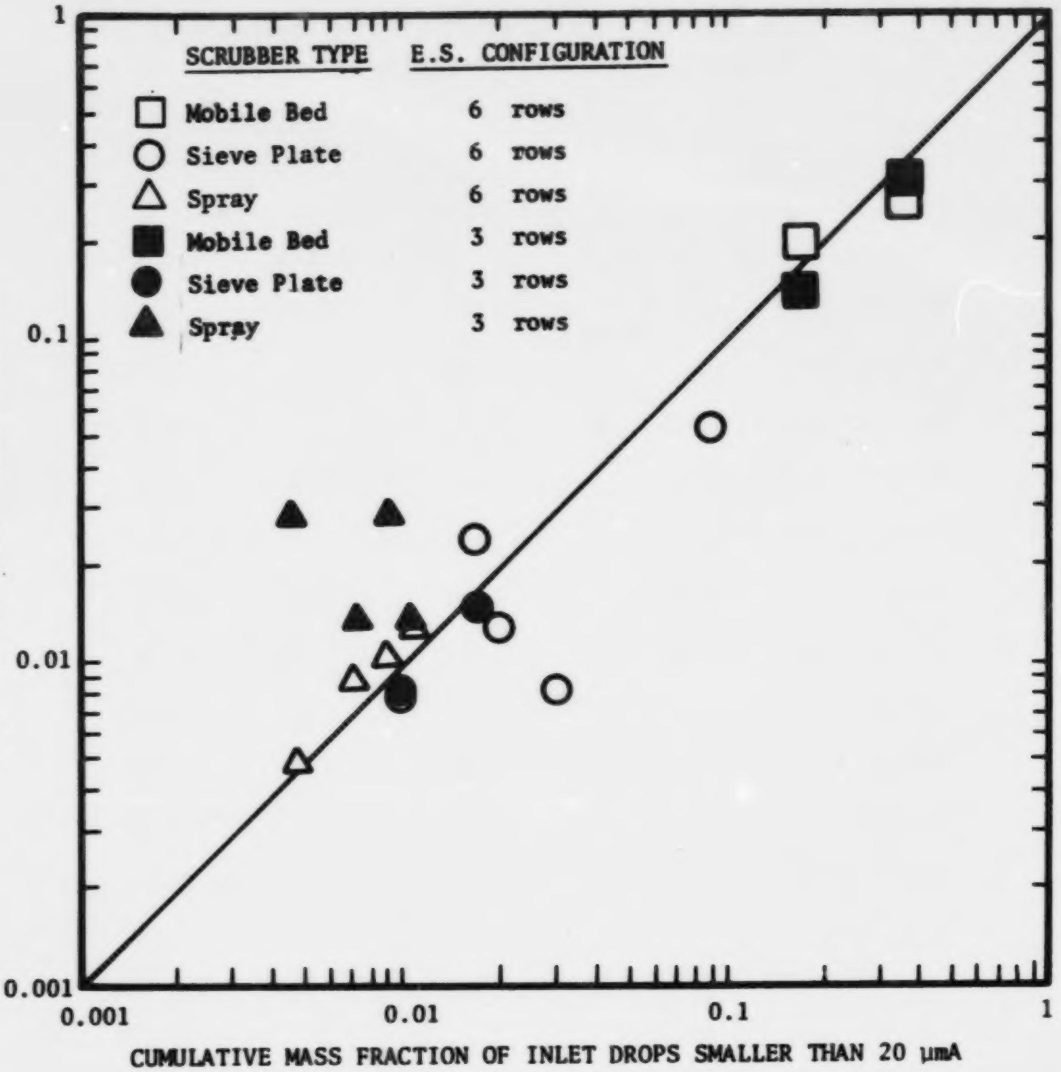

Figure 47. Measured overall penetration correlated to cumulative mass fraction of drops smaller than 20 μmA.

COMPARISON WITH THEORETICAL MODEL

The theoretical efficiency of zigzag baffles was predicted in Section 3, based on the model developed by Calvert, et al. (1974). Theoretical grade efficiencies were presented in Figures 4, 5, and 6 for the geometry and gas velocities used in the pilot E.S.

For 3 rows the predicted cut diameters (50% efficiency) were between 30 and 50 μm while for 6 rows they ranged from 21 to 36 μm. Predictions of collection efficiency for 15 μm diameter drops ranged from 0.05 to 0.3 which agrees with the experimental results that most of the drops smaller than 15 μm diameter penetrated the E.S.

When compared to the entrainment size distributions given in Figures 35 to 45, these results show the expected trends of lower penetrations for higher velocity and larger drop sizes. The low penetrations during the high velocity mobile bed tests indicate that reentrainment was not occurring. The relatively high penetrations for the sieve scrubber operation are due to a combination of the small drop size from the scrubber and the low gas velocity in the E.S.

The data agree with the model and do not indicate any errors in the model. The accuracy of the grade penetration curves was limited, so the model could not be tested with precision. The model is useful for design purposes, where ignorance of the entrainment drop size distribution usually imposes a severe limitation on one's ability to predict performance.

PRESSURE LOSS

The pressure loss in the E.S. was measured for superficial gas velocities between 2.2 and 7.0 m/s for 3 and 6 rows of baffles. The data correlate to the following equations:

$$\text{for 6 rows, } \Delta P = 5.88\ u_G^2\text{, Pa} \qquad (42)$$

$$\text{for 3 rows, } \Delta P = 2.65\ u_G^2\text{, Pa} \qquad (43)$$

where ΔP = pressure loss, Pa

u_G = superficial gas velocity, m/s

These data agree with those of Calvert, et al. (1974). The data may be correlated to a general pressure loss equation as follows. Assume the equation has the form,

$$\Delta P = \sum_{i=1}^{n} f_p \frac{1}{2} \rho_G (u_{Gi}')^2 \qquad (44)$$

where f_p = pressure loss coefficient, dimensionless

ρ_G = gas density, kg/m³

u_{Gi}' = actual velocity between baffles of row i, m/s

n = number of rows of baffles

for our geometry,

$$u_{Gi}' = \frac{u_G}{\cos 15°} \qquad i = 1 \qquad (45)$$

$$u_{Gi}' = \frac{u_G}{\cos 30°} \qquad i > 1 \qquad (46)$$

then,

$$\Delta P = f_p \frac{1}{2} \rho_G u_G^2 \left(\frac{1}{\cos^2 15°} + \frac{n-1}{\cos^2 30°} \right) \qquad (47)$$

The average value of f_p based on the data, was $f_p = 1.2$.

Conversion of Units to cm W.C.

It is often convenient to express pressure loss in cm of water column. The conversion factor is: 1 cm W.C. = 98.06 Pa. Thus equation (44) would become:

$$\Delta P \text{ (cm W.C.)} = 0.0102 \sum_{i=1}^{n} f_p \frac{1}{2} \rho_G (u_{Gi}')^2 \qquad (48)$$

REENTRAINMENT CHARACTERISTICS

A few runs were made to determine the onset of reentrainment for the 6 rows of vertical baffles. The determination of onset of reentrainment was made visually. With all 6 rows in place reentrainment was not observed even at the limit of system performance: volume flow rate = 2.6 m^3/s, superficial gas velocity, u_G = 8.4 m/s, and spray scrubber Q_L/Q_G, = 2.4 ℓ/m^3.

When 2 rows were removed (4 baffles in place) reentrainment was observed beginning at a volume flow rate of 2.12 m^3/s, u_G = 6.9 m/s and spray scrubber, Q_L/Q_G, = 2.97 ℓ/m^3. Heavier reentrainment was observed at higher velocities.

The onset of reentrainment occurred simultaneously with the flow of the liquid from the front baffle surface to the rear surface. The flow of the liquid around the rear edge and onto the rear surface was caused by the combination of the large liquid film thickness due to heavy loading and the transverse drag of the high velocity gas on the film. Apparently as the liquid flowed around the baffle edge, some of it was sheared off and consequently reentrained into the gas flow.

The fact that reentrainment will occur at lower velocities when a fewer number of rows of baffles are used indicates that the final rows are collecting reentrained drops from the forward baffles. In many installations where the entrainment loading is high, extra rows are needed for this reason and not to increase the primary efficiency. If the entrainment drop sizes are relatively large, there is little advantage to more than about 3 rows for a system such as our pilot E.S. unless the loading is heavy enough to cause reentrainment in the forward rows at the operating velocity.

E.S. OUTLET SOLIDS EMISSION LEVELS

The penetration data of this section of the report and the inlet size distribution data of the previous section can be used to estimate E.S. solids emissions from the configurations we tested. Slurry concentrations of 15 wt. % and 25 wt. % were used to compute solids emissions over the range from the usual level to a convservatively high one.

Table 12 presents the solids emission concentrations for the E.S. used in this program. Emissions from the mobile bed E.S. would range from 4 to 14 mg/DNm^3 for 25% slurry and from 2.3 to 8.4 mg/DNm^3 for 15% slurry. The highest emission occurred for mode 5, for which the liquid/gas ratio in the scrubber was the highest studied.

In the section on design (Section 3) we assumed that the E.S. operating on entrainment from a scrubber similar to our Mobile Bed, Mode 1, would emit 4 mg solids/DNm^3 while we measured an emission level corresponding to a 6 mg/DNm^3 solids. Since the entrainment emission rate from the scrubber in the present study was twice that assumed for the specification of design efficiency, while the E.S. emission rate is only 1.5 times the design rate, it is obvious that the E.S. is more efficient than specified. Predicted solids emissions are within an acceptable limit for the mobile bed and sieve plate scrubbers, even for 25% slurry. Spray scrubber emissions are higher, due to the high E.S. inlet liquid loadings, but could be tolerated at 15% slurry concentration. The use of a more efficient pre-separator would be advisable for the spray scrubber in order to reduce entrainment emission and ease the required scrubber efficiency.

TABLE 12. E.S. OUTLET SOLIDS EMISSIONS BASED ON DROP PENETRATION

Scrubber Configuration	E.S., ΔP cm W.C.*	Inlet Liquid Drop Conc., ml/DNm^3	$\overline{Pt}$ for 6 rows %	Outlet Solids Conc. in Gas @25% solids	mg/DNm^3 @15% solids
Mobile Bed					
Mode 1	2.9	2.44	0.82	6.0	3.6
Mode 2	2.9	1.54	0.84	3.9	2.3
Mode 3	2.9	1.26	1.3	4.9	2.9
Mode 4	2.2	1.19	2.5	8.9	5.3
Mode 5	1.7	0.85	5.5	14.0	8.4
Sieve Plate					
Low	0.3	0.086	26.0	6.7	4.0
High	0.7	0.14	20.0	8.4	5.0
Spray - 5	1.3	9.15	0.49	13.5	8.1
Spray - 7	1.3	7.32	0.89	19.5	11.7
Spray - 4	1.3	3.22	1.3	12.6	7.6
Spray - 6	1.3	3.76	1.1	12.4	7.4

*1 cm W.C. = 98.06 Pa

SECTION 6

SOLIDS DEPOSITION

INTRODUCTION

The characteristics of solids deposition in the pilot scrubber/E.S. were determined during operation with a limestone slurry scrubbing liquid. The deposition rate on the baffle surfaces was measured for a series of run conditions and E.S. configurations. Comparison with predictions was made and attempts were made to modify the model to more accurately predict the deposition rate.

SLURRY

The slurry consisted of commercially available fine limestone ($CaCO_3$) powder, nominally 325 mesh size. When sized with a Coulter counter the mass median particle diameter was found to be 12 μm. The particle density of $CaCO_3$ is 2.7 g/cm^3.

PROCEDURES

The character of the solids deposition on the zigzag baffle surfaces was determined by operating the pilot system in a normal manner with slurry. For each condition the scrubber was operated approximately 7 hours per day for at least 7 days. The slurry was well stirred before starting each day and samples were taken twice a day for concentration.

At the end of a run set the entrainment separator (E.S.) baffles were removed, inspected, and photographed. The deposits were non-uniform in most cases, but average thickness could be estimated. These average deposit thicknesses were used to determine a rate of deposition, or a thickness buildup rate for each run set.

MEASUREMENTS

A total of 6 series of runs were made, each lasting a number of days. The run conditions and observations were as follows:

Run Set 1

Scrubber nozzles: 6 Bete ST24FCN
Scrubber nozzle pressure: 69 kPa gauge (10 psig)
Duration: 6 days; 38 hours, total
Average slurry concentration: 2.7% by mass
Entrainment separator configuration: 6 rows of vertical baffles
E.S. superficial gas velocity: 4.6 m/s

Because of inadequate mixing, the slurry solids concentration was only 2.7% by mass while the goal was 10%. The first 3 rows had no solids deposition and the last 3 had slight uniform deposition. The fifth row had the thickest deposit, which was still less than 1 mm. The back surfaces of all 6 rows showed no deposition.

Run Set 2

Scrubber nozzles: 5 Spraying System Company 1/2B50
Scrubber nozzle pressure: 207 kPa, gauge (30 psig)
Duration: 9 days; 48.5 hours, total
Average slurry concentration: 6.4% by mass
E.S. configuration: 6 rows of vertical baffles
E.S. superficial gas velocity: 4.6 m/s

The same trends were noticed as for the previous run set but the deposition was heavier. The first 3 rows had no deposition except at the top, leading edge of the first row. The last 3 rows had uniform deposition over the front surface with row No. 5 having the heaviest deposition, reaching a thickness of about 3 mm. No deposition occurred on the back surface of the baffles.

Run Set 3

Scrubber nozzles: 5 Spraying System Company 1/2B50
Scrubber nozzle pressure: 207 kPa, gauge (30 psig)
Duration: 8 days; 54 hours, total
Average slurry concentration: 6.4% by mass
E.S. configuration: 6 rows of vertical baffles
E.S. superficial gas velocity: 4.6 m/s

The solids deposition characteristics were:

1. The first 3 rows were clean, front and back, except the first row had slight buildup on the leading edge for 5 cm from the top.
2. Row 5 had heaviest deposition - about 3 mm thick over the first third of the front surface.
3. Row 6 had about 1 mm of deposition, uniformly distributed over the front surface.
4. The back surfaces of rows 4, 5, and 6 had slight deposition.

Run Set 4

Scrubber nozzles: 4 Bete ST24FCN
Scrubber nozzle pressure : 69 kPa, gauge (10 psig)
Duration: 13 days; 87.4 hours, total
Average slurry concentration: 5.3% by mass
E.S. configuration: 6 rows of vertical baffles
E.S. superficial gas velocity: 4.6 m/s

The solids deposition characteristics were:

1. Row 1 - Front has thick deposit on the top 12 cm. At the front edge the thickness was the maximum, 0.6 cm. The lower 49 cm of the front surface and the rear surface were clean except for a slight (<0.1 cm) deposit on the trailing edge.
2. Row 2 - Pattern similar to Row 1 but less in extent. The rear surface was generally clean.
3. Row 3 - Front surfaces clean except for the baffle next to the wall. This baffle had about 0.5 cm deposit over the lower 40 cm of surface. The top of the baffles also had deposits up to 1 cm thick on the front edge. The rear surface had a very thin even deposit (<<0.1 cm).

4. Row 4 - The lower 5 cm of the front surface was clean and there was an even deposit about 0.2 cm thick on the upper 56 cm of the baffle. The rear surface had a thin (<0.1 cm), even deposit.

5. Row 5 - Front surface had no deposit on lower 5 cm nor at the very top. Thickness varied from top to bottom with a maximum of 0.3 cm deposit 40 cm from the top. The rear surface had an even, thin (<0.1 cm) deposit.

6. Row 6 - Front surface had a thin deposit (~0.1 cm average) with the maximum at 53 cm from top. The lower 8 cm were clean. The rear surface had a very slight deposit.

Run Set 5

Scrubber nozzles: 4 Bete ST24FCN
Scrubber nozzle pressure: 69 kPa, gauge (10 psig)
Duration: 8 days; 52.9 hours, total
Average slurry concentration: 3.3% by mass
E.S. configuration: 6 rows of baffles, sloped 30° forward of the vertical
E.S. superficial gas velocity: 4.6 m/s

The solids deposition characteristics were:

Row 1 - Front surface was clean except for the top 5 cm which had lumps on the front edge. The baffle next to the wall had deposits over most of the front surface about 0.1 mm thick. The rear surfaces were clean.

Row 2 - Same as row 1 except the baffle next to the wall was clean.

Row 3 - Same as row 1 except the baffle next to the wall had a deposit thickness of about 0.5 mm.

Row 4 - The upper third of the front surfaces had deposits 0.1 to 0.5 mm thick; the lower 40 cm was clean. The baffle next to the wall had a 0.1 mm thick, uniform deposit on the front surface. The rear surfaces were clean.

Row 5 - The baffle next to the wall was heaviest, but all the baffles had 0.1 to 0.5 mm thick deposit on the upper 40 cm of the front surface. The lower third was almost clean. The rear surfaces were clean.

Row 6 - All the baffles had a thin (0.1 mm) deposit on the upper 45 cm of the front surface, except for the baffle next to the wall. Its entire front surface was coated. The back surfaces were clean.

Run Set 6

Scrubber: Sieve plate @ 1.0 m^3/s, Q_L/Q_G = 9.1 ℓ/m^3

Duration: 7 days; 47.8 hours, total

Average slurry concentration: 4.5% by mass

E.S. configuration: 6 rows of vertical baffles

E.S. superficial gas velocity: 3.4 m/s

The solids deposition characteristics were:

Row 1 - The upper 50 cm had 1 mm thick deposits in patches, not uniform. Channels or clean vertical spaces were present. The rear surface was clean.

Row 2 - Thick (1-2 mm) deposits occurred in spots. The thickest region was 30 cm from the top and the thinnest was at 55-61 cm from the top. The rear surface was clean.

Row 3 - The front surfaces had a thin, 0.1 mm deposit. Slight carry-over around the leading edge to the rear surface was present, resulting in a thin coating near the leading edge.

Row 4 - A slight (<0.1 mm) deposit occurred on the front surfaces. The rear surfaces were clean.

Row 5 - A very thin, even deposit coated the front surfaces. There was nothing on the rear surfaces.

Row 6 - Same as row 5.

RESULTS

Figures 48 and 49 present the average thickness rates for spray scrubber and sieve plate scrubber operation, respectively. The thickness rate has been normalized for a 10% slurry for comparison purposes. Curves have been drawn for the average of each row that had a measurable deposit.

The first 3 rows of the E.S. during spray scrubber operation had no deposit except over a few centimeters at the top, leading edge. There was no measurable deposit on the rear surfaces of

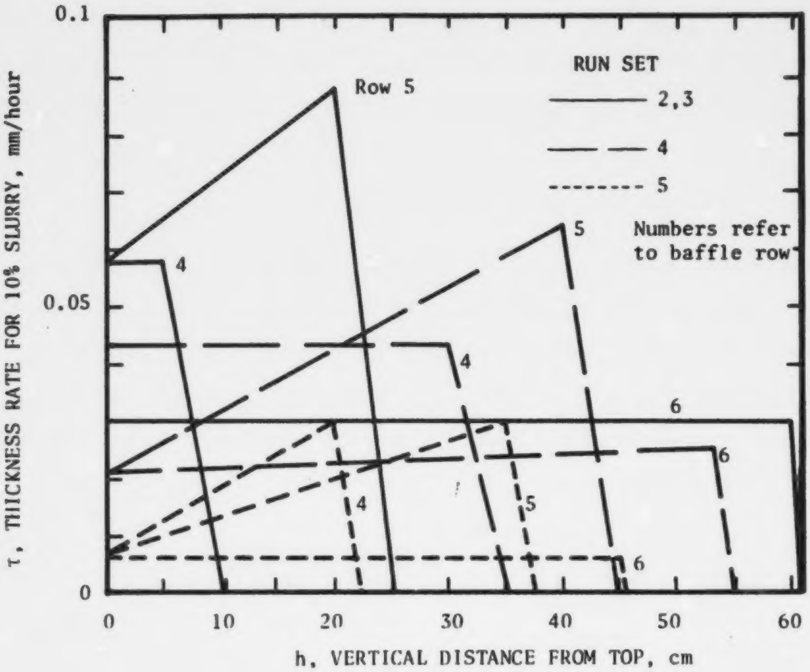

Figure 48. Measured deposition thickness rate for spray scrubber operation.

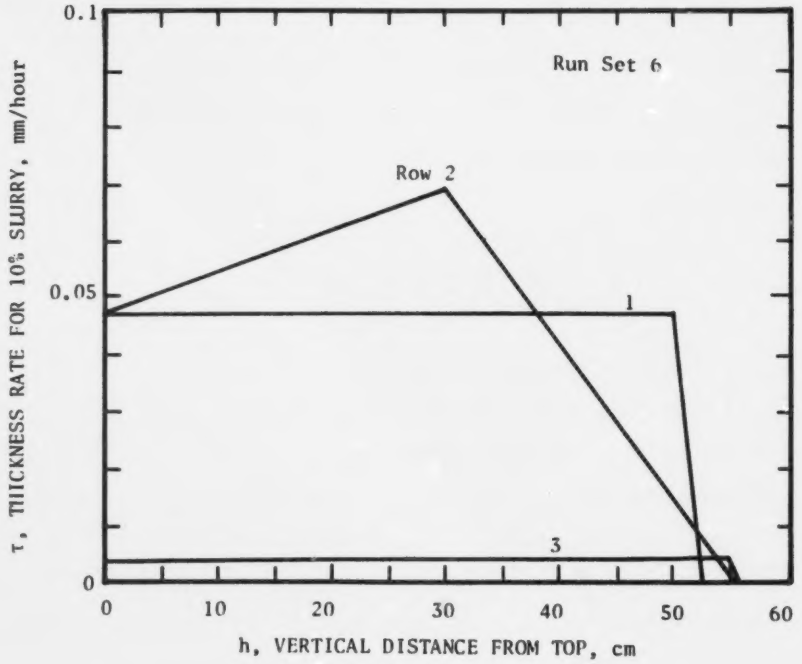

Figure 49. Measured deposition thickness rate for sieve plate scrubber operation.

the baffles of any row. Based on the thickness rates shown in the figures, it would take at least 100 hours of operation before the deposits became thick enough to affect the pressure drop

COMPARISON WITH SOLIDS DEPOSITION MODEL

Using data from a small single baffle, Calvert, et al (1974) derived an empirical equation for the solids deposition rate. We have modified the model slightly to account for slurry particle size and to account for the deposition occurring while the dry baffle surface is being wetted. The equation for deposition rate is,

$$R_s = W \Phi \exp [-k (\delta - d_{pmm})] \tag{49}$$

where $k = 0.13 + 0.53 \Phi$, μm^{-1}

and R_s = solid deposition rate on a vertical flat surface, mg/cm^2-s

W = weight fraction of solid in slurry

Φ = slurry flux, mg/cm^2-s

δ = laminar liquid film thickness, μm

d_{pmm} = slurry particle mass median diameter, μm

The laminar film thickness is,

$$\delta = \left(\frac{3 \mu_L h \Phi}{1{,}000 \rho_L^2 g} \right)^{1/3} \times 10^4 \tag{50}$$

where μ_L = liquid viscosity, g/cm-s

h = vertical length of film travel, cm

ρ_L = liquid density, g/cm^3

$g = 980$ cm/s^2

Equation (49) applies when $\delta \geq d_{pmm}$; and when $\sigma < d_{pmm}$:

$$R_s = W \Phi \tag{51}$$

The thickness rate is related to the deposition rate by

$$\tau = \frac{36\ R_s}{\rho_s} \qquad (52)$$

where τ = thickness rate, mm/hour
ρ_s = solid deposit density, g/cm^3

At the start of each daily run the deposit on the baffle surface is dry. Before any slurry will run off the surface it must be wetted. To account for the solids deposition occurring during this initial wetting of the surface, the following equation has been derived:

$$\tau' = \tau(1+f_\tau)^m \qquad (53)$$

where τ' = corrected thickness rate, mm/hour
m = number of times the dry surface is wetted

and

$$f_\tau = \frac{\varepsilon\ f_v}{1-f_v-\varepsilon} \qquad (54)$$

with ε = porosity of surface deposit, fraction
f_v = volume fraction of slurry particles in the slurry, fraction

The slurry flux, Φ, was not measured directly. It was calculated based on the entrainment loading and size distribuiton and the penetration through the various rows of the E.S. The penetration model was essentially that derived by Calvert et al. (1974). The calculated slurry fluxes for the operating conditions of the spray and sieve plate scrubbers are given in Table 13.

The model is compared with the data in Figures 50 and 51 for the 5-nozzle spray scrubber and the sieve plate scrubber, respectively. The agreement is fairly good for row 6 of the

TABLE 13. CALCULATED SLURRY FLUX ON ROWS 1 THROUGH 6*

Scrubber	u_G in E.S. m/s	Total Loading ml/m^3	d_{dg} µmA	σ_g	Φ_1 (mg/cm^2-s)	Φ_2 (mg/cm^2-s)	Φ_3 (mg/cm^2-s)	Φ_4 (mg/cm^2-s)	Φ_5 (mg/cm^2-s)	Φ_6 (mg/cm^2-s)
Spray 5	4.6	9.0	160	1.6	2.4	1.3	0.31	0.097	0.037	0.016
Spray 4	4.6	3.2	130	1.5	0.71	0.49	0.14	0.049	0.019	0.0086
Sieve-High	3.4	0.14	100	1.5	0.017	0.016	0.0066	0.0031	0.0015	0.0008

* Method described with equations (56) - (58) in Section 7.

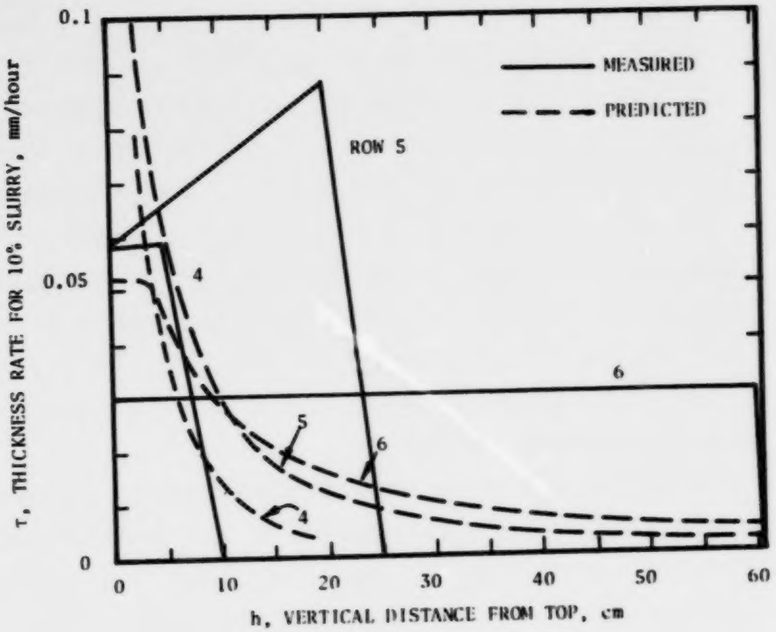

Figure 50. Comparison of measured and predicted deposition rate for spray scrubber run sets 2 and 3.

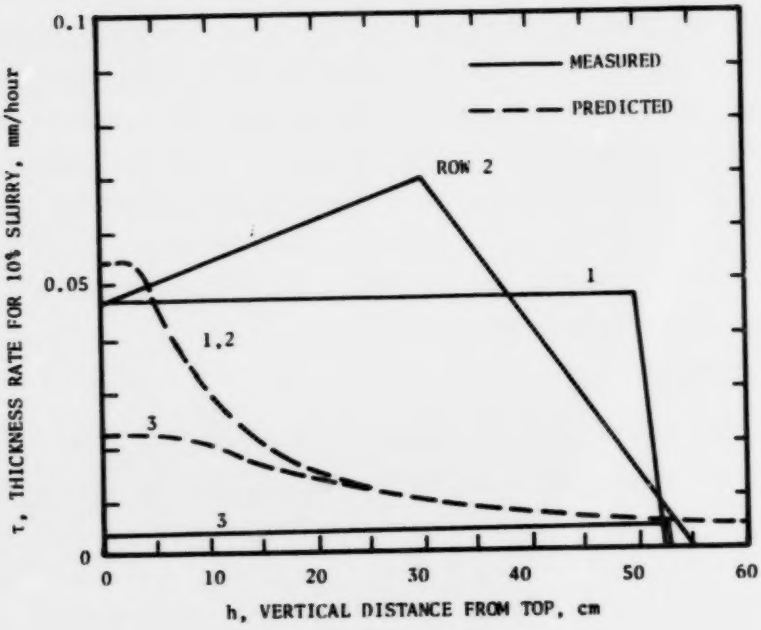

Figure 51. Comparison of measured and predicted rates for the sieve plate scrubber operation.

spray scrubber run and row 3 of the sieve scrubber run where the deposit was the most uniform. A significant underestimate is evident for row 5 of the spray scrubber operation and row 2 of the sieve plate operation. It appears that "end effects" or the effects of the ceiling and the end construction of the baffles has caused a downward shift of the location of heaviest deposit. Another real effect causing this shift is gravity which reduces the entrainment loading somewhat on the top few centimeters of the baffles. Also, the higher than predicted deposit thickness could be caused by periods of unsaturated operation.

Should the water drops be evaporating within or upstream of the E.S., the liquid film thickness on the baffle would decrease below that predicted by equation (50). A thinner liquid film would cause a higher deposition rate. The humidity was monitored closely and on days with low ambient humidity an extra fog nozzle was used upstream of the scrubber to keep the air as nearly saturated as possible.

CONCLUSIONS

Because of the non-ideal flow pattern at the top of the E.S., the non-uniform concentration of drops due to gravity and some periods of unsaturated operation, the model underpredicted the solids deposition rate. It was accurate to within an order of magnitude and indicated correctly the rows of the E.S. which should have significant solids deposition. The present model is useful for design purposes but it should be developed further.

OPERATING EXPERIENCE

The main problems encountered due to use of the slurry were pump seal wear and difficulty in mixing of the slurry in the main sump tank. A ceramic mechanical seal was used during the salt solution runs but it quickly wore out during slurry operation. A packing seal was then installed. The seal naturally dripped to enhance lubrication; a fresh water barrier was not used. The seal drippings were pumped back into the scrubber sump with a small venturi pump attached to one of the mixing pumps. Two small pumps were used to circulate the slurry at various locations within the main sump tank to provide extra mixing.

The main pump was a standard design cast iron close-coupled centrifugal pump. During the salt solution runs a bronze, closed impellor was used. However, it became eroded noticeably after a few days of operation on the slurry. A cast iron, open impellor was substituted and no further problems were encountered.

Unsaturated Operation of E.S.

An unsaturated condition was noticed at the outlet of the entrainment separator on a day when the relative humidity was about 50%. Evaporation of drops in the entrainment separator would reduce the amount of liquid flowing on the baffle surface. This was undesirable since solids deposition rate increases as the slurry flux and liquid film thickness decrease.

To try to ensure saturation a fog nozzle was placed between the blower and the scrubber inlet. Thereafter the humidity was closely monitored. The differences between inlet and outlet wet bulb temperatures were kept within 0.5°C. In addition to using the fog nozzle on dry days the E.S. baffle surfaces were closely watched for wetness. Test runs were not begun (blower started) until they were visibly wet from the convection of mist from the fog nozzle and spray scrubber nozzles.

Solids Deposition Outside the E.S.

Solids deposition was significant in only one location other than the E.S. in the pilot system. This was the horizontal section of duct upstream of the E.S. which experienced buildup on its floor. It was flushed periodically with scrubber liquid (slurry). A sloping floor and a shorter horizontal section would alleviate this deposition.

A potential solids buildup location was the turning vane section at the top of the vertical scrubber duct. However, the slurry flux was large enough to keep the vanes self-washed and no significant solids buildup occurred.

Design Considerations -

In general the designer of an entrainment separator system for use on a slurry scrubber should consider the potential for solids buildup throughout the system. For horizontal surfaces solids deposition will occur wherever the liquid flow is slow enough to allow slurry particles to settle out and slow enough not to scour the deposited solids. These horizontal surfaces include any ducting in which entrainment drops may settle out by gravity and horizontal parts of the E.S. which carry away the entrainment collected on the baffle surfaces.

Solids will deposit on vertical surfaces, such as the E.S. baffles, when the liquid flow on the surface is too slow to be self-washing (by scouring, etc.). Prime examples of vertical surfaces that have potential for solids buildup are horizontal ducting bends or turns. As in the E.S. a change in gas flow direction will cause some of the slurry drops to impact on the solid surface, creating a potential for solids buildup.

Both horizontal and vertical surfaces will experience rapid solids deposition if the carrier gas is allowed to become unsaturated. If the gas is not saturated the entrainment will evaporate resulting in either a higher solids concentration in the drops or even dry particles instead of drops. Besides causing a faster deposition rate, evaporation of the entrainment will also reduce the efficiency of the entrainment separator due to the smaller drop size of the entrainment.

The solution to unwanted solids buildup is washing. Spray nozzles should be located so as to wash or flush any surface that has a high potential for solids buildup.

Recirculated slurry can usually be used, although if fresh, make-up water must be added to the system the wash system would be an excellent location.

SECTION 7

WASHING SYSTEM

INTRODUCTION

In this section the need for and requirements of a washing system to remove deposited solids from entrainment separator surfaces will be described. A series of experiments will be discussed to verify the performance of a candidate washing system. Finally, criteria for washing systems of any scale will be developed.

NEEDS AND REQUIREMENTS

There exists a strong possibility that an entrainment separator designer will be unable to avoid solids deposition, either because the entrainment loading will be below that which is self-washing or it will be above the loading which causes an insignificant deposition.

In the previous section on solids deposition it was demonstrated experimentally that a high slurry flux was self-washing and will not permit solids to build up. Also in the case of very light entrainment the deposition rate was insignificant. Between these limits the deposition rate is significant and unavoidable. It would appear that solids deposition could be eliminated by operating at high enough entrainment loading to keep the baffles self-washing. However, at these high loadings the E.S. will probably not have the required efficiency due to either low primary efficiency or reentrainment. Also, solids will always deposit at the top of the leading edges of the first few rows because the film thickness is essentially zero at those locations. In some E.S. installations this buildup could slip down, because of vibrations, etc., and cause significant plugging problems.

The location of the maximum solids buildup can be approximated by differentiating the deposition rate equation with respect to the slurry flux, Φ, setting the result equal to zero, and solving for Φ_{max}. The location on a certain row a certain distance from the top of the baffle is,

$$h = \frac{1{,}000\ \rho_L^2\ g}{3\ \mu_L\ \Phi_R} \left(\frac{10^{-4}}{0.0433 + 0.7067\ \Phi_R} \right)^3 \qquad (55)$$

where Φ_R = slurry flux for which the deposition rate is a maximum, mg/cm²-s

and the other terms were defined in Section 6. If the vertical distance of film travel, h, calculated from equation (55) is between 1 cm and the baffle height then that row of baffles will have the maximum deposition rate at that height. If the "h" calculated from equation (55) is much less than 1 cm the slurry flux is too great for significant solids deposition. And, if the "h" calculated is much greater than the baffle height then the deposition rate is insignificant, because the slurry flux is so low. Equation (55) is plotted on Figure 52 for typical conditions.

For the typical conditions given and a baffle height of 61 cm, Figure 52 shows that the rows for which the slurry flux, Φ was between 0.005 and 0.06 mg/cm²-s would have significant solids buildup. These rows would be the ones requiring washing.

Requirements/Constraints

The basic requirements of the washing system is that it wash the baffle surfaces in a short time using a minimum of liquid and pumping power. If spray nozzles are used, they must be arranged to provide coverage of at least the upper half of the baffles. Recycled slurry should be used unless the system requires fresh make-up water, which could be conveniently introduced in the wash system.

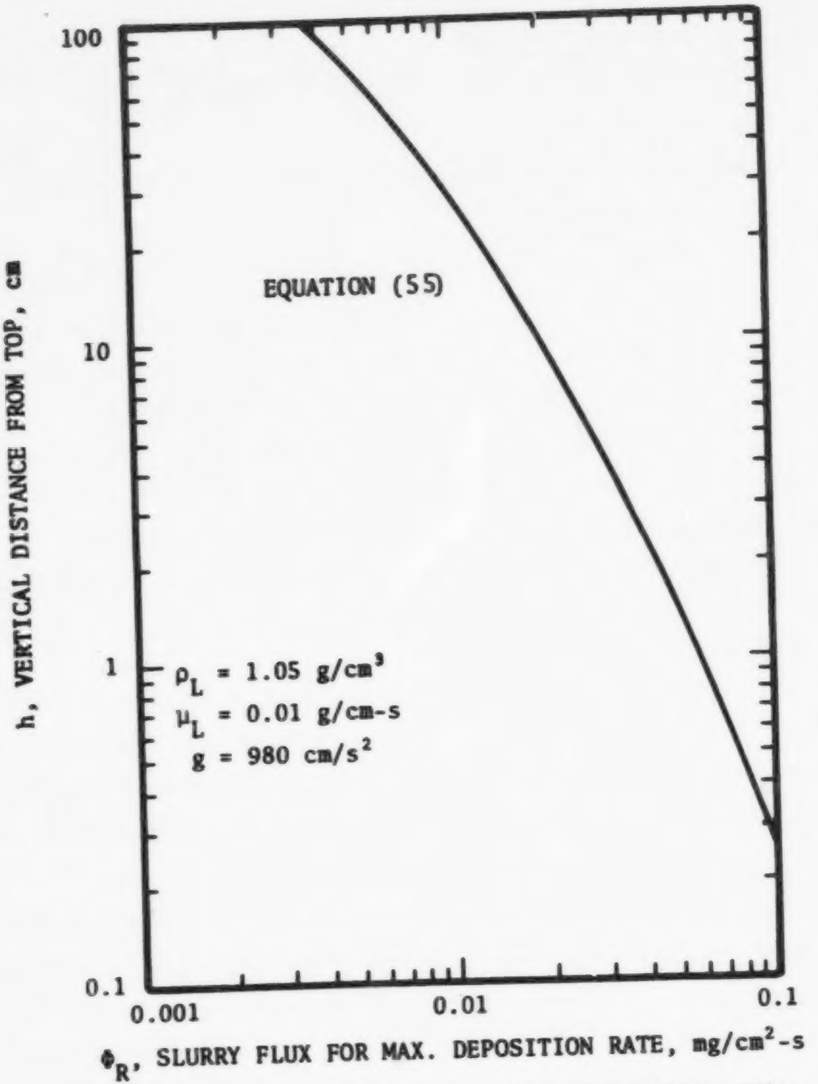

Figure 52. Slurry flux for maximum deposition rate.

EXPERIMENTAL DESIGN

The wash system for experimentation consisted of several small spray nozzles on a manifold located about 23 cm upstream of the E.S. The nozzles were Spraying Systems Company Model 1/4-B-3 of type 316 stainless steel. They were operated at 210 and 350 kPa gauge pressure (30-50 psig) using slurry and the drops produced had mass median diameters of 400 and 360 μm, respectively. The rate of washing was controlled by the number of nozzles and the pressure.

The washing system was tested at the end of solids deposition runs and using artificially coated baffles. An intermittent mode was found to be satisfactory with the wash system being run for only 10 minutes during the cycle.

RESULTS

The results of the wash system tests are shown in Figures 53 and 54 where the washing flux on each row of baffles is plotted against the percent of the surface cleaned. Since the "percent cleaned" may be imprecise due to the non-uniformity of the deposit, these figures should be used primarily to determine the washing flux required for total cleaning. The washing flux was calculated from the liquid flow rate, the spray drop size distribution, the gas velocity, and the E.S. geometry.

Washing Flux Calculation

The flux of washing slurry, Φ_w, hitting each baffle depends on the amount of slurry penetrating the baffles of the upstream rows.

Equation (8) is used for calculating the penetration of zigzag baffles:

$$Pt = \exp\left\{-\frac{w}{\bar{b}}\left[\frac{u_{D1}}{u_G} + (n-1)\,\frac{u_D}{u_G}\right]\right\} \qquad (56)$$

where the terms were defined in Section 3.

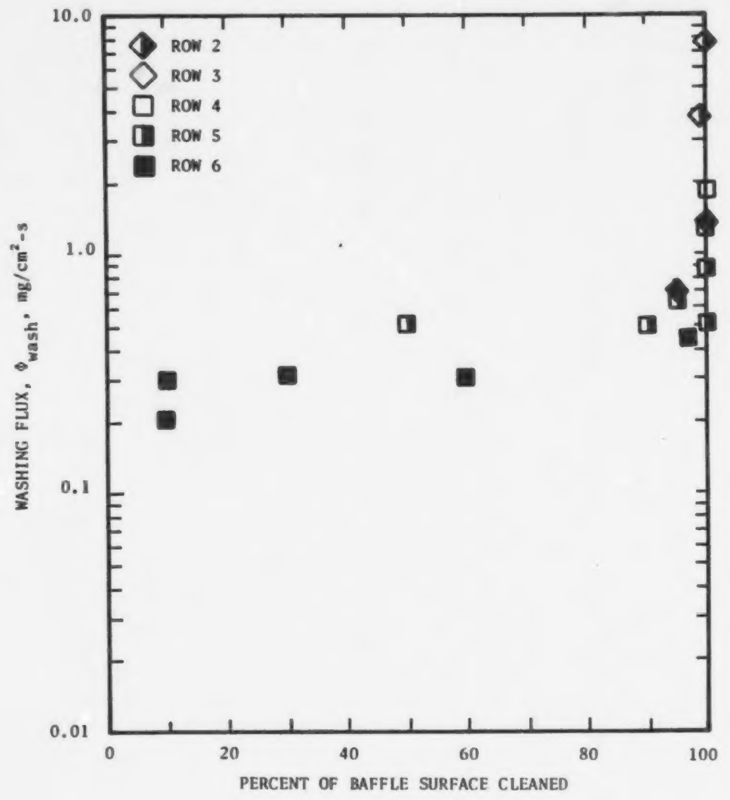

Figure 53. Washing flux vs percent of baffle surface cleaned after 10 minutes of u_G = 2.3 m/s.

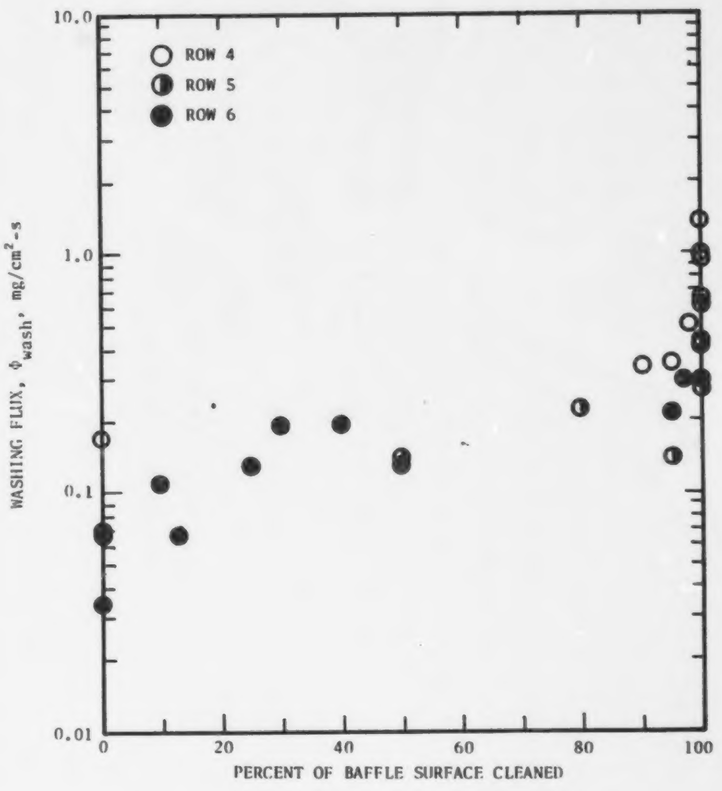

Figure 54. Washing flux vs percent of baffle surface cleaned after 10 minutes for u_G = 3.4 m/s.

The deposition velocities, u_{D1}, and u_D, are evaluated using the general drag coefficient relation, equation (7). The overall penetration, $\overline{Pt}$, is equation (8) integrated over the size distribution.

The loading hitting each row, n, can then be found from:

$$C_n = C_T\,(\overline{Pt}_{n-1} - \overline{Pt}_n) \qquad (57)$$

where n = row number

C_n = loading hitting row n, ml/m³

C_T = total loading, ml/m³

$\overline{Pt}_0 = 1.0$

and the loading hitting each row is related to the flux on the surface by

$$\Phi_n = \frac{\rho_L\, C_n\, u_G}{10} \qquad (58)$$

where ρ_L = liquid density, g/cm³

u_G = superficial gas velocity, m/s

Φ_n = slurry flux on row n, mg/cm²-s

The calculated penetrations are given in Table 14 for the 4 conditions under which the wash system was run. The loading, C_T, was calculated from the liquid flow rate through the nozzle, accounting for wall losses.

Minimum Flux Required

For the superficial gas velocities of 2.3 and 3.4 m/s the minimum slurry flux required to clean the baffles was 0.9 and 0.6 mg/cm²-s, respectively. The difference due to velocity is probably the result of more reentrainment from upstream rows at the higher velocity. The flux calculation is conservative as it assumes no reentrainment.

TABLE 14 . CALCULATED PENETRATIONS OF WASH SPRAY DROPS

		Overall Penetration, $\overline{Pt}_n$, fraction			
	u_G, m/s	2.3	2.3	3.4	3.4
Row n	d_{dg}, µm	360	400	360	400
	σ_g	2.2	2.2	2.2	2.2
1		0.27	0.24	0.24	0.21
2		0.069	0.057	0.053	0.043
3		0.029	0.023	0.020	0.016
4		0.016	0.012	0.0102	0.0077
5		0.0096	0.0072	0.0059	0.0043
6		0.0064	0.0047	0.0038	0.0027

Comparison with Prediction

The solids deposition model is not directly applicable for predicting required washing fluxes. However, from Figure 52 one would predict that the washing flux should be greater than 0.1 mg/cm^2-s. This value was also the flux, above which no deposition occurred in the solids deposition experiments. Since this is the flux required to continuously wash the baffles it is logical that a somewhat higher flux would be required for short duraction intermittent washing of accumulated deposits. Thus, the experimentally determined washing fluxes do not conflict with the deposition model but they could not be predicted with any precision by the model.

DESIGN CRITERIA

The variable that determines the washing effectiveness is the washing flux on the baffles. It is a function of the total wash spray flux into the E.S. and the penetration of the spray drops through the preceding rows of baffles. Since the penetration is a function of the E.S. geometry, gas velocity, and the wash spray drop size distribution, the calculation of the flux is complicated.

Typical Design

In order to estimate the amount of washing required in a typical E.S. installation, we will assume the following typical conditions:

E.S. geometry- as we used (Figure 3)
E.S. superficial gas velocity = 4.6 m/s (15 ft/s)
Spray drop size distribution:

$$d_{dg} = 400\ \mu m$$
$$\sigma_g = 2.2$$

Washing duration = 10 minutes
Required washing flux, $\Phi_{wash} = 0.6\ mg/cm^2$-s

The calculated overall penetrations for each row are:

Row, n	1	2	3	4	5	6
$\overline{Pt}_n$	0.161	0.0301	0.0104	0.0048	0.0026	0.0016

The total washing spray flux required upstream of the first row to wash row n is then,

$$\Phi_T = \frac{0.6}{\overline{Pt}_{n-1} - \overline{Pt}_n} \quad , \text{ mg/cm}^2\text{-s} \qquad (59)$$

which is given in Table 15 in terms of both spray flux (liquid flow rate per unit E.S. cross section) and Q_L/Q_G. Rows 4, 5, and 6 would probably require less washing than shown since there would be considerable reeentrainment from preceding rows at these high liquid loadings. The amount of washing could be reduced by decreasing the gas velocity or lowering the spray drop size at the cost of E.S. efficiency or increased spray nozzle pressure, respectively. Washing rates could be significantly reduced by separating a 6-row E.S. into two 3-row modules, also at the cost of E.S. efficiency.

TABLE 15. PREDICTED TOTAL WASHING RATES FOR TYPICAL E.S. FOR TEN-MINUTE OPERATION (u_G = 4.6 m/s)

	Row					
	1	2	3	4	5	6
Wash Spray Flux						
ℓ/m^2-s	0.0072	0.046	0.30	1.1	2.7	6.0
GPM/ft^2	0.011	0.068	0.44	1.6	4.0	8.8
Wash Spray Q_L/Q_G						
ℓ/m^3	0.0016	0.010	0.065	0.24	0.59	1.30
gal/1,000 ft^3	0.012	0.075	0.49	1.8	4.4	9.8

SECTION 8

FUTURE RESEARCH RECOMMENDATIONS

The major goals of this research were met, however, additional work on some problems would be useful. Since the major goals of the project were attained, the superior E.S. design should be used in a demonstration phase. This phase would prove that the design can maintain high performance and not be degraded by a slurry in an actual practical application. Demonstration at a coal-fired utility boiler that uses a lime or limestone flue gas desulfurization scrubber would be desired. The design gas flow rate should be an order of magnitude greater than the present; i.e., at least 14 actual m^3/s (30,000 ACFM).

GRADE EFFICIENCY

The nature of E.S. operation is such that precise measurement of the drop size distribution and concentration is extremely difficult. Drop size and concentration vary greatly in three dimensions, especially at the upstream side of the E.S., where large drops abound. One would have to make a tedious traverse across the inlet face of the E.S. along a plane close enough to the face so that drop sedimentation has a tolerably small effect.

The lack of a good drop sizing method for the 20 to 50 µm diameter range is another deterrent to good drop size analysis. Consequently, one does not have a good measurement of the average drop size and concentration going into the E.S. The outlet drops are better defined but the net result is that measurement of drop collection efficiency as a function of drop diameter is subject to considerable error if done for polydisperse entrainment from a scrubber.

We have done some exploratory experiments which showed that the use of monodisperse liquid drops is a promising way to measure E.S. collection efficiency. Drops in the broad range of 10 to 100 μm diameter are relatively easy to generate with such devices as the spinning disk atomizer.

Sampling and analysis based on the use of a tracer compound in the drops or optical methods can provide the data needed to compute drop collection efficiency. Problems of drop distribution across the E.S. face and along the axis of the gas flow can be readily resolved.

REENTRAINMENT LIMIT

Extension of our knowledge of the reentrainment limit of the zigzag E.S. was not a part of the present study but it would be useful to do. Several E.S. configurations which have been developed in recent years are claimed to have high limiting gas velocities and these should be investigated in addition to the zigzags.

Because these newer configurations are complex and generally involve the use of hooks or small depressed passages for liquid flow, they are probably subject to plugging by solids. The influence of solids deposition on the performance of such E.S. configurations should be determined experimentally.

SOLIDS DEPOSITION MODEL

The only available model for solids deposition was not satisfactory for anything more than predicting general trends. It was based on a simplified theoretical treatment which yielded a semi-empirical equation. Constants in the equation were evaluated with data taken in a limited experimental program. In that experiment a single impaction baffle was sprayed with slurry from an air-atomizing nozzle.

Observations made in the present study showed that air flow patterns and drop deposition on the single element are not the same as on one baffle among a zigzag assembly. It is clear that a more realistic and extensive experiment should be performed to obtain good data on solids deposition rate.

A special experiment is required because the rate of solids deposition in a simulated scrubber system such as used in the present study is so low that the experimental run requires at least several days of operation. An accelerated deposition experiment, perhaps with automated, continuously operated equipment, is needed.

The recommeded program should investigate important variables, such as E.S. Type, surface cake type, surface roughness and wettability, and slurry particle size. From the data and applicable theory, engineering models should be developed to predict deposition rate more accurately.

DEMONSTRATION PROGRAM

The advantages and performance of the type of entrainment separator described in this report would be demonstrated at a large scale pilot facility. The facility should be a large coal-fired boiler that has a lime or limestone wet scrubber to control sulfur dioxide and particulate emissions. The scale of the demonstration should be at least an order of magnitude greater than the small pilot facility used in the program described in this report; i.e., 14 m^3/s (30,000 ACFM).

Program Objectives

The program objectives would be to demonstrate that the E.S. performs with the desired efficiency and operates economically without being adversely affected by solids deposition. Overall economics of this E.S. relative to other types used on similar applications would be estimated.

Program Plan

The general program would be conducted as follows:

1. Site Selection:

A utility that has a pilot scale wet scrubber operating on flue gas from a large coal-fired boiler is the desired facility. An ideal site would be the EPA Alkali Scrubbing Test Facility at the TVA Shawnee Power Station, Paducah, Kentucky. This facility has 3 pilot scrubbers, each capable of treating up to 16.5 m^3/s (35,000 ACFM) of flue gas at 150°C. The scrubber outlet gas glow rates are about 80% of the inlet because of the pressure and temperature drops through the scrubber. Two of the pilot scrubbers are currently in operation: a venturi/spray tower and a mobile bed. Both have horizontal zigzag baffle entrainment separators located at the top of vertical scrubbing towers.

2. Source Evaluation:

The drop size distribution, entrainment loading, and liquid and gas properties and flow rates would be determined by a source test. The efficiency of the present E.S. (if any) would be measured to permit performance and cost comparison. Overall description of the scrubber/E.S. system would be compiled to determine available structures and equipment that could be adapted for a new E.S. and to facilitate evaluation of the impact of the new E.S. on overall system performance and economics.

3. Preliminary Design:

The basic E.S. design will be the same as the vertical zigzag baffles described in this report. Several design variables must, however, be considered:

a. Height of the vertical disengagement space above the scrubber.
b. Incorporation of a pre-separator, such as turning vanes in the vertical-to-horizontal elbow duct transition.
c. Length and slope of horizontal duct between the scrubber tower and the E.S.
d. Cost/performance trade-off to decide pressure drop, superficial gas velocity, scrubber cross sectional, and number of rows of baffles.
e. E.S. baffle length.
f. E.S. drainage and slurry recirculation system.
g. Washing system design - slurry or make-up water.
h. Materials.
i. Provisions for performance testing.

j. Instrumentation.

k. Test plan.

4. Engineering Design:

This phase would produce engineering fabrication, construction and installation, drawings and procedures based on the design decided upon in the preliminary design phase. Detailed costs would be determined and prospective subcontractors and equipment vendors would be evaluated.

5. Installation:

Procurement of equipment, selection of subcontractors and construction and installation of the E.S. system would occur in this phase.

6. Startup:

During this phase the various problems that accompany the operation of new equipment and systems would be solved. Inspection and maintenance procedures would be set up. Special instrumentation required for performance testing would be installed and checked out.

7. Performance Testing:

As in the source evaluation phase the upstream and downstream entrainment and gas properties and conditions would be measured to allow determination of overall and grade efficiencies. The following variables would be evaluated:

a. Number of rows in E.S.

b. Superficial gas velocity and pressure drop.

c. Washing rate, frequency, and liquid.

d. Slurry concentration, particle size, and chemistry.

e. Materials - plastic versus stainless steel.

8. Evaluation:

This phase would involve the analysis and evaluation of the data taken during the testing phase. The effects of the several variables on the E.S. performance would be determined. The economic benefits of the E.S. system would also be evaluated.

Program Schedule

The demonstration program would be performed over a 2-year period and involve 6 months of performance testing. A proposed schedule is presented in Figure 55.

Program Costs

The program would cost approximately $400,000 and the breakdown is presented in Table 16.

TABLE 16. PROGRAM COST ESTIMATE

Task	Labor	Other
1	$ 20,000	$ 1,000
2	30,000	5,000
3	50,000	
4	50,000	
5	30,000	30,000
6	10,000	
7	90,000	10,000
8	40,000	
9	30,000	2,000
	$350,000	$48,000

Figure 55. Proposed program schedule.

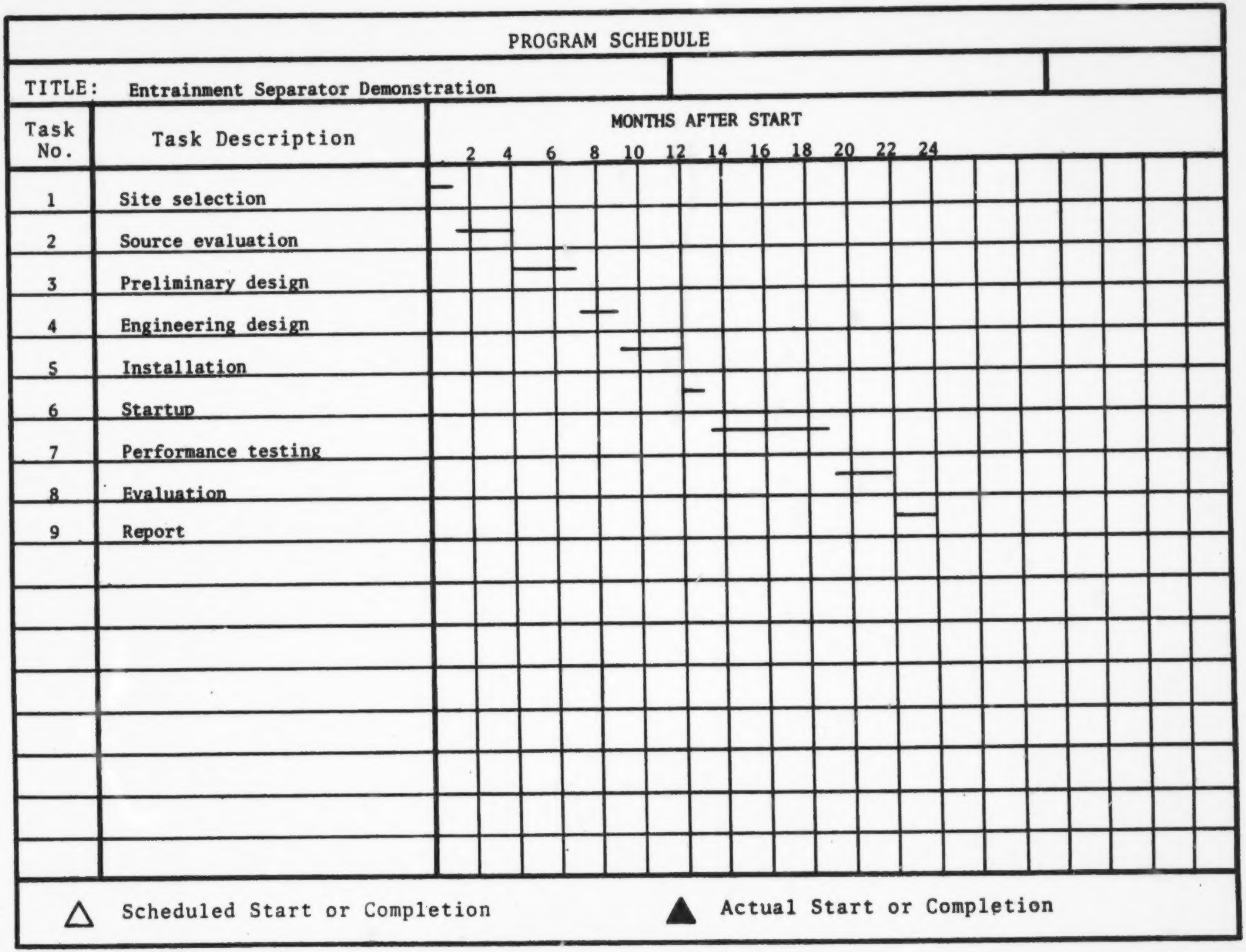

REFERENCES

Bell, C.G. and W. Strauss. Effectiveness of Vertical Mist Eliminators in a Cross Flow Scrubber. J. Air Pollution Control Assoc. 23:967-969, 1973.

Calvert, S. Venturi and Other Atomizing Scrubbers; Efficiency and Pressure Drop. American Inst. of Chemical Engineers J. 16:392-396, 1970.

Calvert, S. State-of-Art Survey of Mist Elimination in the USA. In: Second US/USSR Symposium on Particulate Control. EPA 600/7-78-037, 1978. pp 180-193.

Calvert, S. Guidelines for Selecting Mist Eliminators. Chemical Engineering. pp 109-112, Feb. 27, 1978.

Calvert, S., J. Goldshmid, D. Leith, and D. Mehta. Scrubber Handbook. PB 213-016, 1972.

Calvert, S., I.L. Jashnani, and S. Yung. Entrainment Separators for Scrubbers. J. of Air Pollution Control Assoc. 24:971-975, 1974.

Calvert, S., S. Yung, H.F. Barbarika, and L.E. Sparks. Entrainment Separators for Scrubbers. In: Second EPA Fine Particle Scrubbers Symposium. EPA 600/2-77-193. pp 75-95, 1977.

Calvert, S., S. Yung, and J. Leung. Entrainment Separators for Scrubbers - Initial Report. EPA 650/2-74-119a. PB 241-189, 1974.

Calvert, S., S. Yung, and J. Leung. Entrainment Separators for Scrubbers - Final Report. EPA 650/2-74-119b. PB 248-050, 1975.

Calvert, S., S. Yung, and L.E. Sparks. Liquid Entrainment from a Mobile Bed Scrubber. J. Air Pollution Control Assoc. 27:768-770, 1977.

Carter, W.J. A Literature Survey and Analysis of Mists 1-10 μ Size and Moisture Separators, MSAR 70-10, January 21, 1970.

Chan, J.K. and M.W. Golay. Comparative Evaluation of Cooling Tower Drift Eliminator Performance. MIT-EL 77-004. PB 272-366, June 1977.

Chan, J. and M.W. Golay. Comparative Performance of Current Design Evaporative Cooling Tower Drift Eliminators. Atmospheric Environment. 11:775-781, 1977.

Chaput, L.S. Federal Standards of Performance for New Stationary Sources of Air Pollution. J. of Air Pollution Control Assoc. 26:1055-1060, 1976.

Conkle, H.N., H.S. Rosenberg, and S.T. Dinovo. Guidelines for the Design of Mist Eliminators for Lime/Limestone Scrubbing Systems. EPRI FP 327, December 1976.

Davies, R. A Review of the Methods for the Particle Size Analysis of Droplets, Sprays, and Mists. Dechema Monogr. 79, n 1589-1615, pt B, pp 115-134, 1976.

Dickinson, D.R. and W.R. Marshall, AIChE Journal. 14:541-552, 1968.

Epstein, M. EPA Alkali Scrubbing Test Facility: Summary of Testing through October 1974. EPA 650/2-75-047. NTIS PB 244-901, 1975.

Epstein, M. H.N. Head, S.C. Wang, and D.A. Burbank, Results of Mist Elimination and Alkali Utilization Testing at the EPA Alkali Scrubbing Test Facility. In: Proceedings: Symposium on Flue Gas Desulfurization New Orleans, March 1976, Volume I. EPA 600/2-76-136a, 1976. pp 145-204.

Fuchs, N.A. The Mechanics of Aerosols. Pergamon Press, New York, 1964.

Galeski, J.B. Particle Size Definition for Particulate Data Analysis. EPA 600/7-77-129, 1977.

Gieseke, J.A. and R.I. Mitchell. Size Measurement of Collected Drops. J. of Chemical and Engineering Data. 10:350-353, 1965.

Head, H.N. EPA Alkali Scrubbing Test Facility: Advanced Program, Second Progress Report. EPA 600/7-76-008. NTIS PB 258-783, 1976.

Head, H.N. EPA Alkali Scrubbing Test Facility: Advanced Program, Third Progress Report. EPA 600/7-77-105, 1977.

Hollinden, G.A., R.F. Robards, N.D. Moore, T.M. Kelso, and R.M. Cole. TVA's 1-MW Pilot Plant: Vertical Duct Mist Elimination Testing - Progress Report, PRS-14. EPA 600/7-76-021, October 1976.

Hollinden, G., R. Robards, N. Moore, T. Kelso, and R. Cole. TVA's 1-MW Pilot Plant: Final Report on High Velocity Scrubbing and Vertical Duct Mist Elimination, PRS-19. EPA 600/7-77-019. NTIS PB 269-850, March 1977.

Houghton, J.G. and W.H. Radford. Trans. Am. Inst. of Chemical Engineers. 35:427, 1939.

Johnson, L.D. and R.M. Statnick. Measurement of Entrained Liquid Levels in Effluent Gases from Scrubber Demisters. EPA 650/2-74-050. NTIS PB 233-739, June 1974.

Medecki, H., M. Kaufman, and D.E. Magnus. Design, Development, and Field Test of a Droplet Measuring Device. EPA 650/2-75-018, 1975.

McIlvaine Company. The McIlvaine Scrubber Manual. Northbrook, Illinois, 1978.

Nannen, L.W. and K.E. Yeager. Status of the EPRI Flue Gas Desulfurization Development Program. In: Proceedings: Symposium on Flue Gas Desulfurization, New Orleans, March 1976, Vol. I. EPA 600/2-76-136a, 1976. pp 102-113.

Roffman, A. and L.D. Van Vleck. The State-of-the-Art of Measuring and Predicting Cooling Tower Drift and Its Deposition. 24:855. J. Air Pollution Control Assoc. 1974.

Sekhar, N. Demister Design for Limestone Slurry Scrubber, Paper No. 77-17.3. Presented at 70th Annual Meeting of APCA, Toronto, Ontario, Canada, June 20-24, 1977.

Weir, A., L.T. Papay, D.G. Jones, J.M. Johnson, and W.C. Martin. Results of the 170 MW Test Modules Program. Mohave Generating Station, Southern California Edison Company. In: Proceedings: Symposium on Flue Gas Desulfurization, New Orleans, March 1976, Volume I. EPA 600/2-76-136a, 1976. pp 325-353.

Williams, J.E. Mist Eliminator Testing at the Shawnee Prototype Lime/Limestone Test Facility. In: Second US/USSR Symposium on Particulate Control. EPA 600/7-78-037, 1978. pp 194-214.

Yao, S.C. and V.E. Schrock. Aerodynamic Design of Cooling Tower Drift Eliminators, Transactions of the ASME: Journal of Engineering for Power, 450-456. October 1976.

APPENDIX "A"

ENTRAINMENT SEPARATOR INLET AND OUTLET ENTRAINMENT CONCENTRATION AND SIZE DISTRIBUTION DATA

TABLE A-1. ENTRAINMENT SEPARATOR INLET DATA MOBILE BED SCRUBBER OPERATION

Concentration (ml/DNm³) based on 4 collection methods

Run No.	E.S. Drainage	7.6 cm dia. Sphere Drainage	3.8 cm dia. Sphere Drainage	Sample Train w/Cascade Impactor				
				Cum. Total	Conc. Less Than (μmA) 14	8	5	1.5
			Scrubber Mode 1					
13-3	(1.65)	2.37	2.69	2.08		.034	.032	.011
13-4	(1.45)	2.05	2.47	1.86		.049	.029	.011
14-4	(1.61)	2.29	2.82	2.83	.010	.006	.001	
13-15	3.55	2.41	3.33	2.68		.016	.012	.007
13-16	3.61	2.41	3.30	2.51		.018	.012	.007
13-26	3.17	2.38	2.88	1.86	.012	.008	.001	
13-27	3.36	2.28	2.91	2.40	.003	.002		
13-5		2.89	2.64	2.03		.022	.020	.007
13-6		2.23	2.69	2.08		.049	.040	.015
14-5	4.07	2.47	2.89	3.28	.028	.012		
13-19	4.39	2.34	2.61	3.36		.036	.035	.032
13-20	3.87	2.40	2.95	2.56		.010	.010	.005
13-24	4.45	2.22	2.69	2.98	.006	.004	.001	
13-25	4.45	2.10	2.75	1.67	.004	.004	.001	
Average	3.88	2.35	2.83	2.44		.019	.016	.012
			Scrubber Mode 2					
13-11	4.65	2.13	2.75	1.47		.035	.028	.014
13-12	4.49	2.19	2.89	1.60		.046	.043	.011
Average	4.57	2.16	2.82	1.54		.040	.036	.012

TABLE A-1. (continued)

Run No.	E.S. Drainage	7.6 cm dia. Sphere Drainage	3.8 cm dia. Sphere Drainage	Sample Train w/Cascade Impactor				
				Cum. Total	Conc. Less Than (μmA) 14	8	5	1.5
			Scrubber Mode 3					
13-13	4.13	2.03	2.34	.955		.024	.023	.007
13-14	4.13	1.84	2.41	1.57		.016	.013	.012
Average	4.13	1.94	2.38	1.26		.020	.018	.010
			Scrubber Mode 4					
13-17	2.75	1.47	1.15	1.47		.017	.012	.007
13-18	3.48	1.57	1.98	1.15		.016	.011	.009
14-1	3.04	1.56	1.85	0.637	.005	.003		
14-2	2.93	1.64	1.93	1.31	.006	.004		
13-1	(5.29)	1.59	1.85	1.24		.033	.029	.020
13-2	(4.97)	1.43	1.46	1.27		.011	.010	.008
13-7	(4.67)	1.33	1.46	0.817		.028	.020	.010
13-8	3.87	1.54	2.24	0.720		.031	.025	.018
14-6	3.62	1.62	2.00	1.94	.010	.005		
13-21	4.34	1.54	1.54	1.20	.037		.036	
13-22	4.05	1.67	2.06	-	-		-	-
13-23	4.34	1.64	1.84	1.42	.008		.007	
14-3	4.27	1.61	2.24	1.06	.023	.012	.001	
Average	3.67	1.55	1.82	1.19		.016	.017	.012

TABLE A-1. (continued)

Run No.	E.S. Drainage	7.6 cm dia. Sphere Drainage	3.8 cm dia. Sphere Drainage	Sample Train w/Cascade Impactor Cum. Total	Conc. Less Than (μmA) 14	8	5	1.5
			Scrubber Mode 5					
13-9	3.61	0.81	0.99	0.344		.056	.046	.029
13-10	3.32	0.77	1.05	1.36		.145	.132	.040
14-7	3.17	0.79	1.01	0.852	.005	.003		
Average	3.37	0.79	1.02	0.852		.068	.089	.035

*Note: Figures in ( ) not included in averages.

TABLE A-2. ENTRAINMENT SEPARATOR INLET DATA SIEVE PLATE SCRUBBER OPERATION

Concentration (ml/DNm³) based on drainage from entr. sep. and sample train w/cascade impactor collection

Run No	E.S. Drainage	Sample Train w/C.I.			
		Cum. Total	Conc. Less Than (µmA)		
			20	11	7
	Low Pressure Drop Operation				
14-19	(.451)	.081	.023	.018	.016
15-3	(.291)				
14-17	.516	.092	.043	.041	.036
14-21	.773	.089	.028	.025	.020
14-10	-	.126	.039	.030	.018
14-11	.387	.074	.027	.022	
14-12	.451	.085	.014	.013	.009
14-13	.773	.092	.028	.027	.018
15-6	.507	.048		.016	.013
14-23	.773	.094	.033	.028	.020
14-24	.773	.120	.034	.029	.022
14-26	.677				
14-27	.516	.087	.031	.025	.014
14-28	.644	.040	.030	.021	.017
14-29	.516	.056	.035	.027	.019
15-1	.581	.131	(.122)	(.115)	(.108)
15-2	.387	.068	.033	.022	.014
Average	.591	.086	.031	.025	.018

TABLE A-2. (continued)

Run No	E.S. Drainage	Sample Train w/C.I. Cum. Total	Conc. Less Than (µmA) 20	10	6	1.8
	High Pressure Drop Operation					
14-18	(.483)	.208	.024	.022	.018	
15-4	(.327)					
14-16	.878	.197	.016	.015	.009	
14-20	1.23	.133	.020	.018	.011	
14-8	1.06	.167	.013	.009		.001
14-9	1.32	.108	.020	.018	.013	
14-14	1.23	.136	.026	.024	.013	
14-15	1.06	.101	.018	.017	.012	
15-5	1.14	.038		.016	.014	.011
14-22	1.23	.106	.032	.030	.016	
14-25	1.32	.197	.047	.041	.018	
Average	1.16	.139	.024	.021	.014	.006

Note: Figures in parentheses ( ) not used in average calculation.

TABLE A-3. ENTRAINMENT SEPARATOR INLET DATA
SPRAY SCRUBBER OPERATION

Concentration (ml/DNm^3) based on 4 collection methods

Run No.	E.S. Drainage	7.6 cm dia. Sphere Drainage	3.8 cm dia. Sphere Drainage	Sample Train w/Cascade Impactor				
				Cum. Total	Conc. 17	Less Than (µmA) 8	5	1.5
			5 ea. 1/2-B-50 Spray Nozzles					
15-21	(5.04)	-	-	8.01	.060	.039		.024
22	(4.44)	-	-	8.19		(.171)		
17	8.80	6.22	8.77	9.28	.058	.036		.020
23	9.23	6.24	8.14	8.74	.040	.026		.014
16A	10.8	6.19	9.03	9.17	.026	.018		.010
16B	10.4	6.24	9.03	11.9	.048	.033		.008
26	11.0	6.32	8.61	8.77	.028	.020		.012
Average	10.0	6.24	8.72	9.15	.043	.029		.015
			7 ea. 1/2-B-50 Spray Nozzles					
15-19	(4.45)	-	-	7.17		(.132)	(.121)	
20	(4.14)	-	-	10.8	.053	.041	.017	
18	7.18	5.52	7.59	7.05	.061	.047		.015
24	8.10	5.13	6.91	6.40	.028	.020		.012
12	8.17	4.09	5.62	5.10		.055	.044	
13	8.38	4.97	7.23	6.56		(.134)	(.112)	
14	8.31	5.31	7.23	6.18	.088	.075		.012
15	8.66	5.55	7.33	9.84	.047	.032		.018
25	9.65	4.58	6.17	6.76	.033	.022		.012
Average	8.35	5.02	6.87	7.32	.052	.042	.031	.014

TABLE A-3. (continued)

Run No.	E.S. Drainage	7.6 cm dia. Sphere Drainage	3.8 cm dia. Sphere Drainage	Sample Train w/Cascade Impactor Cum. Total	Conc. Less Than (μmA) 17	8	5	1.5
		4 ea. ST-24-FCN Spray Nozzles						
16-3	(2.99)	-	-	3.12		.033	(.030)	
16-4	(3.47)	-	-	2.03	.069	.060		.043
16-5	6.12	2.51	2.70	3.21	.022	.017		.012
15-29	6.31	2.75	4.14	3.64	.016	.012		.009
16-8	8.17	2.74	3.77	3.64	.024	.018		.010
15-28	7.75	2.36	3.45	3.66	.038	.030		.017
Average	7.09	2.59	3.52	3.22	.034	.028		.018
		6 ea. ST-24-FCN Spray Nozzles						
16-1	(3.18)	-	-	4.04	.038	.029		.019
16-2	(2.69)	-	-	4.82		.031	.027	
16-6	6.12	1.74	3.66	2.83	.032	.028		.019
15-30	6.29	2.20	3.56	3.65	.030	.024		.015
16-7	7.46	2.13	3.03	2.57	.021	.015		.009
15-27	7.46	2.33	3.25	4.62	.048	.040		.034
Average	6.83	2.10	3.38	3.76	.034	.028	.027	.019

TABLE A-4. ENTRAINMENT SEPARATOR OUTLET DATA
MOBILE BED SCRUBBER OPERATION

Concentration (ml/DNm^3) based on sample train w/cascade impactor collection

		Cum. Conc. Less Than (µmA)			
Run No.	**Scrubber Mode**	**Total**	**8**	**5**	**1.5**
	No Entrainment Separator (Blank Run)				
13-3	1	.607	.021	.013	.008
13-4	1	.302	.021	.020	.016
14-4	1	.333	.021	.019	.013
	3 Rows of Vertical Baffles				
13-15	1	.031	.021	.019	.015
13-16	1	.022	.016	.014	.013
13-17	4	.017	.012	.012	.010
13-18	4	.015	.014	.014	.012
	3 Rows of Slanted Baffles				
13-26	1	.015	.012	.012	.011
13-27	1	.011	.008	.008	.007
14-1	4	.025	.019	.017	.013
14-2	4	.016	.011	.010	.008
	6 Rows of Vertical Baffles				
13-5	1	.018	.014	.013	.010
13-6	1	.056	.042	.036	.028
14-5	1	.032	.018	.016	.012
13-11	2	.013	.010	.009	.006
13-12	2	.012	.010	.010	.008
13-13	3	.016	.014	.014	.012
13-14	3	.016	.015	.010	.010
13-1	4	.010	.009	.007	.007
13-2	4	.011	.010	.009	.006
13-7	4	.042	.032	.028	.021
13-8	4	.061	.055	.048	.038
14-6	4	.031	.022	.020	.015
13-9	5	.085	.068	.059	.040
13-10	5	.036	.032	.027	.023
14-7	5	.019	.015	.013	.010

TABLE A-4. (continued)

Run No.	Scrubber Mode	Cum. Conc. Less Than (μmA) Total	8	5	1.5
		6 Rows of Slanted Baffles			
13-19	1	.012	.009	.008	.007
13-20	1	.004	.004	.004	.004
13-24	1	.012	.012	.010	.008
13-25	1	.016	.016	.010	.009
13-21	4	.034	.030	.029	.025
13-22	4	.010	.010	.010	.010
13-23	4	.014	.012	.012	.011
14-3	4	.034	.028	.024	.018

TABLE A-5. ENTRAINMENT SEPARATOR OUTLET DATA
SIEVE PLATE SCRUBBER OPERATION

Concentration (ml/DNm^3) based on sample train with cascade impactor collection

	Scrubber	Cum	Conc. Less Than (μmA)		
Run No.	ΔP	Total	8	5	1.6
No Entrainment Separator (Blank Run)					
14-19	Low	.051	.017	.016	.012
14-18	High	.102	.017	.015	.009
3 Vertical Rows of Baffles					
14-17	Low	.037	.032	.028	.025
14-16	High	.019	.012	.011	.006
3 Slanted Rows of Baffles					
14-21	Low	.019	.013	.011	.007
14-20	High	.022	.014	.013	.008
6 Vertical Rows of Baffles					
14-10	Low	.039	.036	.026	.021
14-11	Low	.012	.009	.009	.006
14-12	Low	.010	.008	.007	.006
14-13	Low	.022	.016	.015	.015
15-6	Low	.015	.013	.012	.009
Average	Low	.020	.016	.014	.011
14-8	High	.078	.073	.019	.014
14-9	High	.013	.011	.009	.005
14-14	High	.010	.009	.008	.005
14-15	High	.015	.012	.012	.008
15-5	High	.022	.020	.019	.016
Average	High	.028	.025	.013	.010
6 Slanted Rows of Baffles					
14-23	Low	.027	.024	.021	.014
14-24	Low	.031	.027	.026	.020
Average	Low	.029	.026	.024	.017
14-22	High	.019	.016	.015	.008
14-25	High	.038	.030	.023	.013
Average	High	.029	.023	.019	.011

TABLE A-6. ENTRAINMENT SEPARATOR OUTLET DATA
SPRAY SCRUBBER OPERATION

Concentration (ml/DNm^3) based on sample train w/cascade impactor

Run No	Spray Config.[1]	Total	Cum. Conc. Less Than (μmA) 17	8	5	1.5
			No Entrainment Separator (Blank Run)			
15-21	5	2.73		.057	.041	.021
15-22	5	3.88	.165	.132		.079
15-19	7	4.43	.061	.042		.022
15-20	7	1.95		.061	.048	
16-3	4	.590	.024	.017		.013
16-4	4	1.30		.033	.027	
16-1	6	.914		.030	.026	
16-2	6	.467	.023	.019		.015
		3 Vertical Rows				
15-17	5	.355		.299	.288	.269
15-18	7	.128		.061	.051	.037
16-5	4	.059		.019	.016	.012
16-6	6	.109		.018	.015	.012
		3 Slanted Rows				
15-23	5	.198		.095	.084	.071
15-24	7	.069		.031	.026	.020
15-29	4	.036		.019	.016	.013
15-30	6	.075		.039	.034	.028
		6 Vertical Rows				
15-16A	5	.043		.019	.015	.009
15-16B	5	.046		.031	.027	.017
15-12	7	.042		.027	.021	.011
15-13	7	.107		.073	.065	.046
15-14	7	.041		.026	.023	.014
15-15	7	.064		.039	.032	.022
16-8	4	.051		.040	.035	.031
16-7	6	.030		.016	.015	.012

TABLE A-6. (continued)

Run No	Spray Config.[1]	Cum. Conc. Less Than (μmA)				
		Total	17	8	5	1.5
		6 Slanted Rows				
15-26	5	.051		.033	.028	.022
15-25	7	.053		.036	.031	.024
15-28	4	.045		.034	.031	.024
15-27	6	.045		.031	.027	.022

---

[1] Spray Configurations:
5 - 5 ea. 1/2-B-50 spray nozzles
7 - 7 ea. 1/2-B-50 spray nozzles
4 - 4 ea. ST-24-FCN spray nozzles
6 - 6 ea. ST-24-FCN spray nozzles